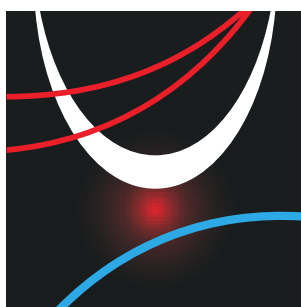




Book of abstracts



Advanced Properties and Processes in
Optoelectronic Materials and Systems
APROPOS 18

5-7 October, 2022

Vilnius, Lithuania

apropos.ftmc.lt



Organizers



Sponsors



Friends



ISBN 978-609-96355-0-7

© Center for Physical Sciences and Technology, 2022
Savanorių ave. 231, LT-02300 Vilnius, Lithuania
<http://apropos.ftmc.lt>
apropos@ftmc.lt

CONTENTS

Committees [4](#)

A Word of Welcome [5](#)

Programme [6](#)

Section 1: Semiconductor nanostructures and advanced photonics systems [10](#)

Special session “Semiconductor chips trends and issues” [13](#)

Section 2: Materials for optoelectronics [15](#)

Section 3: Ultrafast and THz phenomena [21](#)

Section 4: Quantum optics [24](#)

Section 5: United Lithuanian-Polish workshop “Lublin Readings” dedicated to express solidarity with Ukrainian scientists [29](#)

Section 6: THz technologies [39](#)

Section 7: Organic materials for optoelectronics [55](#)

Section 8: Nano and Biophotonics [59](#)

Section 9: Semiconductor nanostructures and advanced photonics systems [66](#)

Poster session [73](#)

3-min award poster session [106](#)

Author index [107](#)

COMMITTEES

CHAIR

Gintaras Valušis, *Vilnius, Lithuania*

PROGRAMME COMMITTEE

Vidmantas Gulbinas, *Vilnius, Lithuania*

Saulius Juršėnas, *Vilnius, Lithuania*

Andriy Kadashchuk, *Kiev, Ukraine*

Jacek Kossut, *Warsaw, Poland*

Wojciech Knap, *Warsaw, Poland*

Arūnas Krotkus, *Vilnius, Lithuania*

Polina Kuzhir, *Joensuu, Finland*

Edmund H. Linfield, *Leeds, U.K.*

Valdas Pašiškevičius, *Stockholm, Sweden*

Carlito S. Ponseca, *Kuwait City, Kuwait*

Hartmut G. Roskos, *Frankfurt/M, Germany*

Chiko Otani, *Sendai, Japan*

Gediminas Račiukaitis, *Vilnius, Lithuania*

Roman Sobolewski, *Rochester, NY, USA*

Sigitas Tamulevičius, *Kaunas, Lithuania*

Gintautas Tamulaitis, *Vilnius, Lithuania*

LOCAL ORGANIZING COMMITTEE

Renata Butkutė (Secretary)

Domas Jokubauskis

Renata Karpič

Ramunė Kriaučionytė

Rimgaudas Žaliauskas

Evaldas Tornau

Marius Vinciūnas

Milda Tamošiūnaitė-Survilienė

Linas Galkauskas

Intro

A WORD OF WELCOME



This conference APROPOS 18 was specific – it took place during a time of war in Ukraine caused by Russian invasion. This particular circumstance introduced appropriate context and additional dimension in discussion atmosphere. It was also reflected in the program of joint section of Poland – Lithuania scientific cooperation aiming usually to present bilateral projects or research. This year, due to the war in Ukraine, the section was different – it was started with a lecture by prof. Rimvydas Petrauskas, the Rector of Vilnius University, dedicated to review the historical relations between Lithuania and Poland, as well as to highlight the historical links with Ukraine. A guest from Kiev, prof. Andrey Kadashchuk, presented situation in Ukraine and its science situation marked by the war.

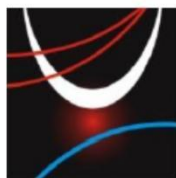
The APROPOS 18 was distinct due to the important milestone – it indicated 50 years tradition of the conference starting in 1971 as the symposium entitled "Plasma and Instabilities in Semiconductors". This event has been associated with Vilnius all these years, and the event is organized initially by former Semiconductor Physics Institute and the Center for Physical Sciences and Technology (FTMC) currently.

The conference has continued a tradition to mirror current and scientific breakthrough trends in optoelectronic materials and technologies, semiconductor physics and photonics. A special session dedicated to discuss semiconductor chip technologies and their development directions from both technological and industrial points of view was organized. The latest achievements of terahertz technologies, terahertz imaging and new research trends in development of future generations of communication and space technologies were presented. A particular attention was dedicated to the latest achievements in the technology of organic semiconductor materials, development in organic electronics and optoelectronics devices as well as their applications in solar energy.

Another special feature of this conference with more than 120 participants from 14 countries was a MasterClass in scientific writing and presentation for PhD students organized by European Marie-Curie training network. This coupled event with 27 international participants was held within the frame of the project "TERAOPTICS" funded by the European Commission.

We are highly indebted to the Research Council of Lithuania and Go Vilnius for making this event possible. Highest possible appreciations go to our sponsors – Light Conversion, Teltonika IOT Group, Inospectra and Science and Technology Park of Institute of Physics for the establishment of Young Researcher Awards.

Gintaras Valušis
Chair of the APROPOS 18



APROPOS 18

Advanced Properties and Processes in Optoelectronic Materials and Systems

5-7 October, 2022 - Conference
2-4 October, 2022 - Masterclass

PROGRAMME

DAY 1, October 5		
Center for Physical Sciences and Technology (FTMC) Saulėtekio av. 3, Vilnius, Lithuania Conference hall A101		
8:30-9:00	FTMC	Registration
9:00	FTMC A101	CONFERENCE OPENING <i>Mayor of Vilnius Remigijus Šimašius</i> <i>Vice-Minister of Education, Science and Sport Ramūnas Skaudžius</i> <i>Chair of APROPOS 18 Conference Gintaras Valušis</i>
Section 1: Semiconductor nanostructures and advanced photonics systems <i>Chair: Vidmantas Gulbinas</i>		
9:10	S1-I1-P	Karl Leo (TU Dresden, Germany) – <i>Organic semiconductors for novel optoelectronic devices – Plenary</i>
9:40	S1-I2	Vytautas Getautis (KTU, Lithuania) – <i>Advanced Organic Molecules for New Generation Solar Cells: from Idea to Commercialization – Invited</i>
10:10-10:30 Coffee break		
Special session “SEMICONDUCTOR CHIPS TRENDS AND ISSUES” <i>Chair: Linas Minkevičius</i>		
10:30	S-I1	Robert Lo , Deputy General Director of EOSL/ITRI (Hsinchu, Taiwan) – <i>The Next Generation of Semiconductor: Trends in chip technology and 3D heterogeneous integration – Invited</i>
11:00	S-I2	Jo De Boeck , IMEC (Belgium) – <i>Invited</i>
11:30	S-I3	Ernestas Zdaniauskis , Teltonika (Vilnius, Lithuania) – <i>TELTONIKA towards new industries: from EMS to semiconductor chips – Invited</i>
12:00-13:00 Lunch break		
Section 2: Materials for optoelectronics <i>Chair: Hartmut Roskos</i>		
13:00	S2-I1	Chiko Otani (RIKEN Center for Advanced Photonics, Japan) – <i>Development of 300 GHz walk-through body scanner for security gate inspections – Invited</i>
13:30	S2-I2	Yi-Jen Chiu (National Sun Yat-sen University, Taiwan) – <i>Above 100Gb/s by Wafer-bonding Hybrid Si Photonics integration – Invited</i>
14:00	S2-I3	Alessandro Surrente (Wrocław University of Science and Technology, Poland) – <i>Magnetically brightened dark excitons in two-dimensional metal halide perovskites – Invited</i>
14:30	S2-O1	C. P. V. Nguyen – <i>First comparison of rhodium- and iron-doped InGaAs photoconductive THz emitters for continuous-wave terahertz emission</i>
14:45	S2-O2	A. Apostolakis – <i>Broadband amplification of terahertz electromagnetic radiation from semiconductor superlattices under coherent phonon driving</i>
15:00-15:15 Coffee break		
Section 3: Ultrafast and THz phenomena <i>Chair: Daniel Mittleman</i>		
15:15	S3-I1	Taiichi Otsuji (Tohoku University, Japan) – <i>Invited</i>
15:45	S3-I2	Wojciech Knap (Warsaw, Unipress, Poland) – <i>Towards on-chip plasmonics amplifiers of THz radiation – ERC – advanced project – Invited</i>
Section 4: Quantum optics <i>Chair: Heinz-Wilhelm Hübers</i>		
16:15	S4-I1	Georgy Fedorov (Institute of Photonics, University of Eastern Finland, Finland) – <i>Graphene based devices for terahertz radiation detection and beyond – Invited</i>
16:45	S4-I2	Fedor Jelezko (Ulm University, Germany) – <i>Quantum sensing enabled by spin qubits in diamond – Invited</i>
17:15	S4-I3	Gediminas Juzeliūnas (Vilnius University, Lithuania) – <i>Topology for Electrons in Solids, Photons and Ultracold atoms – Invited</i>
17:45	S4-I4	Stephan Winnerl (Institute of Ion Beam Physics and Materials Research, Helmholtz-Zentrum Dresden-Rossendorf) – <i>Nonequilibrium carrier dynamics in Landau quantized graphene and mercury cadmium telluride – Invited</i>
18:15-18:30 Coffee break		
18:15-19:00 POSTER SESSION / Networking		

DAY 2, October 6 VU Library Scholarly Communication and Information centre (MKIC) Saulėtekio av. 5, 10222 Vilnius Conference hall A103		
8:30-9:00	MKIC	Registration
Section 5: SPECIAL SESSION – United Lithuanian-Polish workshop “LUBLIN READINGS” <u>dedicated to express solidarity with Ukrainian scientists</u> Chair: Gintaras Valušis		
9:00	MKIC A103	Ambassador Extraordinary and Plenipotentiary of the Republic of Poland in Lithuania
9:10	S5-I1	Rimvydas Petrauskas (Vilnius University, Lithuania) – <i>historical lecture at “Lublin Readings” – Invited</i>
9:40	S5-I2	Tribute to those who died for Ukraine’s freedom. Andrey Kadashchuk (Kiev – Bayreuth (Ukraine-Germany)) – <i>Monitoring the charge-carrier occupied density-of-states in disordered organic semiconductors under non-equilibrium conditions – Invited</i>
10:10-10:30 Coffee break		
Chair: Andrey Kadashchuk and Agnieszka Siemion		
10:30	S5-I3	Egidijus Auksorius (FTMC, Lithuania) – <i>Imaging of the human retina and cornea in vivo with high-resolution ultrafast optical coherence tomography – Invited</i>
11:00	S5-O1	M. Dub – <i>Low frequency noise as a quality control of novel AlGaIn/GaN devices</i>
11:15	S5-O2	V. Stankevič – <i>Measurement of short pulsed magnetic fields</i>
11:30	S5-O3	D. Pashnev – <i>Optimization of 2D plasmons excitation in grating-gated AlGaIn/GaN high electron mobility transistor structures</i>
11:45	S5-O4	M. Maciaszek – <i>ab initio modeling of the photoionization of NV centers in diamond OR Thermodynamical modeling of carbon related defects in hexagonal boron nitride</i>
12:00	S5-O5	V. Čižas – <i>Dissipative parametric generation in a biased superlattice: the case of small signal gain</i>
12:15	S5-O6	P. Sai – <i>Interplay of THz plasmon modes in AlGaIn/GaN grating-gate structures</i>
12:30-13:30 Lunch break		
Section 6: THz technologies		
Chair: Wojciech Knap		
13:30	S6-I1	Heinz-Wilhelm Hübers (German Aerospace Center, Berlin, Germany) – <i>Terahertz technology for remote sensing of the Earth’s atmosphere – Invited</i>
14:00	S6-I2	Hartmut G. Roskos (Goethe-university, Frankfurt/M, Germany) – <i>High-harmonic generation in p-doped Si pumped with intense terahertz pulses – Invited</i>
14:30	S6-O1	I. Grigelionis – <i>Excitation of magnetic polaritons in n-GaAs/GaAs/metal structure in the terahertz range</i>
14:45	S6-O2	K. Kumar – <i>Towards electronically-controlled reconfigurable terahertz beam steering based on phase-change metasurfaces</i>
15:00	S6-O3	R. Balagula – <i>Efficient electrooptic THz beam modulator based on drifting space-charge domains in gallium nitride structures</i>
15:15	S6-O4	D. But – <i>Optimization of self-mixing effect in integrated BiCMOS sources for reflection-type imaging applications</i>
15:30	S6-O5	S.R. Ayyagari – <i>Development of Hybrid phase profile silicon multi-phase zone plate lenses for THz frequencies</i>
15:45-16:00 Coffee break		
Chair: Chiko Otani		
16:00	S6-I3	Daniel Mittleman (Brown University, USA) – <i>Local and non-local terahertz measurements in the near field – Invited</i>
16:30	S6-I4	Tadao Nagatsuma (Osaka University, Japan) – <i>Wireless telecommunications towards Beyond 5G/6G – Invited</i>
17:00	S6-O6	I. Belio-Apaolaza – <i>Optical-THz-Optical bridge at 5Gbps with a photonic-driven Schottky mixer at the receiver</i>
17:15	S6-O7	A. Bandyopadhyay – <i>100 Gbit/s THz Data Transmission and Beyond using Multicore Fiber Combined with UTC Photodiode Array</i>
17:30	S6-O8	M. Tamošiūnaitė-Survilienė – <i>Outdoor THz communications: channel characteristics and statistical uncertainties</i>
17:45	S6-O9	S. Iwamatsu – <i>Ultra-Broadband THz Transition from CPW to Si Rod Waveguide for Future Tbps On-Chip Communications</i>
18:00	S6-O10	K. Ikamas – <i>Data Transmission with Compact All-Electronic THz Wireless System</i>
18:15	S6-O11	K. Spanidou – <i>Optical heterodyne-based module on silicon platform for sub-THz wireless data transmission</i>
19:30 DINNER GALA (Energy and Technology Museum (Rinktinės str. 2, 09312 Vilnius))		

DAY 3, October 7 VU Library Scholarly Communication and Information centre (MKIC) Saulėtekio av. 5, 10222 Vilnius Conference hall A103		
8:30-9:00	MKIC A103	Registration
<u>Section 7: Organic materials for optoelectronics</u> <i>Chair: Irmantas Kašalynas</i>		
9:00	S7-I1	Vidmantas Gulbinas (FTMC, Lithuania) – <i>Charge carrier motion in perovskite films. Role of barriers – Invited</i>
9:30	S7-I2	Tomas Serevičius (Vilnius University, Lithuania) – <i>Towards thermally activated delayed fluorescence compounds with minimized solid-state conformational disorder – Invited</i>
10:00	S7-O1	A. Klein Schuster – <i>Enhanced Mie Scattering on Spoof Plasmonic Surfaces of Terahertz Biosensors</i>
10:15-10:30 Coffee break		
<u>Section 8: Nano and Biophotonics</u> <i>Chair: Georgy Fedorov</i>		
10:30	S8-I1	Valery Zwiller (KTH, Sweden) – <i>Generation, manipulation and detection of light at the single photon level – Invited</i>
11:00	S8-I2	Janis Spigulis (University of Latvia) – <i>Skin-remitted light as a tool for health monitoring – Invited</i>
11:30	S8-O1	L. Naimovičius – <i>Novel diketopyrrolopyrrole-based emitters for NIR-to-visible photon upconversion</i>
11:45	S8-O2	J. Jovaišaitė – <i>Diboranthracene and polymer-based systems for room temperature organic afterglow</i>
12:00	S8-O3	V. Astachov – <i>Controllable growth of two-dimensional palladium sulfide films</i>
12:15	S8-O4	S. Nargelas – <i>Photoluminescence and transient optical absorption in heavily doped lead tungstate</i>
12:30-13:30 Lunch break		
<u>Section 9: Semiconductor nanostructures and advanced photonics systems</u> <i>Chair: Renata Butkutė</i>		
13:30	S9-O1	R. Ivaškevičiūtė-Povilauskienė – <i>Terahertz imaging using diffractive Airy lens</i>
13:45	S9-O2	S. Keraitytė – <i>Growth Optimization and Characterization of MQWs based on InGaAs and GaAsBi for VECSELs and NIR sources</i>
14:00	S9-O3	E. Dudutienė – <i>Effect of substrate temperatures on luminescent properties of GaAsBi/GaAs multi-quantum-wells</i>
14:15	S9-O4	M. Karaliūnas – <i>Experimental Investigation of GaAs(Bi)/AlGaAs Grown Parabolic Quantum Wells in Terahertz Frequency Range</i>
14:30	S9-O5	S. Stanionytė – <i>Structural analysis of thin bismuth layers grown on silicon (111) substrates</i>
14:45	S9-O6	T. Troha – <i>Ultrafast long-distance electron-hole plasma expansion in GaAs mediated by stimulated emission of photons</i>
15:15-15:30 Coffee break		
<u>Section 10:</u> <i>Chair: Renata Butkutė and Gintaras Valušis</i>		
15:30	MKIC A103	SPECIAL SESSION – 3 min award presenters session
16:00		CLOSING REMARKS
16:10	FTMC	Excursion to the laboratories and Clean Room Facilities // Meeting of Scientific conference board

DAY 1, October 5

Center for Physical Sciences and Technology (FTMC)
Saulėtekio av. 3, Vilnius, Lithuania
Main hall near A101

18:15-19:00 POSTER SESSION**Section 1: Semiconductor nanostructures and advanced photonics systems**

S1-P1 – Arnas Pukinskas – Bi-Quantum Dots Formation in-situ in MBE Reactor

S1-P2 – Justinas Jorudas – Comparison of InAlGa_N and AlGa_N HEMT structures

S1-P3 – Monika Jokubauskaitė – Influence of the design of parabolic AlGaAs barriers on the optical properties of GaAsBi quantum wells

S1-P4 – Algimantas Lukša – Intentional modification of nanocrystalline graphene coatings by thermal annealing

S1-P5 – Martynas Skapas – Transmission electron microscopy of Hybrid graphene-lanthanum perovskite structures

S1-P6 – Ezgi Abacioglu – Structural, optical, and mechanical properties of silicon nitride films deposited by inductively coupled plasma enhanced chemical vapor deposition

S1-P7 – Linus Ardaravičius – High-field electron transport measurements in (Be,Zn)MgO/ZnO heterostructures

Section 2: Materials for optoelectronics. Quantum optics

S2-P1 – Darius Urbonis – Double Fano resonance in broken symmetry split-ring resonator array metasurface

S2-P2 – Justina Žemgulytė – Compact rectennas for energy harvesting using SSAIL technique

S2-P3 – Jerzy Lusakowski – Optically detected cyclotron resonance in CdTe-based quantum wells

S2-P4 – Karolis Redekas – Quantum well infrared photodetector operating at room temperature

S2-P5 – Žygimantas Vosylius – Radiometric imaging and pulsed X-ray-based studies of light collection from scintillating crystals

S2-P6 – Jose Javier Fernandez-Pacheto Cuesta – Study of thermo-refractive noise in solid-state dual frequency micro-lasers

S2-P7 – Vytautas Janonis – Optimization of Coherent Thermal Emission from Circular Shape n-GaN Surface Relief Gratings

Section 3: Ultrafast and THz phenomena. THz technologies

S3-P1 – Dominykas Sanda – Application of terahertz time-domain spectroscopy in the study of air components and vapors of organic compounds

S3-P2 – Alexander Chernyadiev – Investigation of sensitivity limits of a near-field THz sensor based on a Si CMOS technology

S3-P3 – Himanshu Gohil – Development of an integrated Schottky based heterodyne THz receiver at 300 GHz using power combining approach.

S3-P4 – Javier Martinez Gil – 270-320 GHz Low Barrier Schottky Diode Mixer

S3-P5 – Mateusz Kaluza – 3D printed THz MIMO diffractive structures

S3-P6 – Mateusz Surma – THz achromatic lens from 3D printing materials

S3-P7 – Ashish Kumar – Cost-effective high pass filter for dielectric rod waveguides

S3-P8 – Abdu Subahahan Mohammed – Low Loss Topological Silicon Valley Photonic Crystal waveguides in Terahertz regime

S3-P9 – Yilmaz Ucar – Cascaded wideband RoF links with LWA for enabling mobile 5G base stations

S3-P10 – Jonas Tebart – Exploiting 3D metal printing for additive manufacturing of waveguide and antenna structures for THz-applications

S3-P11 – Fasil Bashir Wani – Metamaterial based Antenna integrated UTC-PD array for THz communications in 270-330 GHz band

Section 4: Organic materials for optoelectronics. Nano and Biophotonics

S4-P1 – Muhammad Mujahid – Triple cation perovskite/silicon tandem solar cell

S4-P2 – Oleg Kiprijanovic – Strong inverse piezoelectric response in graphene - dielectric structures induced by nanosecond electric pulse

S4-P3 – Ihor Zharchenko – Low and high photon energy induced photoresponse in single junction solar cells

S4-P4 – Yaraslau Padrez – Collagen orientation index determination in wide-field SHG microscopic images of lung tissue

S4-P5 – Šarūnas Mickus – Investigation of surface modification of polycarbonate by picosecond Nd:YVO₄ laser pulses for selective chemical copper deposition

S4-P6 – Karolis Adomavičius – In vivo imaging of human retina with Fourier-Domain Full-Field Optical Coherence Tomography and a Multimode Fiber for Coherence Noise Reduction

S4-P7 – Faustino Wahaia – Characterization of Metal-Organic Frameworks (MOFs) Using THz Techniques

Section 1

SEMICONDUCTOR NANOSTRUCTURES AND ADVANCED PHOTONICS SYSTEMS

S1-I1-P

Organic Semiconductors for Novel Optoelectronic Devices

Karl Leo

TU Dresden, Germany



Photo by Irmantas Gelunas / BNS

S1-I2

Advanced Organic Molecules for New Generation Solar Cells: from Idea to Commercialization

Vytautas Getautis

Department of Organic Chemistry, Faculty of Chemical Technology, Kaunas University of Technology, K. Donelaičio st. 73, 44249 Kaunas, Lithuania

Email: vytautas.getautis@ktu.lt

This lecture will cover results of our recent investigations in the field of molecular engineering of small molecule hole transporting materials for perovskite solar cells. Our group has been successful in creating several classes of novel organic charge transporting materials, which are on a par with or even better than Spiro-OMeTAD. The molecularly engineered new hole transporting materials were synthesized in one or two steps from commercially available and relatively inexpensive starting reagents, resulting in up to several fold cost reduction of the final product compared with Spiro-OMeTAD. High solubility in organic solvents and ease of preparation makes these molecules very appealing for commercial prospects of photovoltaic devices.

Special session

SEMICONDUCTOR CHIPS TRENDS AND ISSUES

Special session “SEMICONDUCTOR CHIPS TRENDS AND ISSUES”

The Next Generation of Semiconductor: Trends in chip technology and 3D heterogeneous integration

Robert Lo

*Deputy General Director of EOSL/ITRI
(Hsinchu, Taiwan)*



Invited talk by IMEC

Jo De Boeck

*Executive Vice President, Corporate Strategy
Officer (CSO) & general manager imec the
Netherlands, IMEC (Belgium)*



TELTONIKA towards new industries: from EMS to semiconductor chips

Ernestas Zdaniauskis

Teltonika (Vilnius, Lithuania)



Section 2

MATERIALS FOR OPTOELECTRONICS

Development of 300 GHz walk-through body scanner for security gate inspections

Chiko Otani^{1,2}, Tomofumi Ikari^{1,3} and Yoshiaki Sasaki¹

¹RIKEN Center for Advanced Photonics, RIKEN, 519-1399 Sendai, Japan.

²Dept. Physics, Tohoku University, Sendai, Japan.

³Spectra Design Co., Ltd., Otawara, Japan.

Email: otani@riken.jp.

Public transportation facilities such as airports and high-speed train stations require various security inspections to prevent terrorism and injury incidents, and millimeter (MMW) and terahertz (THz) waves body scanners have been developed. However, faster inspections are required to perform it without stopping the pedestrians. We have developed a prototype of a 300 GHz body scanner for the walk-through gate with walking speed of more than 4 km hr⁻¹ and the spatial resolution of 10 mm. In this prototype, a beam is irradiated at an angle of 45 degrees to the pedestrian to obtain a 3D image near the chest [1].

Because it uses a single transceiver, we requires beam scans to acquire the 3D information. The horizontal scan is done by using the human gait, moving the detection area from right to left according to the gait. The vertical scan is done by vertical optical beam scanning of the receiving beam. And, the depth measurement is done by the FMCW radar measurement. The frequency sweep for the radar is 275-305 GHz during 10 μ s. The transmitter power is more than 20 mW in the whole frequency range and the ratio of the maximum power to the minimum detectable power is about 105 dB. Typical measurement time of acquire the 3D image is about 0.4 sec. The examples of acquired images are shown in Fig. 1 and 2 for a man who is holding a plastic gun in his pocket.

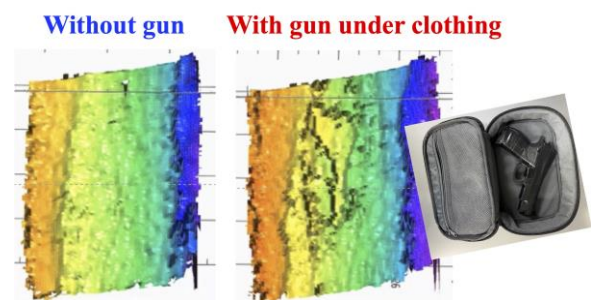


Fig. 1 Acquired images during walking w/o and with a fake gun.

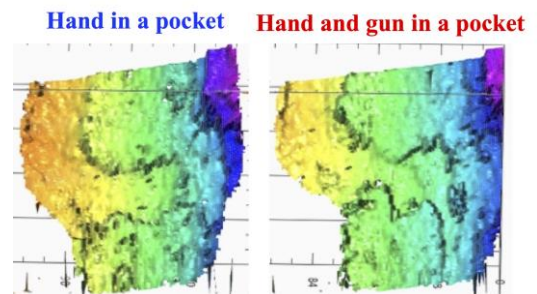


Fig. 2 Acquired images during walking w/o and with a fake gun in hand.

ACKNOWLEDGEMENTS

We thank to Ms. Yoshimi Kudo, Mr. Toshihisa Tanaka and Dr. Yuichi Takigawa of NIKON Co., Ltd. for their technical supports. This work was supported by the JST-ACCEL program (JPMJMI17F2).

REFERENCES

- [1] C. Otani, T. Ikari, Y. Sasaki, Proc. SPIE, **11827**, 11827N (2021).

Above 100Gb/s by Wafer-bonding Hybrid Si Photonics integration

(invited talk)

Yang-Zhen Chen¹, Rih-You Name¹, Chung-Wei Hsiao¹, Yi-Xin Fang¹, Yi-Jen Chiu¹

¹ *Department of Photonics, National Sun Yat-Sen University, Kaoshiung 804, Taiwan.*
yjchiu@faculty.nsysu.edu.tw

Silicon photonics has been treated as one of the key technologies for various emerging applications, such as high-speed data interconnects, data communication, and remote sensor. Through defining the submicron optical waveguide, dense active and passive optical elements can be integrated for different functions through so-called CMOS compatible processing technologies, enabling high-speed optical interconnect, optical communication, and remote sensors. However, two major technology bottlenecks will be formed due to the intrinsic material issues: one is the indirect bandgap of Si-related material and the other is the optical coupling between different material system, which not only restricts the functions of light generation and amplification but also leading to complex fabrication processing in integrating devices.

Thin-film integration using different layer structure of material then becomes one promising solution to enhance the future function in photonic integration. As shown in Fig.1, by integrating layer-by-layer structure through different material system, the coupling between layers is defined by fabricating optical spot size converter (SSC), where wafer bonding was used for connecting two thin-film materials. With such fabrication, the optical active functions, such as gain and light source, could be brought into a Si-based photonic template [1-2]. As a result, the advantages of different material system can be independently taken for performing different functions. In our work, the etching selectivity between materials can be used for self-alignment in vertical processing, enabling 3D photonic integration with just a few simple fabrication steps. Furthermore, hybrid thin-film integration with compact and high-confinement active region, allowing device performance to be built up in a submicron dimension of waveguide. High-speed optical modulation of above 100Gb/s, 10dB/V modulation efficiency, and 8dB optical gain have been demonstrated in such hybrid photonic integration template. High-speed high-power performance with efficiency has also been shown in our recent work. Also, the integration between such chips or material will be proposed with the recent progress for some gyroscope sensor and broadband optical data transmission.

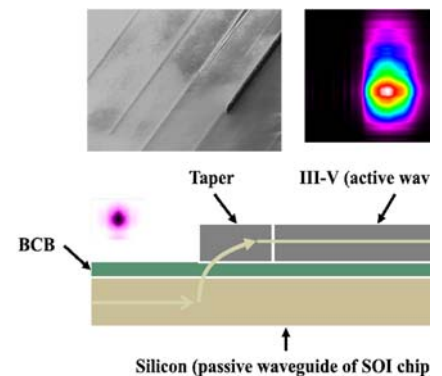


Fig. 1 The schematic diagram of vertically layer-stacked optical spot-size converter (SSC) for Si photonic integration.

REFERENCES

- [1] Yang-Jeng Chen et al, "Vertical Hybrid Integration Devices Using Selectively Defining Underneath Si Waveguide," *IEEE Photonics Technology Letters* v33 23 (2021).
- [2] Yang-Jeng Chen et al, "Hybrid III-V-on-SOI optical spot size converter by self aligned selective undercut dry etching of Si," *Optics Letter*, v45 15 (2020).

Magnetically brightened dark excitons in two-dimensional metal halide perovskites

S. Wang¹, M. Dyksik², C. Lampe³, M. Gramlich⁴, D. K. Maude¹, M. Baranowski², A. S. Urban³, P. Plochocka^{1,2}, A. Surrente²

¹Laboratoire National des Champs Magnétiques Intenses, CNRS Toulouse, France

²Dept of Experimental Physics, Wroclaw University of Science and Technology, Wroclaw, Poland

³Dept of Physics, Ludwig-Maximilians-Universität München, Munich, Germany

Email: alessandro.surrente@pwr.edu.pl

The synthesis of colloidal nanocrystals with near-unity photoluminescence (PL) quantum yields has vastly extended the potential of metal halide perovskites for solid-state lighting and display applications. It is possible to template the growth of nanocrystals to form planar, ultrathin perovskite sheets embedded between long organic molecules, which stabilize the colloids, referred to as nanoplatelets, shown schematically in Fig. 1(a). These colloidal quantum wells are of interest as emitters in the blue spectral region. In the context of light emitters, the splitting between optically dark and optically bright excitons is of paramount importance. After photogenerations, excitons usually relax to the lowest lying dark state, which is detrimental for the device efficiency. We performed optical spectroscopy measurements with an applied in-plane magnetic field to mix the bright and dark excitonic states of CsPbBr₃-based nanoplatelets. The induced brightening of the dark state allows us to directly observe an enhancement of the PL signal on the low-energy side of the spectrum, which we explain as the magnetic-field induced brightening of the dark state, see Fig. 1(b). In-plane magnetic fields allow us to extract accurately the energy splitting between the dark and bright excitons directly, without resorting to further measurements or modelling [see Fig. 1(c)]. The evolution of the PL signal in the magnetic field suggests that at low temperatures the exciton population is not fully thermalized due to the existence of a phonon bottleneck [2].

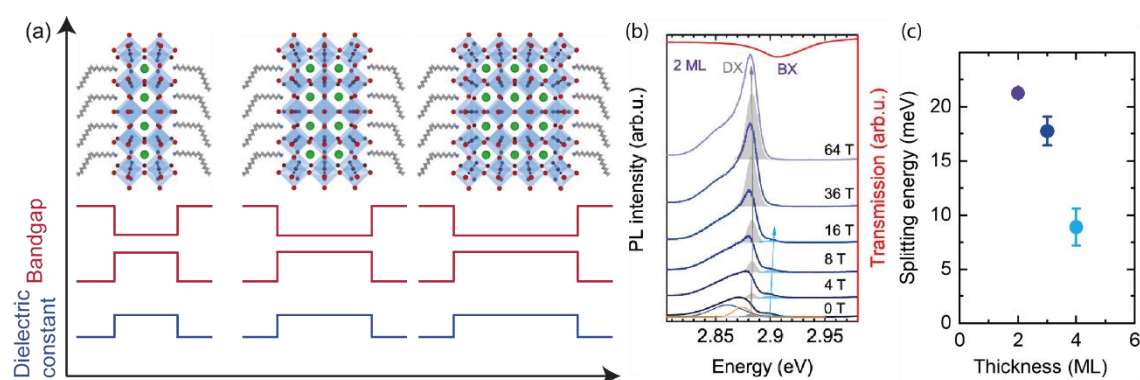


Figure 1. (a) Top: schematic of crystal structure of lead-halide perovskite nanoplatelet. Bottom: spatial dependence of the band gap and the dielectric constant. (b) Magneto-PL spectra of nanoplatelets. BX: bright exciton. DX: dark exciton. (c) Measured bright-dark splitting as a function of nanoplatelet thickness.

REFERENCES

- [1] F. Liu, et al.; *ACS Nano* **11** (2017) pp. 10373-10383.
- [2] S. Wang, et al.; *Nano Letters* **22** (2022) pp. 7011-7019.

First comparison of rhodium- and iron-doped InGaAs photoconductive THz emitters for continuous-wave terahertz emission

Chris Phong Van Nguyen^{1,2}, M. Deumer¹, S. Lauck¹, S. Breuer¹, L. Liebermeister¹,
B. Globisch^{1,2}, M. Schell^{1,2}, R. B. Kohlhaas¹

¹Fraunhofer Institute for Telecommunications, Heinrich Hertz Institute, Einsteinufer 37, 10587 Berlin, Germany

²Technische Universität Berlin, Institute for Solid State Physics, Hardenbergstraße 36, 10623 Berlin, Germany

Email: chris.phong.van.nguyen@hhi.fraunhofer.de

We present the first comparison of rhodium- and iron-doped InGaAs photoconductive antennas (PCA) for use as THz emitters for CW-THz emission. Iron (Fe) and rhodium (Rh) have already been used as dopants for PCAs in THz time-domain spectroscopy (TDS) systems. It was demonstrated that these PCAs offer record levels of emitted THz power and unprecedented responsivity in THz-TDS systems [1][2][3]. For CW-THz detectors, Fe-doped photoconductors have shown improved properties compared to low-temperature grown InGaAs, which are used in state-of-the-art CW detectors [4]. In this work, we conducted the first I-V measurements (Fig. 1a) and continuous wave (CW) THz measurements (Fig. 1b) on emitters, based on Rh-doped photoconductors, and compared them to Fe-doped photoconductors with the same antenna structure. However, the antenna structure, consisting of a stripline antenna with a 25 μm photoconductive gap, is designed for THz-TDS operation and is therefore not optimized for CW-THz operation. Nevertheless, we could show a preliminary qualitative comparison of these promising ultrafast photoconductors. We demonstrated broadband emission capability up to 4 THz and 3 THz bandwidth for Rh- and Fe-based emitters, respectively. We observed a higher peak dynamic range for Rh-based emitters. The I-V-characteristic for the Rh-antenna differed between THz-TDS and CW-THz operation, which hints at a saturation effect occurring in Rh-based emitters. These first measurements show that Rh-doped InGaAs is also a promising candidate for use in CW-THz PCA emitters and could possibly replace Fe as the best choice of dopant in InGaAs for CW-THz emission. A further investigation of these emitters with optimized antennas for CW-THz operation seems very promising.

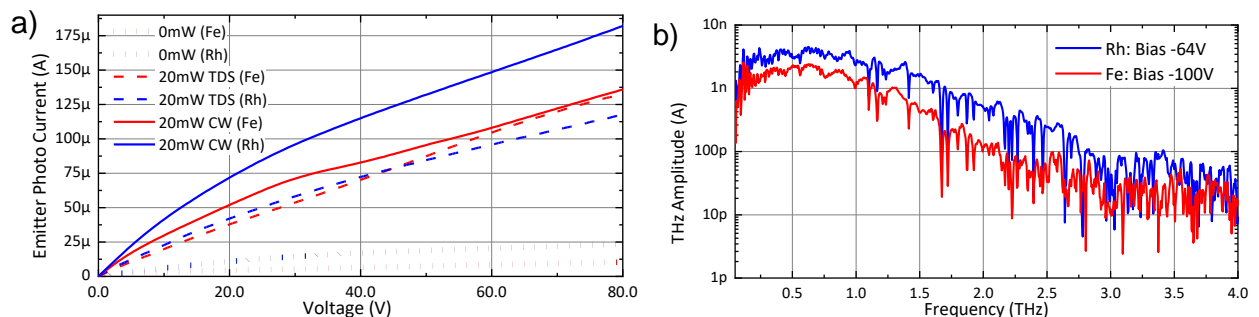


Fig. 1: Comparison of CW-THz emitters based on Fe- and Rh-doped InGaAs. a) I-V-characteristics of the emitter antennas, b) detected CW-THz spectra.

REFERENCES

- [1] B. Globisch et al., Appl. Phys. Lett. 121, 053102 (2017)
- [2] R. B. Kohlhaas et al., Appl. Phys. Lett. 114, 221103 (2019)
- [3] R. B. Kohlhaas et al., Appl. Phys. Lett. 117, 131105 (2020)
- [4] M. Deumer et al., Opt. Express 29, 41819-41826 (2021)

Broadband amplification of terahertz electromagnetic radiation from semiconductor superlattices under coherent phonon driving

A.Apostolakis^{1,2}, K.N.Alekseev^{2,5}, F.V.Kusmartsev^{2,4,5} and A.G.Balanov²

¹*Department of Condensed Matter Theory, Institute of Physics CAS, Na Slovance 1999/2, 182 21 Prague, Czech Republic*

²*Department of Physics, Loughborough University, Loughborough LE11 3TU, United Kingdom*

³*College of Art and Science, Khalifa University, PO Box 127788, Abu Dhabi, United Arab Emirates*

⁴*Microsystem and Terahertz Research Center, Chengdu, 610200, People's Republic of China*

⁵*Center for Physical Sciences and Technology, Vilnius LT-10257, Lithuania*

Miniaturized devices emitting in key spectral windows such as the GHz-THz range are currently in the core of scientific research due to the increasing number of demanding metrological and sensing applications.

Quantum semiconductor superlattices (SLs) by virtue of their nonlinear and high-frequency properties may serve as such active medium to electromagnetic signals which was further confirmed by recent experimental studies showing that the parametric resonance in its narrow energy band can be harnessed for parametric amplification and generation [1].

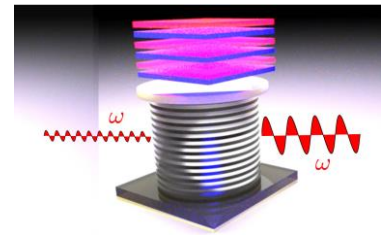


Fig. 1 Schematic diagram of a SL driven by a phonon plane-wave in which the interaction of the electrons with a high-frequency (ω) electromagnetic wave can result in its amplification.

Here we discuss the manipulation of electromagnetic waves by the application of superluminal Doppler effects [2] and nonlinear mechanisms [3, 4] stemming from the phonon driven electron transport in SL minibands (Fig. 1). Within this latter context, the use of the stable gain (SG) approach allows to overcome limitations by the NL-criterion [5], and in such way that heavy doped SLs would not pose the risk of domain formation. Large concentration of carriers, in turn, can result in large magnitude of gain at THz frequencies.

REFERENCES

- [1] V. Čížas et al.; *Phys. Rev. Lett.* **128.23** (2022): 236802.
- [2] A. Apostolakis, A. G. Balanov, F. V. Kusmartsev, K. N. Alekseev; *Phys. Rev. B*-accepted paper (2022): arXiv:2204.04144.
- [3] A. Apostolakis, M. K. Awodele, K. N. Alekseev, F. V. Kusmartsev, A. G. Balanov; *Phys. Rev. E* **95(6)** (2017): 062203.
- [4] Y. M. Gal'perin, V. L. Gurevich, V. I Kozub; *Sov. Phys.-Uspekhi* **22(5)** (1979): 352.
- [5] H. Kroemer; arXiv preprint con-mat/0009311 (2000).

Section 3

ULTRAFAST AND THZ PHENOMENA

S3-I1

Invited talk by Otsuji Lab.

Taiichi Otsuji

Tohoku University, Japan



Towards on-chip plasmonics amplifiers of THz radiation – ERC – advanced project

Wojciech Knap

CENTERA Laboratories, Institute of High Pressure Physics PAS, Warsaw 01-142, Poland

Email: wojciech.knap@unipress.waw.pl

One of the major nowadays scientific challenges lying at the border between physics and electronics, is to find solid state systems that can amplify and generate terahertz frequencies. Around 30 years ago, a new direction in solid state physics and electronics opened with the arrival of plasma-wave electronics. M. Dyakonov and M. Shur theoretically predicted that THz radiation can be rectified/detected by plasma nonlinearities and the current in the nanometer field-effect transistors could lead to the excitation of plasma oscillations. The detection part of the “plasmonics promise” was proven and nowadays THz plasmonic detectors arrays are widely used. In the case of emitters, the task appeared much more complicated.

Only very recently, room temperature, current driven amplification of the incoming THz radiation in graphene grating gate structures with an innovative double grating gate geometry has been shown [1]. These results indicate that, existing model of plasmonic systems should be reconsidered and that use of the new 2D materials or their heterojunctions with semiconductors, once processed with innovative geometries may lead “Towards on-chip plasmonics amplifiers of THz radiation”.

Therefore the ground-breaking objectives of the recently awarded ERC ADVANCED TERAPLASM that will be realized in CENTERA LABS (IHHP PAN 2023-2028) are : i) to understand the physics of the observed THz plasmonic amplification in graphene devices ii) investigate properties of new plasmonic 2D systems like GaN/AlGaN, Hg/HgCdTe and ii) reexamine all existing THz plasmonic amplification mechanisms/theories considering new/ innovative geometries.

By extensive technological, spectroscopic and theoretical research TERAPLASM project will tend to answer 30 years old basic physics and electronics question, about the possibility of realization of on-chip plasmonics amplifiers of THz radiation, important also for society through potential applications of THz radiation in biosensing, security screening as well as for fast wireless telecommunication.

REFERENCES

- [1] Stephane Boubanga-Tombet, Wojciech Knap, Deepika Yadav, Akira Satou, Dmytro B. But, Vyacheslav V. Popov, Ilya V. Gorbenko, Valentin Kachorovskii, and Taiichi Otsuji Room, Temperature Amplification of Terahertz Radiation by Grating-Gate Graphene Structures, Phys. Rev. X 10, 031004 (2020)

Section 4

QUANTUM OPTICS

Graphene based devices for terahertz radiation detection and beyond

Georgy Fedorov

*Institute of Photonics, Department of Physics and Mathematics, University of Eastern Finland,
Joensuu, Finland*

Email: georgy.fedorov@uef.fi.

Graphene has several advantages as a material for detectors of terahertz radiations. These include but are not limited to relatively high mobility, tunability of properties by electrostatic gating and geometric control of the band structure. Graphene has also been proved to support long-living plasma excitations that significantly enhance the range of optoelectronic applications of graphene in terahertz and mid-infrared range.

In this talk I will present several graphene-based detector configurations and show how plasma waves in the graphene channel affect their photoresponse. In particular I will discuss plasmon resonance in a 6-micron long channel formed by a boron-nitride (BN) incapsulated double-layer graphene. I will show that the observed features can be used for analysis of the single-particle spectrum.

Nex I will discuss how plasmonic effects can be unveiled in devices based on graphene grown on a metallic surface by chemical vapor deposition (CVD) and transferred onto a dielectric substrate. Until recently it was generally believed that such graphene has too small mobility for any observable plasmonic effect. Nevertheless, our recent works prove that it is not the case [2, 3]. The data I will present in this talk is interpreted as a fingerprint of plasmon interference inside graphene channel with a length of few microns.

Finally I will report on how tunneling in graphene channel can give rise to strong enhancement of the terahertz detector photo response [4].

REFERENCES

- [1] D. Bandurin, et al, *Nature Communications*, **9** (2018), p 5392
- [2] I A Gayduchenko, et al., *Nanotechnology*, **29** (2018), p 245204.
- [3] Y. Matyushkin, et al., *Nano Letters*, **20** (2020), pp 7296-7303.
- [4] I. Gayduchenko, *Nature Communications* **12**, (2021) p 543.

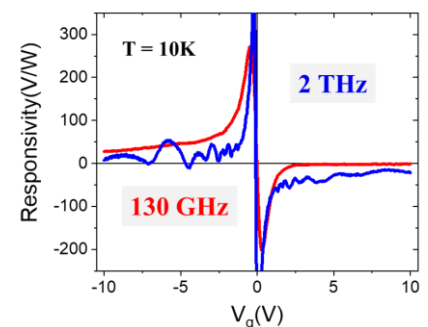


Fig. 1 Illustration of plasmonic resonance effect on the photo response of a by-layer graphene based field-effect transistor [1].

Quantum sensing enabled by spin qubits in diamond

Fedor Jelezko¹

¹ *Institute of Quantum Optics, Ulm University, Germany.*
fedor.jelezko@uni-ulm.de.

Single nitrogen vacancy (NV) color centers in diamond currently have sufficient sensitivity for detecting single external nuclear spins and resolve their position within a few angstroms. The ability to bring the sensor close to biomolecules by implantation of single NV centers and attachment of proteins to the surface of diamond enabled the first proof of principle demonstration of proteins labeled by paramagnetic markers and label-free detection of the signal from a single protein. Single-molecule nuclear magnetic resonance (NMR) experiments open the way towards unraveling dynamics and structure of single biomolecules. However, for that purpose, NV magnetometers must reach performance comparable to that of conventional solution state NMR. We will discuss new techniques allowing to combine high spectral resolution and sensitivity in nanoscale NMR. The ability to sense nuclear spins by NV centers also enables the transfer of polarization from optically polarized spins of NV centers to external nuclear spins. Such diamond based techniques for dynamic nuclear spin polarization are very promising for the enhancement of sensitivity of conventional MRI imaging.

Topology for Electrons in Solids, Photons and Ultracold Atoms

Gediminas Juzeliūnas

*Institute of Theoretical Physics and Astronomy, Vilnius University,
Saulėtekio 3, LT-10257, Vilnius, Lithuania.*

Since the discovery of the quantum Hall effect (QHE) in the early 80s [1] it became clear that the simple division of solids into band insulators and conductors is not complete. In QHE a strong magnetic field confines the bulk motion of electrons in metals making them to move in localised cyclotron orbitals. On the other hand, at the surface electrons undergo skipping cyclotron orbits. This leads to chiral motion of electrons around the edges and thus formation of delocalized surface states. In this way, the two-dimensional metal affected by a strong magnetic field is an insulator in the bulk, whereas it conducts electrons along the surface. Furthermore QHE the chiral edge current appears to be quantised and linked to a certain topological invariant of the bulk bands known as the Chern number [2,3].

Over the last couple of decades it was realised that the external magnetic field is not a necessary element for an insulator to have robust conducting chiral edge states. Instead, the crucial ingredient is nontrivial topology of occupied bands. These systems are generally called the topological insulators [3]. In addition to electrons in solids, the topological insulators can be successfully simulated using ultracold atoms [4] and photonic systems [5].

In the present talk we will present a general overview of the topological insulators for electrons in solids, as well as extension of this concept to other systems including ultracold atoms and photonic systems. We will also present some recent developments on topological effects for ultracold atoms.

REFERENCES

- [1] K. von Klitzing, G. Dorda, and M. Pepper. Phys. Rev. Lett. 45, 494 (1980).
- [2] X.-L. Qi and S.-C. Zhang. Rev. Mod. Phys. 83, 1057-1110 (2011).
- [3] M. Kolodrubetz, D. Sels, P. Mehta and A. Polkovnikov, Phys. Rep. 697, 1 (2017).
- [4] N. Goldman, G. Juzeliūnas, P. Öhberg and I. B. Spielman. Rep. Prog. Phys. 77 126401 (2014).
- [5] T. Ozawa et al. Rev. Mod. Phys. 91, 015006 (2019).

Nonequilibrium carrier dynamics in Landau quantized graphene and mercury cadmium telluride

Stephan Winnerl

*Institute of Ion Beam Physics and Materials Research, Helmholtz-Zentrum Dresden-Rossendorf,
Bautzner landstrasse 400, D-01328, Dresden, Germany
Email: s.winnerl@hzdr.de*

The narrow-gap semiconductor mercury cadmium telluride (MCT) is used for decades as a material for applications in the mid- and far infrared, in particular for detectors. Graphene, on the other hand, has been explored in recent years regarding THz detection, modulation, generation and harmonic generation [1]. In magnetic fields, both materials exhibit strongly non-equidistant Landau-level (LL) systems. Here we present an overview that sheds light into the carrier dynamics of in Landau-quantized Dirac electrons in graphene and Kane electrons in MCT. The non-equidistant Landau-ladder makes these materials highly attractive for realizing the old dream of the semiconductor physics community to fabricate a Landau-level laser. For a recent review on this topic, see Ref. [2]. In such a laser, stimulated emission is achieved between a pair of Landau levels and the emission wavelength can be tuned by the strength of the magnetic field. In graphene, we found evidence for strong Auger scattering for the lowest allowed transitions $LL_{-1} \rightarrow LL_0$ and $LL_0 \rightarrow LL_1$ [3]. These energetically degenerate transitions can be distinguished by applying circularly polarized radiation of opposite polarization. In this configuration, Auger scattering can cause depletion of the LL_0 level even though it is optically pumped at the same time. Recently, we have investigated the $LL_{-2} \rightarrow LL_{-1}$ and $LL_{-1} \rightarrow LL_{-2}$ transition under strong optical pumping. This transition is a candidate for the lasing transition for a Landau-level laser. We observed non-equilibrium carrier distributions by selective pumping before thermalization occurred. MCT, on the other hand, is even more attractive because of much longer relaxation times [4]. They are on the ns scale while in graphene thermalization occurs on a timescale of a few ps. The reason for the longer timescale is the different Landau ladder due to spin splitting.

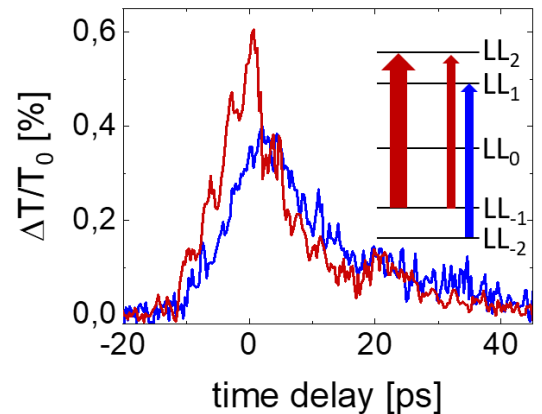


Fig. 1: Pump-induced transmission of graphene for copolarized and counterpolarized excitation with circularly polarized radiation and Landau-level scheme.

REFERENCES

- [1] M. Mittendorff, S. Winnerl, and T.E. Murphy, *Advanced Optical Materials*, **9** 2001500 (2021).
- [2] E. Gornik, G. Strasser und K. Unterrainer, *Nature Photonics* **15**, 875 (2021).
- [3] M. Mittendorff, F. Wendler, E. Malic, A. Knorr, M. Orlita, M. Potemski, C. Berger, W. A. de Heer, H. Schneider, M. Helm und S. Winnerl, *Nature Physics* **11**, (2015).
- [4] D. B. But, M. Mittendorff, C. Consejo, F. Teppe, N. N. Mikhailov, S. A. Dvoretzskii, C. Faugeras, S. Winnerl, M. Helm, W. Knap, M. Potemski und M. Orlita, *Nature Photonics* **13**, 783 (2019).

Special session



**UNITED LITHUANIAN-
POLISH WORKSHOP
“LUBLIN READINGS”
DEDICATED TO EXPRESS
SOLIDARITY WITH
UKRAINIAN SCIENTISTS**

Historical lecture at “Lublin Readings”: Polish-Lithuanian Commonwealth and Ukraine

Rimvydas Petrauskas

Rector of Vilnius University, Lithuania



Monitoring the charge-carrier occupied density-of-states in disordered organic semiconductors under non-equilibrium conditions

Andrei Stankevych^{1,2}, Rishabh Saxena², Heinz Bässler², Anna Köhler² and
Andrey Kadashchuk^{1,2}

¹*Photoactivity department, Institute of Physics of NAS of Ukraine, 03028 Kyiv, Ukraine*

²*Soft Matter Optoelectronics and Bavarian Polymer Institute, University of Bayreuth, 95447
Bayreuth, Germany*

Email: kadash@iop.kiev.ua and Andriy.Kadashchuk@uni-bayreuth.de

In disordered organic semiconductors, charge transport involves energetic relaxation in a broad distribution of localized states, usually assumed to be well-described by a Gaussian distribution characterized by a width σ_{DOS} . Under thermal equilibrium conditions, charges that are injected or photogenerated at a random energy site in the available density-of-states (DOS) proceed by a sequence of energetically downward or upward hops to form an occupied-density-of-states (ODOS), which is placed around an equilibrium energy ($\varepsilon_{eq} = -\sigma_{DOS}^2/k_B T$) below the centre of the DOS with a width σ_{ODOS} equal to the width of the DOS (σ_{DOS}). However, in very thin organic semiconductor layers relevant to organic optoelectronic devices or/and at low temperatures, charge-carriers are not able to reach the thermal equilibrium transport regime prior to being extracted. Therefore, the ODOS under non-equilibrium transport are expected to differ from that under equilibrium condition.

The dynamics of charge carriers in disordered organic semiconductors is inherently difficult to probe by spectroscopic methods. In the present study, we demonstrate that thermally-stimulated luminescence (TSL) technique can be used to determine the low-temperature ODOS distribution for charge-carriers. Another approach to probe charge energy relaxation are kinetic Monte-Carlo (kMC) simulations. Here we use both techniques to monitor the ODOS distribution of charges at low temperatures. We find that the charge dynamics is frustrated, yet this frustration can be overcome in TSL by using an infrared (IR) push pulse, and in kMC by a long simulation time that allows for long-range hopping transitions. Applying the IR-push TSL to pristine amorphous films of 18 commonly used low molecular weight organic light emitting diode (OLED) materials, we find that the width (σ_{ODOS}) of the ODOS universally amounts to about 2/3 of the available DOS. This implies a significant narrowing of the ODOS distribution formed at low temperatures compared to the width of the DOS. The same result is obtained in kMC simulations that consider spatial correlations between the site energies for charge carriers. Without the explicit consideration of the energetic correlations, the experimental value cannot be reproduced, which testifies to the importance of energy correlation effects for charges.

The authors acknowledge funding through the EU Marie Skłodowska-Curie ITN TADFlife grant (GA no. 812872) and support by VW Foundation.

Imaging of the human retina and cornea *in vivo* with high-resolution ultrafast optical coherence tomography

Egidijus Auksorius¹, Dawid Borycki², Piotr Wegrzyn², Kamil Lizewski², Ieva Zickiene¹, Karolis Adomavicius¹, Slawomir Tomczewski² and Maciej Wojtkowski²

¹Center for Physical Sciences and Technology (FTMC), Vilnius, Lithuania.

²International Center for Translational Eye Research (ICTER), Warsaw, Poland

Email: egidijus.auksorius@ftmc.lt

Optical Coherence Tomography (OCT) has become a standard of care for diagnosing and monitoring of the human eye diseases *in vivo*.

Recently, to speed up OCT imaging, Fourier-domain Full-Field OCT (FF-FD-OCT) has been introduced that uses an ultrafast camera and a swept laser source [1].

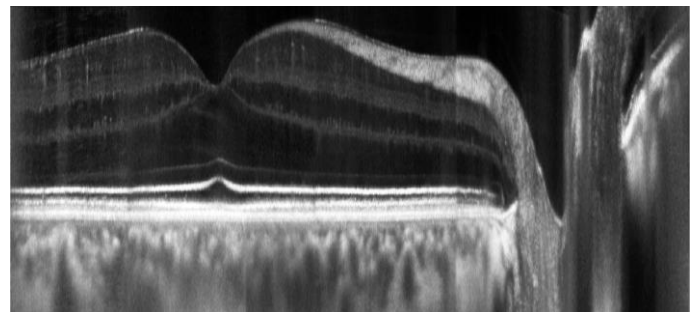


Fig. 1 Cross-sectional image of the human retina.

We have shown that destroying spatial coherence of the swept source laser enables imaging of the human cornea *in vivo* [2], as it prevents laser focusing on the retina. Reducing coherence also allows decreasing crosstalk noise and speckle size when imaging retina [3], which leads to deeper imaging with this technology.

We have further optimized the system by employing a multimode fiber for crosstalk reduction [4, 5] and by implementing a fast preview add-on [6] that enabled acquisition of high-resolution, high-contrast OCT images deep in retina [4], as shown in Fig. 1.

REFERENCES

- [1] D. Hillmann *et al.*, *Scientific Reports*, vol. 6, Art no. 35209, 2016.
- [2] E. Auksorius *et al.*, *Biomed. Opt. Express*, vol. 11, no. 5, pp. 2849-2865, 2020.
- [3] E. Auksorius, D. Borycki, and M. Wojtkowski, *Biomed. Opt. Express*, vol. 10, no. 12, pp. 6390-6407, 2019.
- [4] E. Auksorius *et al.*, *Opt. Lett.*, vol. 47, no. 3, 2022.
- [5] E. Auksorius, D. Borycki, and M. Wojtkowski, *Opt. Lett.*, vol. 46, no. 6, pp. 1413-1416, 2021.
- [6] E. Auksorius, *Opt. Lett.*, vol. 46, no. 18, pp. 4478-4481, 2021.

Low frequency noise as a quality control of novel AlGaIn/GaN devices

Maksym Dub¹, Dmytro B. But¹, Justinas Jorudas², Pavlo Sai¹, Grzegorz Cywiński¹,
Irmantas Kasalynas², Sergey L. Rumyantsev¹ and Wojciech Knap¹

¹*CENTERA Laboratories, Institute of High Pressure Physics PAS, Warsaw 01-142, Poland.*

²*Center for Physical Sciences and Technology (FTMC), Saulėtekio 3, 10257 Vilnius, Lithuania*

Email: mdub@unipress.waw.pl

GaN/AlGaIn high electron mobility field effect transistors (HEMTs) are already used for high power and high frequency applications. GaN/AlGaIn HEMTs can operate within an extremely large temperature range from the lowest possible temperatures up to several hundred degrees Celsius. High bandgap, high electron saturation velocity, extremely high two dimensional concentration on the AlGaIn/GaN interface make this system to be very promising for terahertz applications as well. When these devices are used as oscillators or mixers their low frequency noise is one of the major factors determining the phase noise characteristics. Low frequency noise measurements are also a powerful tool to study impurity and defects in semiconductor structures and to diagnose quality and reliability of contacts and overall semiconductor devices.

We studied the performance and noise properties of AlGaIn HEMTs of several new designs. First, we report experimental results on the low-frequency noise in GaN/AlGaIn transistors fabricated under different conditions and evaluate different methods to extract the effective trap density using the McWhorter model [1].

Second, we studied high-voltage, noise, and radio frequency (RF) performances of AlGaIn/GaN HEMTs fabricated on silicon carbide (SiC) devices without any GaN buffer [2]. Such a GaN–SiC hybrid material was developed in order to improve thermal management and to reduce trapping effects.

Third, AlGaIn/GaN HEMTs with two layers of two dimensional electron gas and a back gate were fabricated and studied experimentally [3]. The back gate allowed reducing the subthreshold leakage current, improving the subthreshold slope and adjusting the threshold voltage. At a certain back gate voltage, transistors operated as normally-off devices. The low frequency noise measurements indicated identical noise properties and the same trap density responsible for noise when the transistors were controlled by either top or back gates.

Fourth, electrical and noise properties of graphene gate AlGaIn/GaN HEMTs were studied experimentally. It was found that graphene on AlGaIn forms a high-quality Schottky barrier [4]. These devices demonstrated ~8 order of magnitude on/off ratio, subthreshold slope of ~1.3, and low subthreshold current in the sub-picoamperes range.

The effective trap density responsible for the low-frequency noise was found within the range of $(1-10) \times 10^{19} \text{ eV}^{-1} \text{ cm}^{-3}$ for all studied devices. These values are of the same order of magnitude as reported earlier in regular AlGaIn/GaN transistors. We found also that contacts do not contribute much to noise in all studied devices indicating their good quality.

These results confirms the perspective of new designs of AlGaIn/GaN HEMTs and proves the effectiveness of the noise studies to asses the quality of the devices and materials.

REFERENCES

- [1] A. L. McWhorter, Semiconductor surface physics, Philadelphia, PA, (1957) pp. 207-228 [2]
J. Jorudas, et al.; *Micromachines*, 11 (2020), p. 1131.
- [3] M. Dub, et. al.; *Micromachines*, 12 (2021) p. 721. [4]
M. Dub, et. al.; *Materials*, 13 (2020) p. 4140.

Measurement of short pulsed magnetic fields

Voitech Stankevič^{*1,2}, Nerija Žurauskienė^{1, 2}, Skirmantas Keršulis¹, Justas Dilys¹, Vytautas Bleizgys¹, Vilius Vertelis¹, Mindaugas Viliūnas³, Valentina Plaušinitienė^{1,4}, Saulius Balevičius¹

¹*Department of Functional Materials and Electronics, Center for Physical Sciences and Technology, Sauletekio ave. 3, LT-10257 Vilnius, Lithuania,*

²*Faculty of Electronics, Vilnius Gediminas Technical University, Naugarduko 41, LT-03227 Vilnius, Lithuania*

³*Institute of Chemical Physics, Faculty of Physics, Vilnius University, Saulėtekio ave. 3, LT-10257 Vilnius, Lithuania*

⁴*Institute of Chemistry, Faculty of Chemistry and Geosciences, Vilnius University, Naugarduko 24, LT-03225 Vilnius, Lithuania*

Recently, it was demonstrated that high amplitude pulsed magnetic fields could be measured using novel CMR-B-scalar sensors based on the colossal magnetoresistance effect (CMR) of polycrystalline manganites [1-3]. To measure short magnetic field pulses such sensors need to be fast enough to measure magnetic fields of microsecond duration. Our previous study shows that changing the chemical composition of manganites allows to reduce magnetic memory effects and magnetization relaxation in different range of temperatures [4, 5]. However, in the real sensors the electromotive force (EMF) induced in the measuring circuit causes some measurement problems. The output signal of these sensors contains two components: the voltage (current) change caused by the sensor's magnetoresistance, and the parasitic voltage caused by the EMF induced in the loop of connecting wires. This problem can be partially solved by using a twisted pair of wires or an additional compensation loop [6]. However, for the measurement of magnetic field pulses with high amplitudes and durations of microseconds, this task becomes difficult.

In this study, we propose a magnetic field meter that compensates EMF using the bipolar pulse supply of the CMR-B-Scalar magnetic field sensor. The proposed meter consists of a high-frequency bipolar pulse power generator and differential analog to digital converter (ADC). A half-bridge circuit that generates rectangular shape pulses with a 10 MHz frequency is used as the main power source for the CMR sensor. The ADC, which is synchronized with the pulse generator, records the peak-to-peak voltage at a frequency of 25 MHz. The output data of ADC are processed by a microprocessor which subtracts two neighboring samples (voltage of positive sign and negative sign). As a result, the EMF is eliminated from the measured signal and only the voltage change caused by the magnetic field change is measured. Such meter allows measurement of fast pulsed magnetic fields.

REFERENCES

- [1] T. Stankevič, L. Medišauskas, V. Stankevič, S. Balevičius, N. Žurauskienė, O. Liebfried, M. Schneider, Rev. Sci. Instrum. 85 (2014) 044704.
- [2] T.L. Haran, R.B. Hoffman, S.E. Lane, IEEE Trans. Plasma Sci. 41 (2013) 1526–1532.
- [3] S. Balevičius, N. Žurauskienė, V. Stankevič, S. Keršulis, V. Plaušinitienė, A. Abrutis, S. Zherlitsyn, T. Herrmannsdörfer, J. Wosnitza, F. Wolff-Fabris, Appl. Phys. Lett. 101 (2012) 092407.
- [4] N. Žurauskienė, D. Pavičionis, J. Klimantavicius, S. Balevičius, V. Stankevič, R. Vasiliauskas, V. Plaušinitienė, A. Abrutis, M. Skapas and R. Juškešas, IEEE Trans. Plasma Sci. 45 (2017) 2773–2779.
- [5] N. Žurauskienė, V. Rudokas, S. Keršulis, V. Stankevič, D. Pavičionis, V. Plaušinitienė, M. Vagner, S. Balevičius, J. Magn. Mater. 539 (2021) 168340.
- [6] S. Balevičius, N. Žurauskienė, V. Stankevič, T. Stankevič, J. Novickij, and M. Schneider, IEEE Trans. Plasma Sci. 41 (2013) 2885–2889.

Optimization of 2D plasmons excitation in grating-gated AlGaIn/GaN high electron mobility transistor structures

Daniil Pashnev¹, Roman M. Balagula¹, Maksym Dub², Maciej Sakowicz², Justinas Jorudas¹, Liudvikas Subačius¹, Pavlo Sai², Grzegorz Cywinski² and Irmantas Kašalynas¹

¹THz photonics laboratory, Center for Physical Sciences and Technology, Vilnius, Lithuania.

²CENTERA, Institute of High Pressure Physics PAS, Warsaw, Poland.

Email: daniil.pashnev@ftmc.lt.

An electrical strength, high temperature, and chemical stability of III-nitride heterostructures are attractive features realized in the high electron mobility transistor (HEMT) with high-density two-dimensional electron gas (2DEG) conductive channel [1]. One of many applications of HEMTs were found in electrically-driven tunable-frequency terahertz (THz) oscillators based on 2D plasmons excitation in grating-gated AlGaIn/GaN heterostructures [2]. In this work, the optimal parameters for 2D plasmon excitation in grating-gated AlGaIn/GaN HEMT structures were investigated.

The plasmonic samples were fabricated by positioning periodic gate electrodes on the top surface over an area of about $2 \times 2 \text{ mm}^2$ between the source and drain terminals of HEMT. Three gratings with a filling factor of 50 % and periods of 600 nm, 800 nm, and 1000 nm were investigated. Electrical pulses, the duration of which varied from 100 ns up to 100 ms, were applied to the lateral source and drain terminals monitoring the current and voltage traces on oscilloscope, while the integral THz radiation power was measured with a fast LHe-cooled bolometric detector and lock-in amplifier in order to obtain current-voltage-power characteristics of the samples. The optimal operation for 2D plasmon emission was found at applied voltages ranging below the saturation of current and radiation power characteristics.

The absorption and emission spectra of the plasmonic samples were measured by means of THz spectroscopy. The emission spectra revealed well-defined 2D plasmon peaks with the same positions as those obtained from measured and numerically calculated transmission spectra [3]. The shape and position of 2D plasmon peaks in emission spectra were found at different polarities and amplitudes of the bias voltage. The Rabi splitting of the fundamental plasmon mode was observed in the emission spectra of the plasmonic samples demonstrating large splitting values up to 345 GHz.

The work was supported by Research Council of Lithuania through the “T-HP” project (grant No.01.2.2-LMT-K-718-03-0096).

REFERENCES

- [1] H. Morkoç, *Nitride Semiconductor Devices: Principles and Simulation Properties of Group-IV, III-V and II-VI Semiconductors Nitride Semiconductors* (2008).
- [2] M. S. Shur, *IEEE Sens. J.* **21**, 12752 (2021).
- [3] D. Pashnev et al., *Appl. Phys. Lett.* **117**, 051105 (2020).

Ab initio modeling of the photoionization of negatively charged NV centers in diamond

Lukas Razinkovas¹, Marek Maciaszek^{1,2}, Friedemann Reinhard³, Marcus W. Doherty⁴, and Audrius Alkauskas^{1,5}

¹*Center for Physical Sciences and Technology (FTMC), Vilnius LT-10257, Lithuania*

²*Faculty of Physics, Warsaw University of Technology, Koszykowa 75, 00-662 Warsaw, Poland*

³*Institute of Physics, University of Rostock, 18059 Rostock, Germany*

⁴*Laser Physics Centre, Research School of Physics, Australian National University, Australian Capital Territory 2601, Australia*

⁵*Department of Physics, Kaunas University of Technology (KTU), Kaunas LT-51368, Lithuania*

Email: marek.maciaszek@ftmc.lt

In this contribution we present theoretical analysis and *ab initio* calculations of the photoionization processes of the negatively charged nitrogen-vacancy (NV) center in diamond. Photoionization thresholds and cross-sections are determined for the photoionization from the triplet ground state 3A_2 , triplet excited state 3E , and singlet state 1E . Moreover, the stimulated emission from 3E and intradefect absorption $^3A_2 \rightarrow ^3E$ are also considered. Technical difficulties related to calculations of cross-sections are discussed (necessity of using very dense k-meshes; unfolding technique overcoming the problem of the artificial periodicity of the supercell approach introducing the minigaps in the conduction band). Presented results provide a comprehensive picture of the photoionization mechanisms of NV^- , which can serve as a “map” for designing future optical experiments on NV centers. Finally, we discuss obtained results in the light of existing experimental data: we propose an explanation of the signal observed in ESR experiments attributed to the 4A_2 state, and we interpret data on the wavelengths corresponding to the efficient photoionization obtained using dual-beam excitation technique.

Dissipative parametric generation in a biased superlattice: the case of small signal gain

Vladislovas Čižas¹, Liudvikas Subačius¹, Natalia Alexeeva¹, Dalius Seliuta¹,
Timo Hyart^{2,3}, Klaus Köhler⁴, Kirill Alekseev^{1,5}, and Gintaras Valušis^{1,6}

¹Center for Physical Sciences and Technology, Saulėtekio Ave. 3, LT-10257, Vilnius, Lithuania.

²International Research Centre MagTop, PAS, Lotnikow Ave. 32/46, Warsaw, Poland.

³Department of Applied Physics, Aalto University, 0076 Aalto, Espoo, Finland.

⁴Fraunhofer-Institut für Angewandte Festkörperphysik, Tullastrasse 72, Freiburg, Germany.

⁵Department of Physics, Loughborough University, Loughborough LE11 3TU, United Kingdom.

⁶Institute of Photonics and Nanotechnology, Vilnius University, Saulėtekio 3, Vilnius, Lithuania.

Email: vladislovas.cizas@ftmc.lt.

Semiconductor superlattices are considered as an engaging structure for the investigation of high-frequency processes [1,2]. One of the possible fields of particular interest is their ability to serve as a platform for the development of small, powerful, and efficient THz frequency range emitters.

Parametric gain in semiconductor superlattices was theoretically predicted more than 3 decades ago exploiting feature of the structure to be set into a negative differential mobility regime under specific biasing conditions. It was shown that the amplification effect can be observed within a wide frequency range, however, there was no experimental evidence of the effect up to now.

In this communication, we present the first experimental demonstration of the dissipative parametric generation in AC-pumped and biased GaAs/AlGaAs superlattice at room temperature [3]. Multifrequency spectra was recorded exhibiting both degenerate and nondegenerate parametric gain. Employing small-signal gain model to describe the conditions for the generation multiphoton processes occurring simultaneously are resolved and discussed. Large signal gain case – it manifests itself in the case when the probing field is amplified high enough and cannot thus be further neglected -- is considered as well.

REFERENCES

- [1] V.G. Lyssenko, G. Valušis, F. Löser, T. Hasche, and K. Leo; *PRL* **79** (1997), pp. 302-304.
- [2] A. Sibille, J.F. Palmier, F. Mollot, H. Wang, and J.C. Esnault; *PRB* **37** (1989), pp. 6272.
- [3] V. Čižas, L. Subačius, N.V. Alexeeva, D. Seliuta, T. Hyart, K. Köhler, K.N. Alekseev, G. Valušis; *PRL* **128** (2022), pp. 236802.

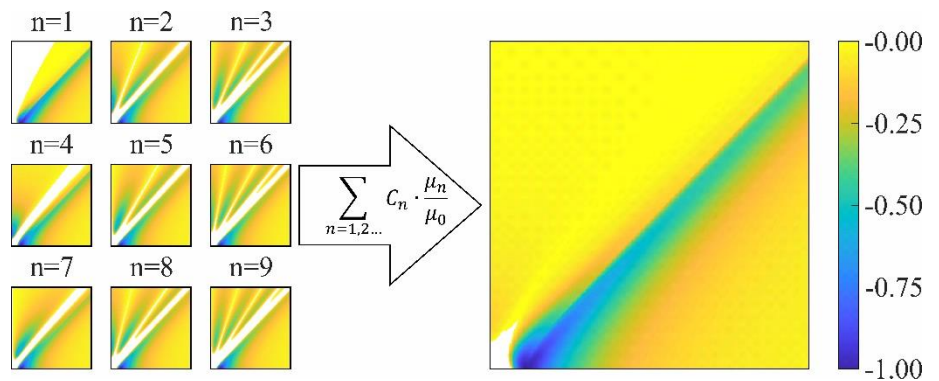


Fig. 1 Sketch displaying the process of single multiphoton parametric gain profile superposition to illustrate simultaneity of single multiphoton generation/amplification processes for the case of small-signal gain model.

Interplay of THz plasmon modes in AlGaIn/GaN grating-gate structures

P. Sai¹, M. Dub¹, D. B. But¹, Yu. Ivonyak¹, G. Cywinski¹, M. Słowikowski², M. Filipiak², M. Sakowicz¹, K. Stelmaszczyk¹, S. Rumyantsev¹, Yu. M. Liaschuk³, V.V. Korotyeyev³, W. Knap¹

¹ CENTERA Laboratories, Institute of High Pressure Physics PAS, Warsaw, Poland.

²Centre for Advanced Materials and Technologies, Warsaw University of Technology, Warsaw, Poland.

³V.Ye. Lashkaryov Institute of Semiconductor Physics (ISP), NASU, Kyiv, 03028, Ukraine
Email: psai@unipress.waw.pl

We have performed THz Fourier-spectroscopy measurements and electrodynamic simulations of the low-temperature (10 K) transmission spectra of large area grating-gated field-effect transistors based on AlGaIn/GaN quantum-well heterostructure in the spectral range of 0.50-3.25 THz. The detailed description of the similar structures and the fabrication process are described in Ref.[1]. In this work we found that transmission spectra possess multiple resonances with an essential variation of their position and sharpness under applied gate-to-channel voltages in the range from +0.5 V to -10 V (Fig.1). In the range of sub-threshold voltages (from +0.5 V to -2 V), we observed multiple resonant structures of the transmission spectra that attributes to the excitation of 2D-plasmons modes of different order in 2DEG channel with a weakly modulation of lateral profile of electron concentration. In the range of upper-threshold voltages (< -3.5 V) total depletion of the gated region of 2DEG occurs and specific 2DEG-strip grating is formed. As a result, we observed a single resonance attributed to the excitation of grating mode in the 2DEG-strip grating. We demonstrated that an increase in the voltage amplitude leads to the essential blue shift of this resonance. It was explained by the effect of the additional depletion of the ungated region. We suggest that the presented results can be important for a deeper understanding of THz plasma physics and the development of all-electrically tuning devices for THz optoelectronics.

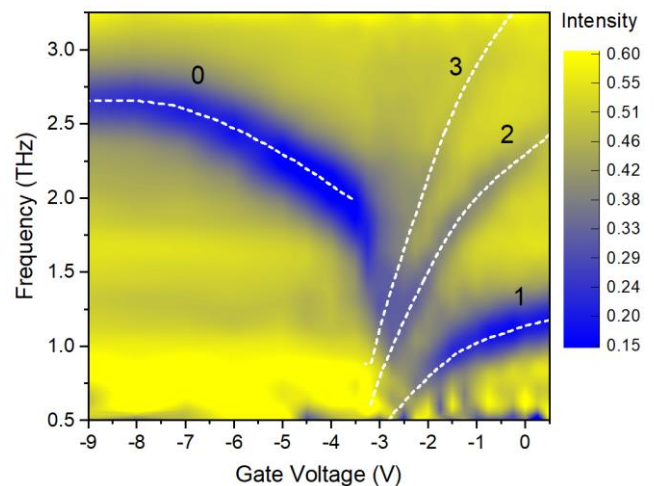


Fig. 1. Experimental mapping of the transmission spectrum of AlGaIn/GaN grating-gate plasmonic structures with 1.5 μ m grating period. Dashed curves are calculated and they show the positions of the minima of the first three 2D-plasmon resonances (marked as 1,2,3) and strip-grating resonance (marked by 0).

REFERENCES

[1] Sai, P., et al. Physical Review B, 104(4), 045301.

Section 6

THZ TECHNOLOGIES

Terahertz technology for remote sensing of the Earth's atmosphere

Heinz-Wilhelm Hübers

German Aerospace Center, Berlin, Germany



High-harmonic generation in p-doped Si pumped with intense terahertz pulses

Hartmut G. Roskos

Goethe-university, Frankfurt/M, Germany



S6-I3

Local and non-local terahertz measurements in the near field

Daniel Mittleman

Brown University, USA



Wireless telecommunications towards Beyond 5G/6G

Tadao Nagatsuma

Osaka University, Japan



Excitation of magnetic polaritons in n -GaAs/GaAs/metal structure in the terahertz range

I. Grigelionis¹, V. Čižas¹, K. Ikamas², V. Jakštas¹, D. Jokubauskis¹,
A. Urbanowicz¹, M. Treideris¹, R. Butkutė¹, and L. Minkevičius¹

¹Center for Physical Sciences and Technology, Saulėtekio Ave. 3, LT-10257, Vilnius, Lithuania

²Institute of Applied Electrodynamics and Telecommunications, Vilnius University,
Saulėtekio Ave. 3, LT-10257, Vilnius, Lithuania

Compact terahertz (THz) imaging systems are of great demand in the fields of medicine, industry and scientific research. Quite a variety of small THz detectors are available for such systems, however, further development and applications are hindered by the lack of compact and effective THz sources [1]. As a solution, solid-state metamaterial structures sustaining magnetic polaritonic excitations can be used. A typical example consists of a sandwich of single metallic and dielectric layers with a periodically structured metal layer on the top, forming thus a pair of single-negative materials where a strong coherent resonant absorption/emission in the THz range can be achieved via excitation of magnetic polaritons [2].

In this work, the excitation of magnetic polaritons in n -GaAs/GaAs/metal metamaterial structure is demonstrated and investigated. The cross-section of the sample is depicted in Fig. 1A, showing the layers of doped GaAs and undoped GaAs as well as periodically positioned metallic square metacells. Four samples of different surface geometries with resonant frequencies in 0.7 THz – 1.3 THz range were prepared. The investigation consisted of reflection measurements at 293 K using THz time-domain spectroscopy and emission measurements using Fourier spectrometer when samples were heated up to 670 K. The experimentally obtained reflectance spectra of the samples with different metacell dimensions are shown in Fig. 1B. The resonant frequency dependence on metacell geometry extracted from reflection measurements is presented as points in Fig. 1C. A good agreement between experimental results and theoretically calculated dependency using LC circuit model [2] to describe magnetic polariton resonances provided in (curve in Fig. 1C) is observed. This paves the way for the further development of magnetic polariton-based THz devices and the possibility of integration of such devices to GaAs THz optoelectronics.

Funding by a grant (No. S-MIP-22-76) from the Research Council of Lithuania is acknowledged.

REFERENCES

- [1] G. Valušis, A. Lisauskas, H. Yuan, W. Knap, and H.G. Roskos; *Sensors* 21 (2021) pp. 4092.
- [2] B. J. Lee, L. P. Wang, and Z. M. Zhang; *Opt. Express* 16 (2008) pp. 11328-11336.

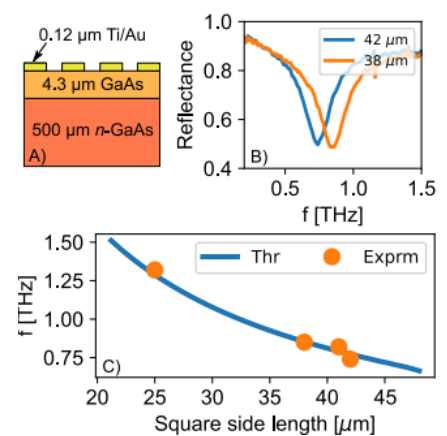


Fig. 1 Structure cross-section (A), recorded reflectance spectra (B), experimental (dots) and calculated (curve) magnetic polariton spectral positions as a function of a square metacell lateral dimensions (C).

Towards electronically controlled reconfigurable terahertz beam steering based on phase-change metasurfaces

Krishna Kumar^{1,2}, Borja Vidal², and Carlos Garcia-Meca¹

¹DAS Photonics, ²Universitat Politècnica de Valencia; Valencia, Spain, 46022.

Email: kkumar@dasphotonics.com

Phase change materials (PCMs) such as Ge-Sb-Te compounds (GST) are a promising platform for the development of reconfigurable devices. By incorporating this kind of material in a metasurface, electronically controlled fast and non-volatile beam steering devices have been experimentally demonstrated in the infrared [1] and GHz regions [2]. THz metasurfaces that can achieve beam steering have also been experimentally demonstrated [3]. However, in this case, changing the steering angle requires a variation of the beam frequency, while reconfigurable steering for a fixed THz frequency has not been reported so far. Here, we explore such a possibility by using a PCM-based metasurface. The states of various PCMs, such as GST or VO₂, present a high contrast in their optical properties at THz frequencies. With proper heating, the PCMs state can be dynamically switched, even achieving highly stable intermediate states. For example, applying electrical pulses across transparent heating electrodes placed below and on top of a thin GST layer would perform crystallization and re-amorphization of GST states [1].

We propose to add a thin PCM layer to passive C-shaped split ring resonators (SRRs) [3] to actively tune the SRR resonance frequency and thus control the phase shift it introduces. For full control of the transmitted THz beam, it is important to achieve a large phase shift (ideally 2π) upon the PCM states transition. However, this is a challenging task. To solve this problem, we use a few-element array so that the full 2π range has not to be covered. We present CST simulations on the performance of a C-shaped SRR over GST (Figure 1) that introduces a maximum phase shift of 40° upon GST states transition at a frequency of 0.6 THz without significant anomalous transmission loss (Figure 1b). Further focusing the incoming THz radiation on the beam steering device, it is possible to dynamically tune the cross-polarized steering angle by dynamically switching the GST state.

REFERENCES

- [1] S. Abdollahramezani, *Nature Communications*, **13** (2022) 1696
- [2] Md. Reza M. Hashemi, *Sci. Reports*, (2016) 35439.
- [3] S. Zhang, *Photonics Research*, **10** (2022) pp. 1731-1743.

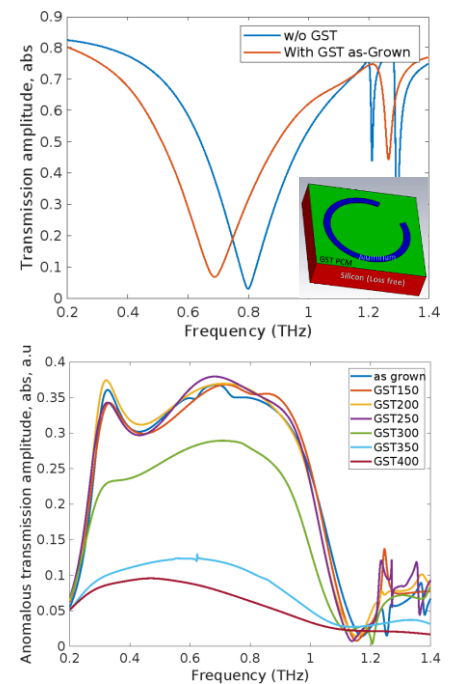


Fig. 1 (a) Effect of introducing a 50 nm GST layer on resonance frequency and (b) Effect of different GST intermediate states (as a function of temperature) on anomalous transmission amplitude.

Efficient electrooptic THz beam modulator based on drifting space-charge domains in gallium nitride structures.

R. M. Balagula¹, L. Subačius¹, P. Prystawko², and I. Kašalynas¹

¹Center for Physical Sciences and Technology (FTMC), Vilnius, Lithuania.

²Institute of High Pressure Physics PAS (UNIPRESS), Warsaw, Poland.

Email: roman.balagula@ftmc.lt.

Improvement of GaN quality is desirable for high-power applications. However, GaN performance under strong electric field is determined by field uniformity that can be reduced by growth- or processing defects as well as current instabilities arising due to formation of space-charge (SC) domains. Gunn domains are among mechanisms utilized in practice, but experimental realization of Gunn effect in GaN faces some technical issues [1]. Nevertheless, the formation of SC domains drifting with speed of acoustic wave in GaN owing to strong piezoelectric interaction was predicted [2].

Drifting SC domains were observed in the 10 μm -thick n -type GaN epilayers grown on semi-insulating GaN substrate. Si-doped layers with $n = 1.1 \cdot 10^{16} \text{ cm}^{-3}$ at $T = 300 \text{ K}$ demonstrated low-field mobility $\mu = 1021(2652) \text{ cm}^2/\text{V}\cdot\text{s}$ at $T = 300(77) \text{ K}$ [3]. Planar ohmic contacts with separation d from 12 μm to 3 mm were developed for application of electric field pulses with rise time $< 1 \text{ ns}$ and duration $\tau \geq 500 \text{ ns}$. Pulsed voltage and current traces were recorded with 6 GHz real-time oscilloscope.

Current traces for samples with $d \leq 65 \mu\text{m}$ repeated rectangular shape of applied voltage pulse up to $E_{\text{breakdown}} = 130(53) \text{ kV/cm}$ at $T = 300(77) \text{ K}$ [3]. However, currents in samples with $d \geq 1 \text{ mm}$ at both temperatures demonstrated decaying oscillations attributed to the drifting SC domains. The ratio between sample length and oscillation period was $\sim 4 \cdot 10^5 \text{ cm/s}$, which is close to the speed of transverse acoustic wave in GaN. The found critical sample lengths for domain formation were $\sim 0.14(0.12) \text{ mm}$ at $T = 300(77) \text{ K}$. The results highlight possible complications for development of large-scale GaN devices for high-field applications. On the other hand, efficient modulation of transmission of THz beam was observed under the applied electric field.

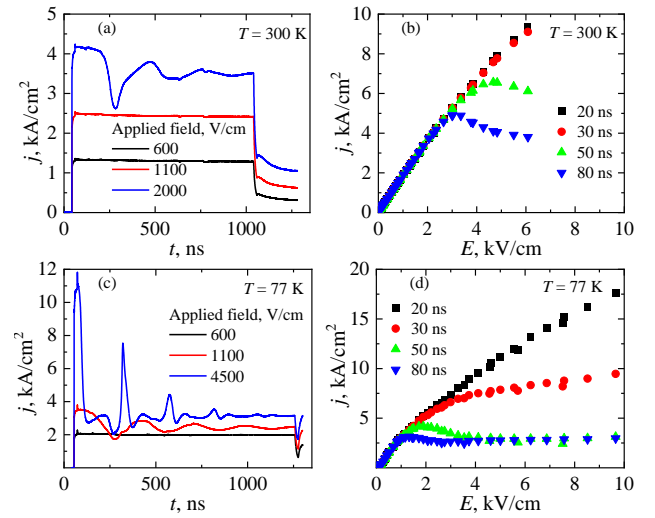


Fig. 1 (a), (c) Traces of j in 1 mm sample at $T = 300$ and 77 K under different E . Traces exhibit formation of current oscillations at $E > E_{\text{critical}}$. (b), (d) Current density dependences on electric field strength at particular time moments of the applied pulse at $T = 300 \text{ K}$ and 77 K .

REFERENCES

- [1] A.S. Hajo, et al., IEEE Access **8**, 84116 (2020).
- [2] S.K. Abdelraheem, D.P. Blyth, and N. Balkan, Phys. Status Solidi **185**, 247 (2001).
- [3] R.M. Balagula, et al., Materials **15**, 2066 (2022).

Optimization of self-mixing effect in integrated BiCMOS sources for reflection-type imaging applications

Dmytro B. But¹, Kęstutis Ikamas^{2,3}, Cezary Kołacinski^{1,4}, Alexander Chernyadiev¹, Ieva Morkūnaitė², Wojciech Knap¹, Alvydas Lisauskas^{1,2}

¹*CENTERA Laboratories, Institute of High Pressure Physics PAS, Warsaw, 01-142, Poland*

²*Institute of Applied Electrodynamics and Telecommunications, Vilnius University, Lithuania*

³*General Jonas Žemaitis Military Academy of Lithuania, 10322 Vilnius, Lithuania*

⁴*Łukasiewicz Research Network - Institute of Microelectronics and Photonics, Warsaw, Poland*

Email: dbut@unipress.waw.pl

We report on the investigations of the self-mixing effect in antenna-integrated voltage-control oscillator (VCO). The VCO employs a pair of heterojunction bipolar transistors implemented in the 130-nm SiGe BiCMOS technology. The source employs a differential Colpitts configuration similarly to our previous work [1], but is optimized for the emission fundamental harmonic. The radiation is outcoupled through the substrate side using a hyper-hemispherical silicon lens. The source emits up to 0.3 mW of propagating power with frequency tenability from 258 to 262 GHz. Due to operation at fundamental harmonic, feedback radiation induces a self-mixing current, which can be detected either in the dc regime or by employing signal modulation techniques. We show the applicability of the self-mixing effect to form reflection-type images.

The self-mixing amplitude achieves 1.5%- 2% of carrier current, as shown in Fig. 1. The application of feedback interferometry based on terahertz transistor oscillators is not limited to imaging applications (see the inset of Fig.1). It can be employed in a wider field of applications such as tracing chemical absorption lines in THz frequency range or accurate distance sensors.

REFERENCES

[1] K. Ikamas, et. all. "All-Electronic Emitter-Detector Pairs for 250 GHz in Silicon," *Sensors* 2021, Vol. 21, Page 5795, vol. 21, no. 17, p. 5795, 2021

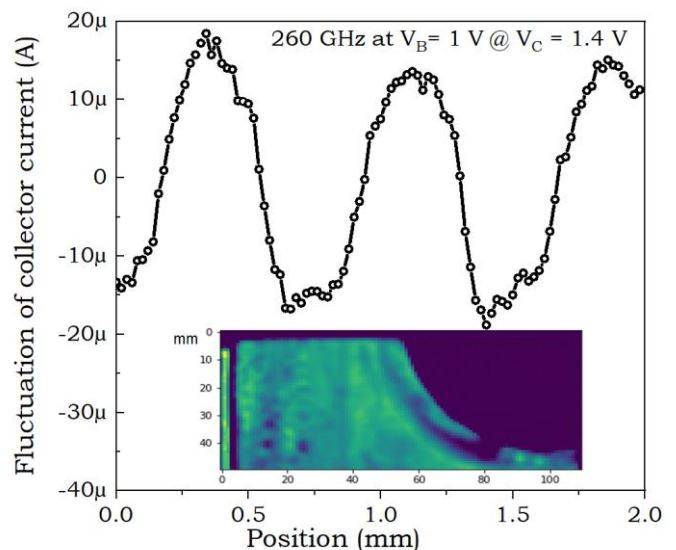


Fig. 1 Fluctuation of the collector-emitter current as a result of the self-mixing effect of 260 GHz radiation reflected from a flat mirror as a function of the mirror position. Inset presents an image of a ceramic part.

Development of Hybrid phase profile silicon multi-phase zone plate lenses for THz frequencies

Surya Revanth Ayyagari¹, Simonas Indrišiūnas², Gediminas Račiukaitis², and Irmantas Kašalynas¹

1 Terahertz Photonics Laboratory, Center for Physical Sciences and Technology (FTMC), Saulėtekio 3, 10257 Vilnius, Lithuania

2 Laser Microfabrication Laboratory, Center for Physical Sciences and Technology (FTMC), Savanoriu ave. 231, LT-02300 Vilnius, Lithuania

surya.revanth@ftmc.lt

Abstract: Engineering of hybrid diffractive optical lenses capable of efficient THz beam focusing is the main aim of this research work. The hybrid multi-phase Fresnel lenses (H-MPFLs) were successfully developed demonstrating up to 10 % higher values as compared to the standard design MPFL at target 0.585 THz frequency. The optimal phase offset was found to be of $+\pi/4$ independently on the hybridization order of the H-MPFL samples.

Diffractive optical elements, such as Fresnel lenses, define the beam shape by describing the phase and amplitude distribution of incident wave at the focal plane. Such Fresnel lenses may have different phase profiles like binary or multi-level step pattern that are of the order of wavelength to achieve a constructive interference of the beam. The MPFL introduces multiple phase shifts in the order of $2\pi/Q$ instead of only phase shift equal to 2π leading to high diffraction efficiency of the beam. The design of standard MPFL and H-MPFL can be described by analytical equation [1,2]:

$$r_n = \sqrt{\frac{2\lambda n \left(\frac{\pi}{Q} + \frac{\lambda}{2Q(\sqrt{\epsilon}-1)} \left(1 + \frac{\pi}{8} \right) \right)}{Q}} + \frac{n^2 \lambda^2}{Q^2}, \quad (1)$$

here r_n is the outer radius of n -th subzone, F is the focal length ($F=13\text{mm}$), λ is the designed wavelength ($\lambda=0.512\text{mm}$), Q – the number of phase quantization levels ($Q=8$), ϵ – the refractive index of HRFZ-Si substrate used ($\epsilon = 3.45$), and m – the optimization factor of phase. The depth of single subzone was defined as $\frac{\pi}{Q} = \frac{\lambda}{Q(\sqrt{\epsilon}-1)} \left(1 + \frac{\pi}{8} \right)$. The H-MPFL with two times smaller amount of phase quantization levels at outer most zones were developed of high resistivity silicon by using the direct laser ablation technology (see Fig.1). The focusing gain of hybrid lenses was found to be up to 10 % higher in comparison to a standard design MPFL validating a new approach suitability for development of new diffractive optical elements with much simpler and less complex fabrication details suitable for on-chip integration with other THz devices.

REFERENCES

- [1] H. D. Hristov, Fresnel zones in wireless links, zone plate lenses, and antennas. Artech House, 2000.
- [2] S. R. Ayyagari et al, "Hybrid Multi-Phase Fresnel Lenses on Silicon Wafers for Terahertz Frequencies," IEEE TTST (under revision).

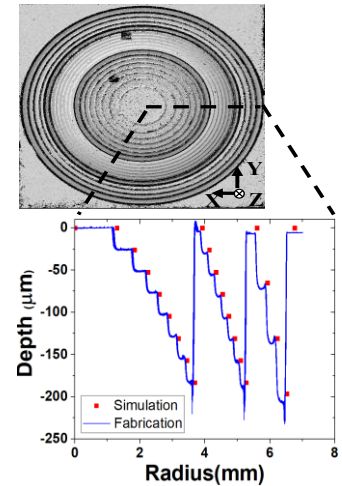


Fig. 1 The microscopic picture of the H-MPFL sample. Inset step profile across the centrum ..

Optical-THz-Optical bridge at 5Gbps with a photonicallly-driven Schottky mixer at the receiver

Inigo Belio-Apaolaza¹, James Seddon¹, Diego Moro-Melgar², Chris Graham¹, Oleg Cojocari², and Cyril C. Renaud²

¹ *Department of Electronic and Electrical Engineering, University College London, London WC1E 7JE, UK*

² *ACST GmbH, Josef-Bautz-Str. 15, 63457 Hanau, Germany*

Email: inigo.apaolaza.21@ucl.ac.uk

THz communications are paving the way for next-generation mobile communications networks, enabling links of data rates beyond 100Gbps [1]. Photonic-based solutions are key players in this field, offering ultra-wide tuneability, agility, and maturity among other advantages. In the transmitter side, typically uni-travelling-carrier photodiodes (UTC-PD) are used as photomixers. In the receiver however, electronic solutions are dominant because of the lack of efficient down-conversion at photonic-based receivers. A particular use of THz communications consists of implementing wireless bridges between two optical ends, connecting seamlessly different segments of a fiber network. Reported examples in literature use heterodyne receivers based on electronically-driven mixers [2], or direct THz-to-optical conversion with ultra-wide bandwidth plasmonic modulators [3]. The first scheme's main limitations are associated with the generation and distribution of the local oscillator signal. The second approach can be very efficient, but down-conversion to an intermediate frequency is not performed, where filtering, amplification, and processing can be applied to the received signal before up-converting into the optical domain.

Here, we present the first 300GHz wireless bridge using a heterodyne receiver based on a subharmonic Schottky mixer driven with a photonic local oscillator. We transmit a 5Gbps OOK signal without errors. The mixer is a prototype operating at 270-320GHz, designed and fabricated at ACST GmbH. The local oscillator signal is generated by optical heterodyning with two 1.55 μ m lasers pumping a waveguide-integrated UTC-PD. The THz transmitter is also based on an UTC-PD photomixer, thus the THz link is all-photonics-based. Our proposed receiver exploits the advantages of photonic local oscillators, such as ultra-wide tuneability and low-loss fiber distribution, combined with high-performance down-conversion of THz Schottky mixers.

REFERENCES

- [1] T. Nagatsuma, G. Ducournau, and C. C. Renaud, "Advances in terahertz communications accelerated by photonics," *Nature Photonics*, vol. 10, no. 6. Springer Science and Business Media LLC, pp. 371–379, May 31, 2016.
- [2] S. Koenig et al., "High-Speed Wireless Bridge at 220 GHz Connecting Two Fiber-Optic Links Each Spanning up to 20 km," *Optical Fiber Communication Conference*. OSA, 2012.
- [3] Y. Horst et al., "Transparent Optical-THz-Optical Link at 240/192 Gbit/s Over 5/115 m Enabled by Plasmonics," *Journal of Lightwave Technology*, vol. 40, no. 6. Institute of Electrical and Electronics Engineers (IEEE), pp. 1690–1697, Mar. 15, 2022.

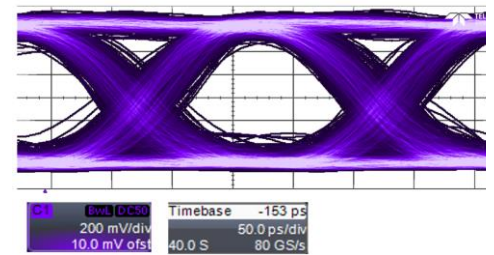


Fig. 1 Eye diagram of a 5Gbps OOK signal captured from the 300GHz wireless bridge

100 Gbit/s THz Data Transmission and Beyond using Multicore Fiber Combined with UTC Photodiode Array

Aritrio Bandyopadhyay¹, Bewindin A. Sawadogo^{1,2}, M. Zegaoui¹, M. Zaknoute¹, P. Szriftgiser², K. Baudelle², M. Bouet², G. Bouwmans², Davy P. Gaillot¹, E. Andresen², Guillaume Ducournau¹, Laurent Bigot²

¹IEMN, University of Lille, 59650 Villeneuve d'Ascq, France.

²PhLAM, University of Lille, 59000 Lille, France.

Email: aritrio.bandyopadhyay@iemn.fr

In a recent report by CISCO, it has been predicted that the global IP traffic will be around 4.8 ZettaOctets by 2022 [1]. In order to cope up with this tremendous increase of data usage, different solutions are being investigated among which is the usage of the Terahertz (THz) frequencies based wireless networks. The range of the THz frequencies are between 100 Gigahertz (GHz) to 10 THz, thus paving the way to Tbit/s wireless links that will meet the requirements of applications such as holograms, vehicle-to-vehicle communications and virtual reality [2]. The “300 GHz band”, corresponding to the 250-320 GHz frequency band that is regulated by IEEE 802.15.3d standard has recently boosted the THz communications research. Currently, Terahertz transmitters (T_x), based on electronics (mixers, SiGe transistors etc.) and a photonics-based one (photomixers, quantum cascade lasers etc.) are being investigated [3].

Generating THz signals via the photomixing technique presents many advantages such as the linearity of the signals over an extended bandwidth. Usually, the THz signal results from the beating of two light waves f_1 and f_2 in an UTC-PD (Unitraveling Carrier Photodiode) or PIN photodiode resulting in a carrier frequency, " $f_{THz} = |f_1 - f_2|$ (1)". The transmitted power is one of the key parameters for any wireless link. Unfortunately, the photonics-based approach suffers from output power limitations that limits the reach of the wireless links.

Hence, there is a need to develop new approaches in order to increase the power of the THz carrier. In this work, an innovative approach based on the use of an UTC-PD array excited by a multicore fiber is proposed to tackle the power issue and enable long distance THz transmissions. Such an approach makes it possible to increase the generated THz power by N , N being the number of UTC-PDs in the array and the number of optical channels that can be multiplexed over the same number of SSMF (Standard Single-Mode Fiber).

In order to achieve this goal, some of the elementary components of the future multipath system have been developed and characterized. The electrical performances of a single UTC-PD operating in the 290-350 GHz range are demonstrated and on-wafer data transmission up to 100 Gbit/s data rates are reported together with Bit Error Rate (BER) measurements at different bit rates.

REFERENCES

- [1] CISCO Visual Networking Index: Forecast and trends, 2017-2022.
- [2] H. Song and T. Nagatsuma, "Present and future of terahertz communications," IEEE Transactions on Terahertz Science and Technology, vol. 1, no. 1, 2011, pp. 256-263.
- [3] Nagatsuma, T., Ducournau, G. & Renaud, C. "Advances in terahertz communications accelerated by photonics". Nature Photon 10, 371–379 (2016). <https://doi.org/10.1038/nphoton.2016.65>.

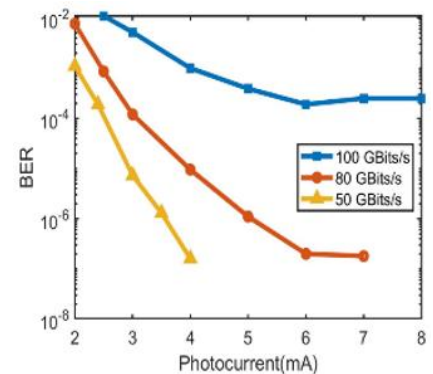


Fig. 1 BER curves obtained at 50, 80 and 100 Gbit/s.

Outdoor THz communications: channel characteristics and statistical uncertainties

Milda Tamošiūnaitė¹, Vincas Tamošiūnas^{1,2} and Gintaras Valušis^{1,2}

¹ *Department of Optoelectronics, Center for Physical Sciences and Technology, Saulėtekio 3, Vilnius, Lithuania*

² *Institute of Photonics and Nanotechnology, Vilnius University, Saulėtekio 3, 10257 Vilnius, Lithuania*

Email: milda.tamosiunaite@ftmc.lt

Terahertz (THz) band telecommunications (0.1-10 THz) envisioned as the key enabling technology for sixth generation (6G) wireless networks. Due to large available bandwidth, 6G is expected to handle exponentially growing mobile data traffic [1]. Furthermore, promising up to terabyte-per-second speeds should spur the development of delay-sensitive technologies, offering novel experience of internet of things and virtual reality.

From the various THz technologies continuously developed, efforts have led to the use of both photonics and electronics-based technologies [2]. For some time lack of compact energy-efficient high-power THz transmitters and low-noise high-sensitivity receivers has limited the practical use of the THz band for communication systems, but recent achievements [3] are closing the technology gap. However, outdoor transmission distance is limited by the atmospheric attenuation and comprehensive test data under varying atmospheric conditions are still quite scarce.

An overview of channel characteristics modelling is presented, as well the efforts to carry out statistical calculations for most probable scenarios (short-range communications with narrow beam high-gain antennas). While THz atmospheric absorption spectra are well described in HITRAN [4] and MODTRAN [5] simulation packages, events of heavy rain are taken into account as attenuation of approximately 10 dB/km. Statistical peculiarities of THz wave attenuation were evaluated emulating drop size distributions of the real rain and the laboratory-controlled rain, described in literature. The shortcomings of the statistical approach are deviations of several percent. Nevertheless, it could be a valuable machine learning tool for estimation of the upper and lower limits in THz communication channels when resilience margin is required.

REFERENCES

- [1] *Ericsson Mobility Report*, June 2022.
- [2] T. Nagatsuma, G. Ducournau and C.C. Renaud; *Nature Photonics* **10** (2016), pp. 371–379.
- [3] I.F. Akyildiz, C.Han, Z. Hu, S. Nie, J. M. Jornet; *IEEE Transactions on Communications* **6** (2022), pp. 4250 – 4285.
- [4] HITRAN online, <https://hitran.org/>
- [5] MODTRAN®, <http://modtran.spectral.com/>

Ultra-Broadband THz Transition from CPW to Si Rod Waveguide for Future Tbps On-Chip Communications

Shuya Iwamatsu¹, Muhsin Ali², Jose Luis Fernandez-Estevez¹,
Sumer Makhoul¹, Guillermo Carpintero², and Andreas Stöhr¹

¹University of Duisburg-Essen, ZHO, Lotharstr. 55, 47057 Duisburg, Germany

²Universidad Carlos III de Madrid, Avenida de la Universidad 30, 28911 Leganés, Madrid, Spain

Email: shuya.iwamatsu@uni-due.de

Recently, terahertz (THz) Si waveguides were utilized as interconnects for cost-effective high data rate (>100 Gbps) on-chip communications thanks to their low loss and low dispersion characteristics [1,2]. However, in [1,2], the Si waveguides were excited from hollow waveguides which limits their operational frequency range to a specific rectangular waveguide (WR) band. Moreover, excitation from a WR prevents from integrating Si waveguides with additional active sources or detector chips which is required for future beyond 100 Gbps transceivers.

In this article, we propose a broadband planar transition between InP-based coplanar waveguide (CPW) and Si dielectric rod waveguide (DRW) [2] using a tapered-slot mode converter [3] as shown in Fig. 1(a). The use of InP targets future monolithic integration with high-power uni-traveling-carrier photodiodes, a promising technology for ultra-broadband THz sources [4]. Experimental results show a coupling efficiency from the InP-based CPW to the Si DRW of about -2 dB in the frequency range of 70-120 GHz and a lower cut-off frequency of 65 GHz (Fig. 1(b)), which agrees with numerical simulation. According to simulations, the 6 dB bandwidth is 265 GHz. Further experimental characterization at different frequency bands will be reported at the conference site.

In conclusion, the proposed planar transition yields broadband operation and is a promising technology for integrating photonic THz active devices with dielectric interconnects for future on-chip Tbps communication.

REFERENCES

- [1] J. Webber, Y. Yamagami, G. Ducournau, P. Szriftgiser, K. Iyoda, M. Fujita, T. Nagatsuma, and R. Singh; *J. Lightw. Technol.* **39** (2021) pp. 7609-7620.
- [2] M. Ali, J. Tebart, A. Rivera-Lavado, D. Lioubtchenko, L.E. Garcia-Muñoz, A. Stöhr, and G. Carpintero; *2022 OFC* (2022) pp. 01-03.
- [3] X. Yu, J.-Y. Kim, M. Fujita, and T. Nagatsuma; *Opt. Express* **27** (2019) pp. 28707-28721.
- [4] B. Khani, S. Makhoul, A. G. Steffan, J. Honecker and A. Stöhr, *J. Lightw. Technol.* **37** (2019) pp. 1037-1044.

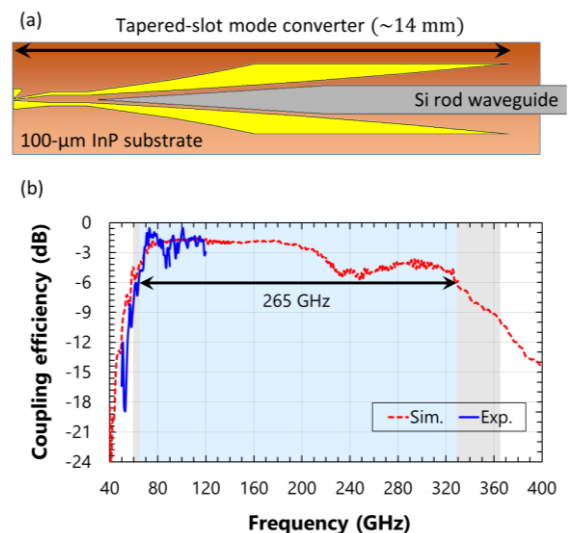


Fig. 1 (a) Schematic of tapered-slot mode converter coupling from InP CPW to Si DRW. (b) Measured and simulated coupling efficiency from InP CPW to Si DRW.

Data Transmission with Compact All-Electronic THz Wireless System

Kęstutis Ikamas^{1,3}, Albert Cesiul¹, Dmytro B. But^{2,4} and Alvydas Lisauskas^{1,2}

¹*Institute of Applied Electrodynamics and Telecommunications, Vilnius University, Vilnius, Lithuania*

²*CENTERA Laboratories, Institute of High Pressure Physics PAS, Warsaw, 01-142 Poland*

³*General Jonas Žemaitis Military Academy of Lithuania, LT-10322 Vilnius, Lithuania*

⁴*CEZAMAT, Warsaw Technical University, 02-822 Warsaw, Poland*

With the continuous increasing demand for higher throughput of wireless communication links, electronic devices are entering into still the least developed terahertz frequency range. A practical communication link requires a variety of fast and efficient THz waves controlling components and devices, such as THz transmitters, receivers, passive optical elements, and fast amplitude modulators [1]. Currently, the most advanced silicon technologies already enable the fabrication of complex electronic circuits directly operating in the microwave frequency range and touching the terahertz band's bottom limit [2]. However, methods and devices for fast data transmission using THz waves are still under development.

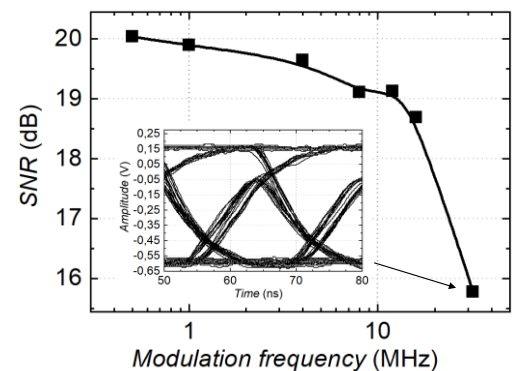


Fig. 1 The transmission line's SNR dependency on the modulation frequency. Inset: the eye diagram of RX output for 32 MHz modulation frequency.

In this work, we report on a free space all-electronic THz communication system, which consists of antenna-integrated Si-CMOS field-effect transistors (TeraFETs). The transmitter (TX) is based on a voltage-controlled two field-effect transistors-based differential Colpitts oscillator coupled with a resonant, slot-type antenna. It is optimized for the third harmonic emission at 252 GHz. The maximum radiated power is -11 dBm [3]. The receiver (RX) is a resonant-antenna-coupled FET quasi-optical detector with a substrate lens. It has a resonance maximum of 254 GHz with a bandwidth of about 25% and a minimal optical NEP of 22 pW/ $\sqrt{\text{Hz}}$.

We employ an on-off keying technique of TX and a self-made low-noise amplifier (LNA) on the RX side. The system demonstrates a signal-to-noise ratio (SNR) of 15.9 dB at a 32 MHz modulation frequency (Fig. 1). The data transmission speed in the current system is limited by used external electronic components – the LNA and the modulator. However, according to the Shannon–Hartley theorem, the theoretical information capacity of the system based on our core CMOS elements could be at **least 100 Gbps per channel**. Implementing state-of-the-art transmitter circuits should allow directly scaling the throughput to 10 Gbps.

REFERENCES

- [1] Nagatsuma T, Ducournau G and Renaud C, *Nature Photonics* **10** (2016) pp. 1749-4893
- [2] Pang J, Maki S, Kawai S, Nagashima N, et. al., 2017 ISSCC pp 424–425
- [3] Ikamas K., But D.B., Cesiul A., et al., *Sensors* **17** (2021), p. 5795

Optical heterodyne-based module on silicon platform for sub-THz wireless data transmission

Kalliopi Spanidou¹, Robinson Guzman¹, Luis Guerrero¹, Luis Orbe² and Guillermo Carpintero¹

¹*Electronic Technology, University Carlos III of Madrid, Av. de la Universidad 30, Leganes, 28911, Spain*

²*Synopsys Photonic Solutions, Enschede, 7521, The Netherlands*
Email: kspanido@ing.uc3m.es

Silicon Photonics (SiPh) is a key contributor to RF photonics as well as a valuable team player on CMOS and InP platforms, for optical interconnecting, filtering, modulation, and detection. Signal processing relies heavily on optical filtering and modulation. Ring-based optical filters and array waveguide grating (AWG)-based wavelength combiners have exhibited great performances by offering high wavelength selectivity and high quality factors (Q) [1]. Optical modulation based on Mach-Zehnder modulators (MZMs) have enabled high-order modulation formats reaching 100Gb/s via plasma dispersion effect [2].

Here, we show the potential of the silicon platform for the development of a sub-THz wireless transmitter. We present the characterization of several building blocks based on Tower's PH18MA Silicon photonics platform, which offers the 180 nm SOI process technology. Figure 1 depicts the envisaged high-speed RF Photonics transmitter, which is based on an external Optical Frequency Comb (OFC) and a SiPh chip for OFC-mode selection and modulation. The SiPh chip is composed of a pair of ring resonators, a modulator and AWG for optical multiplexing. In this paper, we examine the spectral responses of single- and coupled-ring structures in terms of wavelength tunability and flat pass band performance and demonstrate optical transmission data up to 4 Gbps via MZM modulator.

Authors acknowledge TOWER Semiconductor for chip fabrication, Synopsys Photonic Solutions support, financial support by the TERAOPTICS (No. 956857), TERAWAY (No 871668), CONEX-Plus (No. 801538) projects funded by UC3M and the European Union and the European Space Agency (ESA)(No. 4000135351/21/NL/GLC/my).

REFERENCE

- [1] Z. Zhou et. al; *IEEE Photonics Journal*, **10**, no. 1, (2018) pp. 1-12
[2] A. Rahim et. al; *Advanced Photonics*, **3**, no. 2, (2021) pp. 1-23

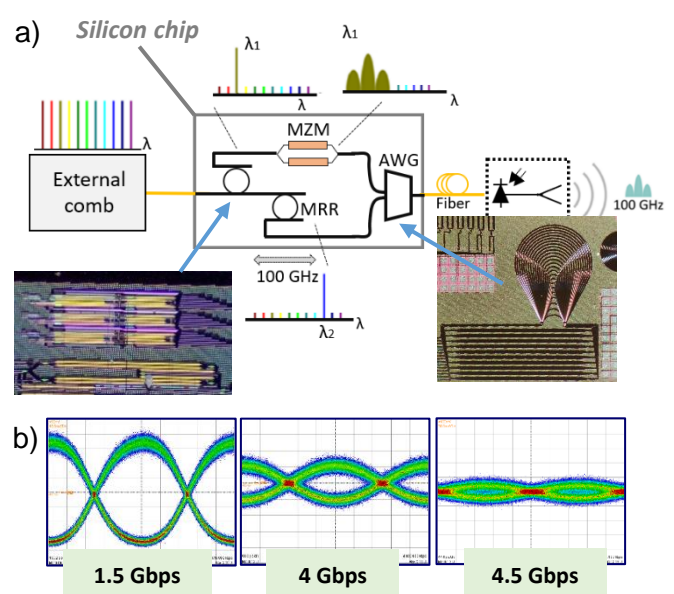


Fig. 1 a) An Illustration of the sub-THz wireless transmitter featuring ring-based filtering, an AWG wavelength multiplexing and data modulation via MZM. b) Optical data modulation up to 4Gbps.

Section 7

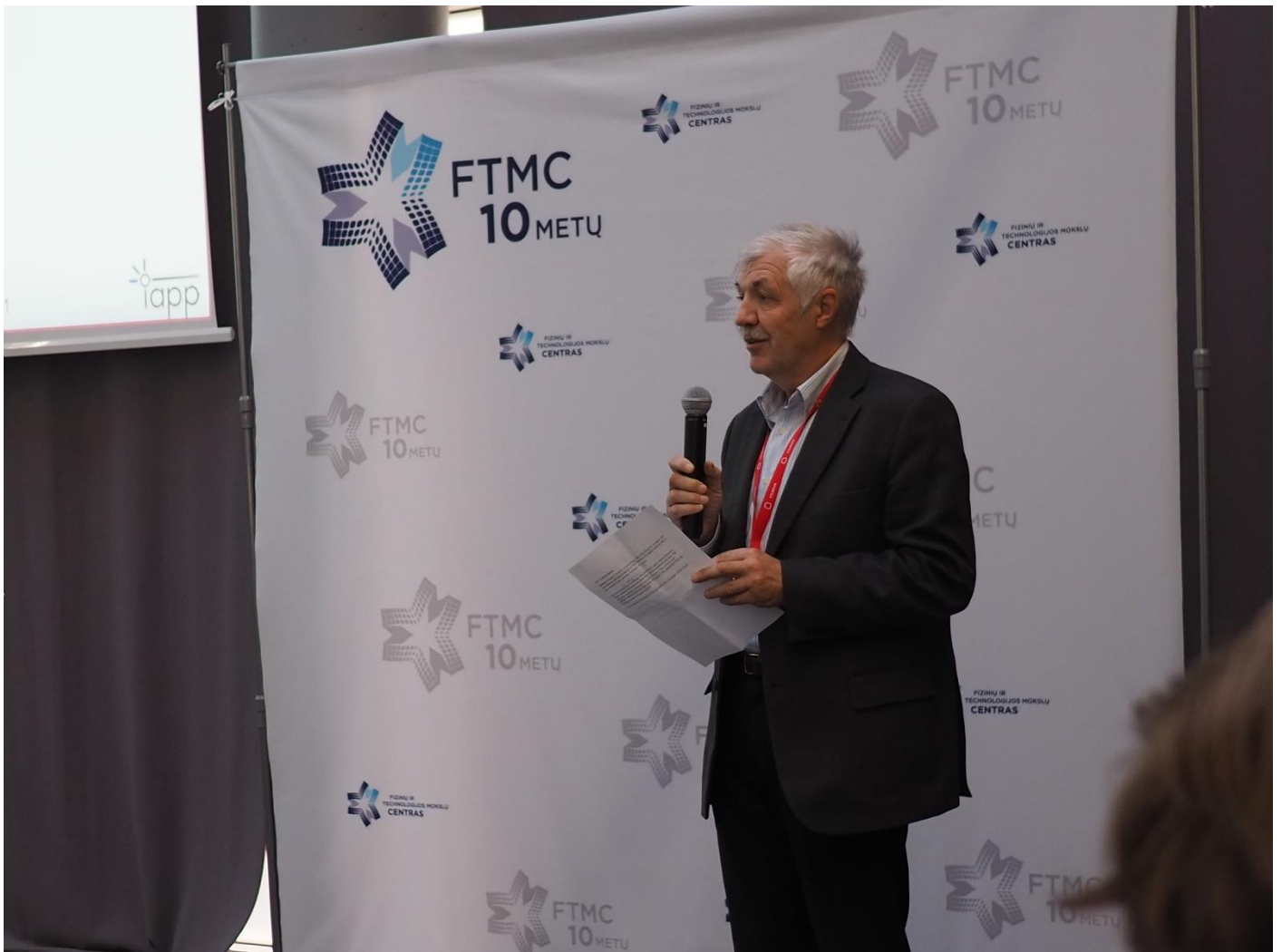
ORGANIC MATERIALS FOR OPTOELECTRONICS

Charge carrier motion in perovskite films.

Role of barriers

Vidmantas Gulbinas

Head of Department of Molecular Compound Physics at FTMC, Lithuania



Towards thermally activated delayed fluorescence compounds with minimized solid-state conformational disorder

Tomas Serevičius

Institute of Photonics and Nanotechnology, Vilnius University, Lithuania



Enhanced Mie Scattering on Spoof Plasmonic Surfaces of Terahertz Biosensors

Andreas K. Klein¹

¹*Department of Optoelectronics, University of Duisburg-Essen, Lotharstr. 55, 47057 Duisburg, Germany*

Email: andreas.k.klein@uni-due.de

Terahertz technology offers the potential for new (bio-) medical applications such as label-less sensing of biomarkers and the identification of relevant biomedical substances due to their spectral “fingerprint” [1]. As most biomarkers of interest are sized in the range of $<1\ \mu\text{m}$, and hence considerably smaller than the wavelength of THz radiation ($1\ \text{THz} \triangleq 300\ \mu\text{m}$). Spoof Surface Plasmon Polariton (spoof SPP) structures are known to increase the sensitivity in spectroscopic applications [2], due to their strong confinement to the surface and the slow-light effect close to the cut-off frequency. The anomalously increased scattering on defects on a spoof SPP surface has previously been reported for surfaces with high defect densities, demonstrating that defects with sizes of $\sim 1\%$ of the wavelength can be detected [3]. Here I investigate the increased Mie scattering on such spoof SPP surfaces for biosensor applications.

To demonstrate the enhancement, the results are compared to scattering on identical particles on metallic and dielectric surfaces. The inset in Fig. 1 shows a micrograph of a particle on a spoof SPP THz sensor. The graph itself shows that the scattering efficiency (blue curve) increases towards the higher-frequency cut-off (left side of the green transmission curve) and reaches enhancement values of ~ 20 at the transmission peak. The peak is preferred for experimental operation, as the even larger enhancement nearer to the cut-off cannot be utilized due to the drop in transmission to nearly zero.

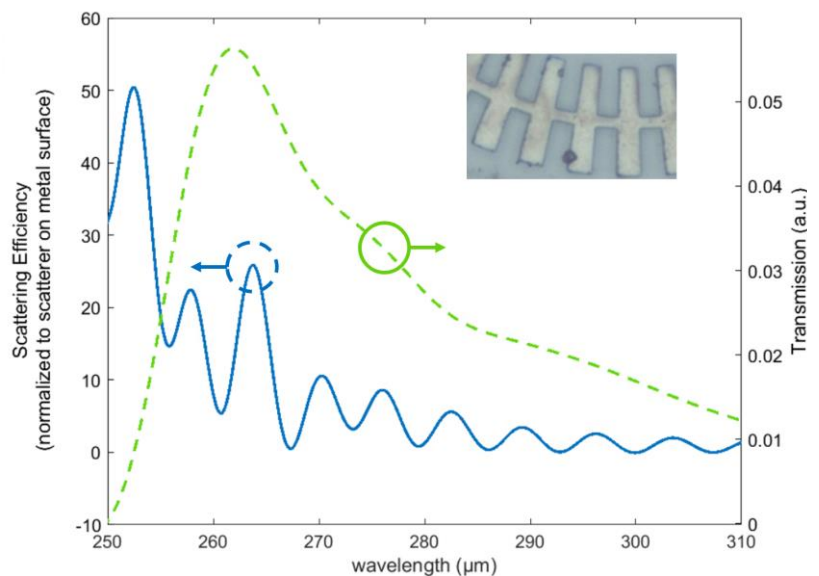


Fig. 1 Increased scattering efficiency of a $1\ \mu\text{m}$ particle on an spoof SPP surface showing increased efficiency by a factor of ~ 20 at the transmission peak (green curve). Inset: Micrograph of a particle on the surface of an THz spoof SPP Biosensor.

REFERENCES

- [1] S. Mallik et al., “High-Sensitive Terahertz Biosensors,” Book Chapter, Advanced Materials for Future Terahertz Devices, Circuits and Systems, Springer (2021), pp- 289-314.
- [2] Ng, B. et al., “Spoof Plasmon Surfaces: A Novel Platform for THz Sensing. Advanced Optical Materials,” Advanced Optical Materials (2013).
- [3] Klein, A. et al., “Scattering of spoof surface plasmon polaritons in defect-rich THz waveguides,” Scientific Reports (2019).

Section 8

NANO AND BIOPHOTONICS

S8-I1

Generation, manipulation and detection of light at the single photon level

Val Zwiller¹, S. Gyger¹, T. Staffas¹, T. Lettner¹, S. Cohen¹, J. Sutton¹, A. Elshaari¹, S. Steinhauer¹, M. Castaneda², J. Chang², R. Gourgues², I. Zadeh², A. Fognini², S. Dorenbos²

¹*KTH Royal Institute of Technology, Quantum Nano Photonics, Stockholm, Sweden*

²*Single Quantum BV, Delft, the Netherlands*



Photo by KTH

Skin-remitted light as a tool for health monitoring

Janis Spigulis

*Biophotonics Laboratory, Institute of Atomic Physics and Spectroscopy, University of Latvia
Jelgavas 3/607, Riga, LV-1004, Latvia*

Email: janis.spigulis@lu.lv

A brief overview on optical technologies suitable for non-invasive monitoring and diagnostics of human health condition will be presented, focusing at information that can be extracted from the skin back-reflected (remitted) signals. The techniques to be surveyed are diffuse reflectance spectroscopy and imaging, laser Doppler flowmetry, contact and remote photoplethysmography, and reflectance pulse oximetry. Laboratory-developed prototype designs will be discussed, as well as examples of clinical measurement results. Existing shortcomings and bottlenecks to be managed in future will be also considered.

REFERENCES

- [1] J.Spigulis, "Multispectral, fluorescent and photoplethysmographic imaging for remote skin assessment", *Sensors*, **17**, 1165 (2017).
- [2] J.Spigulis, I.Kuzmina, I.Lihacova, V.Lukinsone, B.Cugmas, A.Grabovskis, E.Kviesis-Kipge, A.Lihachev, "Biophotonics research in Riga: recent projects and results", *Proc.SPIE* **11585**, 1158502 (2020).

Novel diketopyrrolopyrrole-based emitters for NIR-to-visible photon upconversion

Lukas Naimovičius¹, Edvinas Radiunas², Barbara Chatinovska², Edvinas Orentas², Karolis Kazlauskas²

¹*Institute of Photonics and Nanotechnology, Vilnius University, Saulėtekio av. 3, Vilnius, Lithuania*

²*Department of Organic Chemistry, Vilnius University, Naugarduko str. 24, Vilnius, Lithuania*

Email: lukas.naimovicus@gmail.com

Triplet-triplet annihilation (TTA) mediated NIR-to-visible photon upconversion (UC) operating under incoherent low power density excitations is a rapidly advancing field of organic optoelectronics with many promising applications including photovoltaics, targeted drug delivery and 3D printing. [1,2] Currently, there is a lack of efficient TTA emitters in the visible range as they usually suffer from strong singlet fission, degradation, and self-reabsorption. [2] These limitations result in low UC quantum yield (ϕ_{UC}) preventing the TTA-UC systems from the industrial implementation. Therefore, novel efficient TTA emitters are in high demand.

In this work, the novel diketopyrrolopyrrole (DPP) compounds functionalized with furan, thiophene and phenyl moieties were investigated and applied in TTA-UC systems as alternative emitters to the widely used tetracene [2] and perylene derivatives. The moieties were found to be responsible for the red-shift of emission spectra with extending conjugation while the fluorescence quantum yield (ϕ_{FL}) stayed almost intact. All DPP compounds demonstrated the feasibility for TTA with moderate ϕ_{UC} (0.2% - 3.1%) and high probability factor f (4.4% - 15.6%) to create an emissive singlet from two triplets.

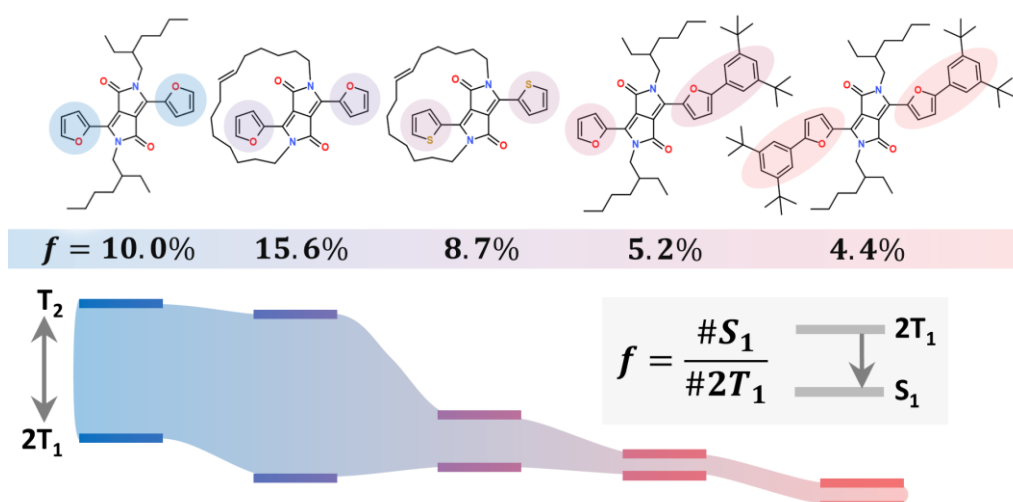


Fig. 1 Molecular structures and probability factor dependence on $2T_1 - T_2$ energy level distribution of studied compounds. Probability factor values indicated.

REFERENCES

- [1] Bharmoria, P. et al., Chem. Soc. Rev. 49, 6529–6554 (2020).
- [2] Radiunas, E. et al., J. Mater. Chem. C 9, 4359–4366 (2021).

Diboraanthracene and polymer-based systems for room temperature organic afterglow

Justina Jovaišaitė¹, Sven Kirshner^{2,3}, Steponas Raišys¹, Gediminas Kreiza¹, Paulius Baronas¹, Matthias Wagner² and Saulius Juršėnas¹

¹*Institute of Photonics and Nanotechnology, Vilnius University, Saulėtekis av. 3, 10257 Vilnius, Lithuania.*

Email: justina.jovaisaite@ff.vu.lt

²*Institut für Anorganische Chemie, Goethe-Universität Frankfurt, Max-von-Laue-Strasse 7, 60438 Frankfurt (Main), Germany.*

³*EaStCHEM School of Chemistry, The University of Edinburgh, David Brewster Road, EH9 3FJ Edinburgh, UK.*

Organic ultralong room temperature phosphorescence (RTP), often referred to as organic afterglow, is an exceptional phenomenon with long emission lifetime, exceeding 100 ms. Recently, it has attracted extensive scientific interest due to promising widespread applications in multidisciplinary fields, such as data encryption, anti-counterfeiting, bioimaging, and sensing. However, the prominent application fields require phosphorescence to be long as well as efficient, that is in principle a conflicting task.

In this work we present two laterally expanded 9,10-dimesityl-9,10-diboraanthracenes (DBA) derivatives as a new class of organic room temperature emission afterglow materials. The compounds demonstrate excellent ultralong and efficient emission properties: emission quantum yields of up to 3% and 15 %, afterglow lifetimes up to 0.8 s and 3.2 s and afterglow durations up to 5 s and 25 s for red and blue-green emitters, respectively. The afterglow emission is comprised of thermally activated delayed fluorescence (TADF) and RTP and was demonstrated by single molecules embedded in a rigid polymer matrix.

The afterglow mechanism can be explained by i) the efficient intersystem crossing between singlet states and upper lying excited triplet states of different nature, ii) the lowest triplet states of locally excited nature with very low non-radiative decay rate, and finally, iii) the intermediate triplet states as well as long-lived population of lowest triplet state that both create the possibility for reverse intersystem crossing, causing the appearance of TADF component.

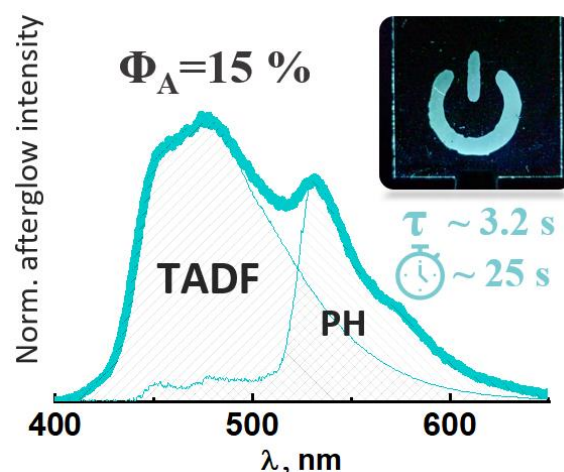


Fig. 1 The emission afterglow spectra of DBA compound. The photograph of thin polymer film doped with DBA material after excitation at 405 nm is turned off.

Controllable growth of two-dimensional palladium sulfide films

Vladimir Astachov¹, Virginijus Bukauskas¹, Audružis Mironas¹, Saulius Balakauskas¹, Jaroslav Dzisevič¹, Ieva Matulaitienė², Marius Treideris¹, Gediminas Niaura², Arūnas Šetkus¹

¹Department of Physical Technologies, Center for Physical Sciences and Technology, Savanorių ave. 231, LT-02300 Vilnius, Lithuania.

²Department of Organic chemistry, Center for Physical Sciences and Technology, Savanorių ave. 231, LT-02300 Vilnius, Lithuania.

Email:

Two-dimensional structures of transition metal dichalcogenides (TMD) are gaining more attention as they are promising basis for novel optoelectronic devices[1]. For example mixing different kinds of TMD with different electrical properties can lead to a new photonic, electronic and gas sensor devices[2]. However, large area growth of TMD films with few monolayer thickness still remains a great challenge.

In this work we present a technological approach for synthesis of palladium sulfide thin films (PdS and PdS₂) obtained by sulfurization of metallic film precursor at atmospheric pressure using chemical vapor deposition (CVD). Si/SiO₂ wafers were used as a substrates.

From our experiments we relate the amount of PdS₂ “islands” with the thickness of the Pd films, as well as the temperature and sulfurization times.

It was found that for the higher sulfurization temperatures (~500 °C) the amount of PdS₂ increases on the thinner film areas (8-4nm). On the contrary when the film thickness exceeds 8nm we observe that the amount of PdS₂ decreases to zero. This effect can be used in order to control the amount of PdS₂ and PdS during sulfurization.

The stability of PdS_x was checked using Raman spectroscopy immediately after the CVD process and in one month. The results demonstrates good stability of PdS_x films at normal conditions (room temp. 1atm pressure).

REFERENCES

- [1] X. Yin, C. S. Tang, Y. Zheng, J. Gao, J. Wu, H. Zhang, M. Chhowalla, W. Chen and A. T. S. Wee; Chem. Soc. Rev., 2021,50, 10087-10115.
- [2] W. Choi, N. Choudhary, G. H. Han, J. Park, D. Akinwande, Y. H. Lee; Volume 20, Issue 3, April 2017, Pages 116-130.

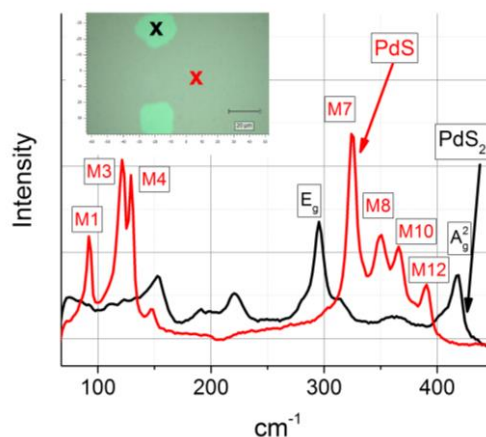


Fig. 1 Raman spectra of PdS₂ “island” and PdS film on the Si/SiO₂ substrate.

Photoluminescence and transient optical absorption in heavily doped lead tungstate

S. Nargelas, A. Vaitkevičius, Y. Talochka, G. Tamulaitis,

*Institute of Photonics and Nanotechnology, Faculty of Physics,
Vilnius University, Saulėtekio av. 3, Vilnius, LT-10257*

The demand for a better time resolution of scintillator-based radiation detectors exploited in high energy physics experiments and medical imaging devices is one of the key guiding trends in the current development of scintillation materials. One of the ways to develop the scintillators with a faster response is reengineering the growth, doping, and codoping properties of well-known mature-technology scintillators to obtain better timing properties. Lead tungstate (PWO) is a scintillator reliably serving already two decades long in CERN experiments. Commercially available PWO crystals are doped by trivalent La and Y ions to heal cationic and anionic vacancies and improve radiation tolerance of the crystal. Typical doping concentrations are at the level of 100 ppm. In this work, we present a study on PWO crystals with substantially larger doping levels by La and Y of up to 1500 ppm and focus on the doping influence on the timing properties of PWO.

The dynamics of nonequilibrium carriers in PWO crystals with different content of trivalent La and Y dopants were studied by exploiting two nonlinear optical techniques with the time resolution in subpicosecond domain: the transient absorption and the light-induced transient grating technique. The study was expanded by using the time-resolved photoluminescence spectroscopy. PWO single crystals were investigated in the temperature range from 10 to 450K and different nonequilibrium carrier densities.

We found that heavy doping of PWO with La and Y results in substantial enhancement of the luminescence decay rate, though at the expense of luminescence efficiency. The observed very low diffusion length of excitations in PWO (<120 nm) is consistent with the interpretation of the excitations as self-trapped excitons, most probable at the regular WO_4^{3-} complexes of the PWO lattice. These features are explained by an assumption that a fraction of the regular WO_4 complexes are distorted at different extent by the impurities located at different positions in the lattice and at different distances from these centers. Strong dipole-dipole interaction enhancing depopulation of emitting centers and resulting in accelerated luminescence decay was revealed at high excitation densities.

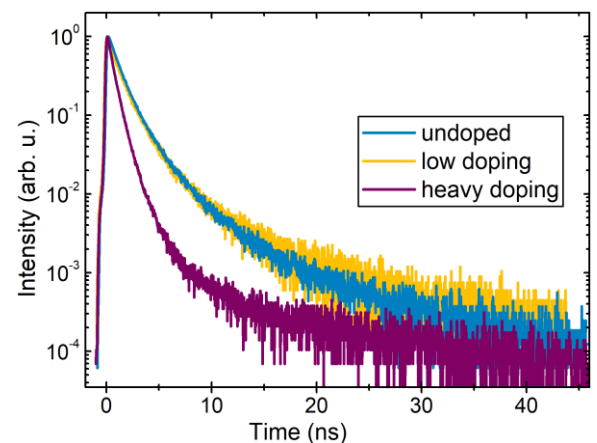


Fig 1. Normalized room temperature photoluminescence kinetics in differently doped PWO single crystals.

Section 9

SEMICONDUCTOR NANOSTRUCTURES AND ADVANCED PHOTONICS SYSTEMS

Terahertz imaging using diffractive Airy lens

Rusnė Ivaškevičiūtė-Povilauskienė¹, Paulius Kizevičius², Ernestas Nacius², Domas Jokubauskis¹, Kęstutis Ikamas³, Alvydas Lisauskas³, Natalia Alexeeva¹, Sergey Orlov², Linas Minkevičius^{1,4} and Gintaras Valušis^{1,4}

¹*Department of Optoelectronics, Center for Physical Sciences and Technology, Saulėtekio av. 3, Vilnius, 10257, Lithuania*

²*Department of Fundamental Research, Center for Physical Sciences and Technology, Saulėtekio av. 3, Vilnius, 10257, Lithuania*

³*Institute of Applied Electrodynamics & Telecommunications, Vilnius University, Saulėtekio av. 3, Vilnius, 10257, Lithuania*

⁴*Institute of Photonics and Nanotechnology, Vilnius University, Saulėtekio av. 3, Vilnius, 10257, Lithuania*

Email: rusne.ivaskeviciute@ftmc.lt

Terahertz (THz) beam engineering can be an important advantage in its further implementation in a variety of applications [1]. Structured light – electromagnetic waves with a strong spatial inhomogeneity of phase, amplitude, and polarization – due to recent innovations in nanotechnology and photonics, can be widely used in various optical research [2].

In this work, we demonstrate compact silicon optics-based THz structured light generation. Laser ablated high-resistivity silicon diffractive optical elements were found suitable for nonparaxial THz light generation in the form of Airy beam and its application in imaging (Fig. 1). Moreover, the accelerating and self-healing nature of this beam was exposed via THz imaging of a partly covered sample using an opaque beam block. Spatial resolution and contrast features in THz imaging were compared using structured light in the form of Airy, Bessel, and Gaussian beams.

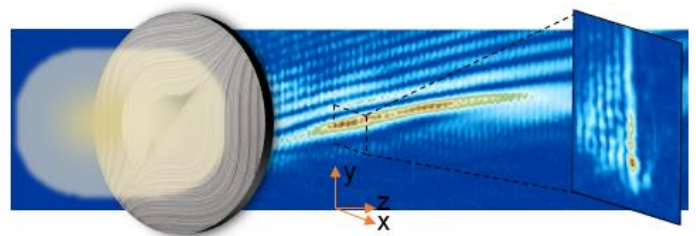


Fig. 1. THz Airy beam generation using diffractive Airy lens. Experimentally obtained THz intensity distribution of the nonparaxial Airy beam in the longitudinal (xz) and transverse (xy) (at the focal point) planes.

Results showed that structured light outperforms the classical Gaussian beam by providing improved resolution and contrast as well as extending thus boundaries of THz imaging applications.

REFERENCES

- [1] G. Valušis, A. Lisauskas, H. Yuan, W. Knap and H. G. Roskos; *Sensors* **21** (2021) 4092.
- [2] H. Rubinsztein-Dunlop, A. Forbes, M. V. Berry, M. R. Dennis, D. L. Andrews, M. Mansuripur, C. Denz, C. Alpmann, P. Banzer and T. Bauer; *Journal of Optics* **19** (2016) 013001.

Growth Optimization and Characterization of MQWs based on InGaAs and GaAsBi for VECSELs and NIR sources

Silvija Keraitytė^{1,2}, Andrea Zelioli², Evelina Dudutienė², Monika Jokubauskaitė^{1,2}, Bronislavas Čechavičius², Sandra Stanionytė², Virginijus Bukauskas² and Renata Butkutė^{1,2}

¹*Optoelectronics Dept. Centre for Physical Sciences and Technology, Saulėtekio av. 3, LT-10257 Vilnius, Lithuania*

²*Institute of Photonics and Nanotechnology, Faculty of Physics, Vilnius University, Saulėtekio av. 3, LT-10257 Vilnius, Lithuania
silvija.keraitytė@ff.stud.vu.lt*

Laser devices are potent in many application fields including optical fiber communication systems, material processing, LiDAR systems, Raman spectroscopy. Most important parameters that define the capabilities of lasers are emission wavelength, beam quality, wavelength tunability, output power and the size of the device [1]. Vertical-external-cavity surface-emitting lasers (VECSEL) are able to execute many of the parameters in a desirable manner and offer circular beam quality lasing with high optical output power [2].

For laser devices, it is important to optimize the active gain region composition and parameters. As such, there are numerous limitations for the growth and optimization of various structures, including non-radiative Auger recombination processes, instabilities due to temperature differences, difficulties in growing homogenous, precise layers [3].

Therefore the goal of this work was to grow and characterize multiple quantum well (MQW) structures based on two different materials – InGaAs and GaAsBi for laser devices operating in the near-infrared (NIR) region and exhibiting strong photoluminescence signals. The structures were grown using molecular beam epitaxy (MBE) system varying quantum well number and thickness, content of active materials.

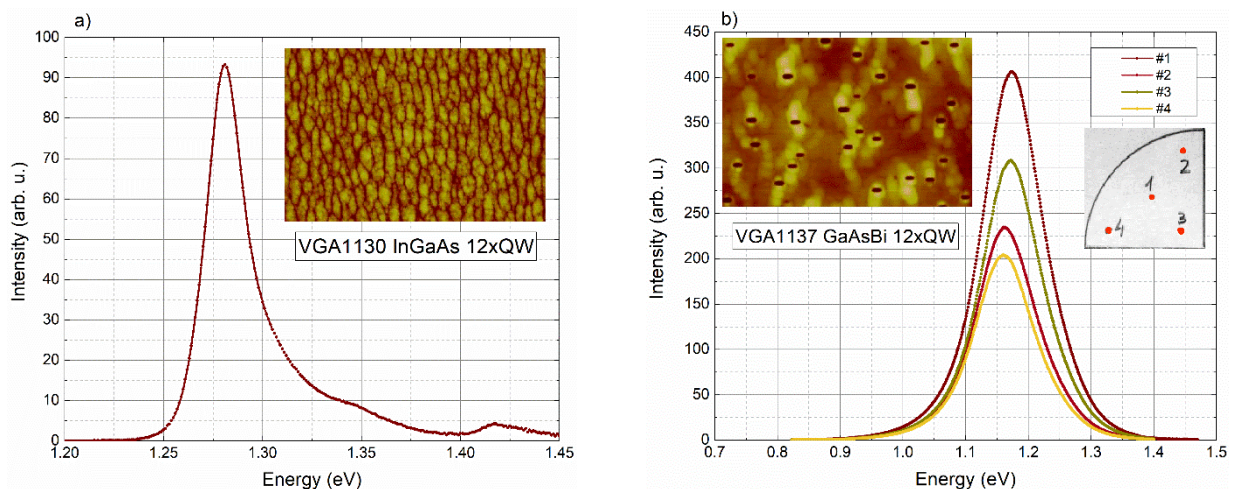


Fig. 1 Photoluminescence spectra of InGaAs (a) and GaAsBi (b) QWs. Insets depict surface morphology.

REFERENCES

- [1] M. Kuznetsov, *Semiconductor Disk Lasers: Physics and Technology* (2010) p. 1-71.
- [2] A.C. Tropper et al., *Journal of Physics D: Applied Physics* 37 R75 (2004).
- [3] M. Guina et al., *Journal of Physics D: Applied Physics* 50 (2017).

Effect of substrate temperatures on luminescent properties of GaAsBi/GaAs multi-quantum-wells

Evelina Dudutienė, Monika Jokubauskaitė, Bronislovas Čechavičius, Algirdas Jasinskas, Sandra Stanionytė, Martynas Skapas and Renata Butkutė

SRI Center for Physical Sciences and Technology, Saulėtekio ave. 3, Vilnius, Lithuania.

Email: evelina.dudutiene@ftmc.lt.

There is high demand for light sources operating in near infrared (NIR) range. Due to favorable properties GaAsBi/GaAs multi-quantum wells (MQW) could be used as an active area in such emitters. However, low growth temperatures required for Bi incorporation and large radius of Bi atoms, if compared with As atoms, reduce the quality of GaAsBi structures. In order to improve emission efficiency, various molecular beam epitaxy growth protocols are used e.g., thermal annealing, in-situ UV irradiation, etc.

In this work, the comparative study of structural and optical properties of GaAsBi/GaAs MQWs grown with conventional single-substrate-temperature (SST) technique and recently for this compound explored two-substrate-temperature (TST) technique [1] was performed. It was demonstrated that despite the better structural quality of GaAsBi/GaAs MQWs grown using SST method, the lower carrier localization and higher emission efficiency was observed for MQWs grown by TST method (see Fig. 1). The higher optical quality of TST grown GaAsBi/GaAs MQWs could be related to thermal annealing of uncovered GaAsBi layers during the growth interruption to increase the substrate temperature for the growth of barrier layers. Moreover, the access Bi evaporation from the surface during the growth pause leads to sharper interfaces between layers and lower localization.

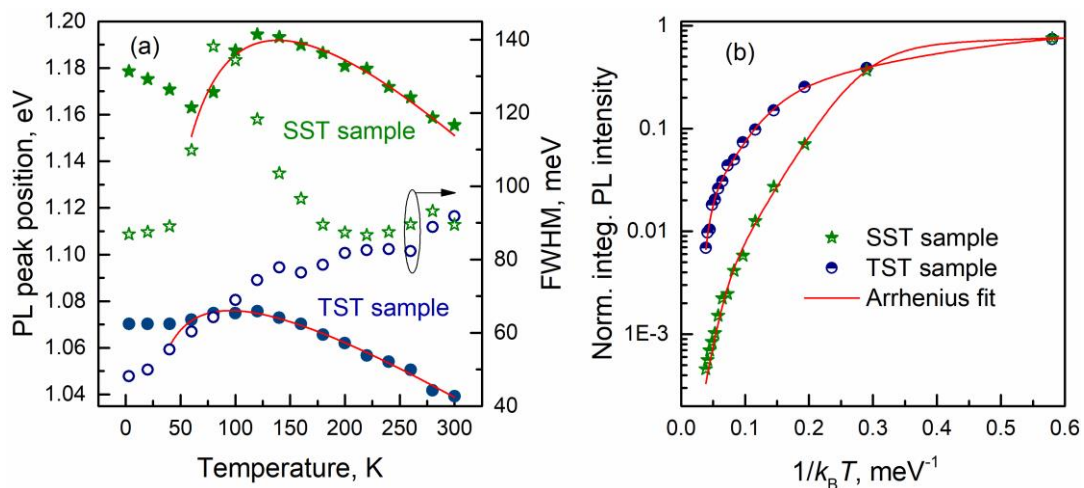


Fig. 1. Temperature- dependence of PL peak position, full-width-at-half-maximum (a) and normalized integrated PL intensity (b) of 12 nm-width GaAsBi/GaAs MQWs.

REFERENCES

- [1] P.K. Patil, F. Ishikawa, S. Shimomura, *Journal of Alloys and Compounds* **725** (2017) pp. 694-699.

Experimental Investigation of GaAs(Bi)/AlGaAs Grown Parabolic Quantum Wells in Terahertz Frequency Range

Mindaugas Karaliūnas, Dominykas Dumbrė, Vytautas Jakštas,
Renata Butkutė, and Gintaras Valušis

*Center for Physical Sciences and Technology, Saulėtekio Ave. 3, 190257
Vilnius, Lithuania*

Email: mindaugas.karaliunas@ftmc.lt

Parabolic quantum wells (PQWs) are promising terahertz (THz) emitters [1]. To increase the THz emission efficiency we implemented advanced carrier depopulation mechanism via bandgap engineering in GaAs [2]. To excite the PQW intersubband (ISB) transitions the electric field of the incident radiation need to be coupled to the PQW, i.e. turned from in-plane to the out-of-plane direction. There are few strategies to fulfill the condition in experiment. In this work we summarize the results of various experiments to characterize PQW samples to measure their performance.

The GaAs(Bi)/AlGaAs nanostructures were grown using molecular beam epitaxy applying the pulsed analog alloy grading technique [3, 4]. There are undoped structures for optical study and doped *pin*-diode-like structures for electrically driven THz emission. The THz frequency range spectra were measured using FTIR spectrometer *Nicolet 8700* by *Thermo Scientific* (USA) with pyroelectric or Golay cell detector. Few configurations were applied to measure the ISB transitions in PQWs: Brewster's angle, metal gratings as well as 45 degree angle incidence geometry. For the last one the PQW sample bar facets had to be polished to 45 degree angle.

Experimental study showed that it is indeed difficult to identify the PQW transitions in the THz frequency range unambiguously [5]. Therefore the comprehensive study of the experimental results in various configurations allowed to address specific spectral features to the 7-THz-designed PQWs.

REFERENCES

- [1] J. Ulrich *et al.*, Appl. Phys. Lett. **74**(21), 3158 (1999).
- [2] M. Karaliūnas, A. Udal, G. Valušis, Lith. J. Phys. **60**(2), 113 (2020).
- [3] M. Karaliūnas, *et al.*, J. Lumin. **239**, 118321 (2021).
- [4] S. Pūkienė, *et al.*, Nanotechnology **30**(45), 455001 (2019).
- [5] M. Karaliūnas, *et al.*, Proc. SPIE **11124**, *Terahertz Emitters, Receivers, and Applications X*, 1112409 (2019).

Structural analysis of thin bismuth layers grown on silicon (111) substrates

Sandra Stanionytė¹, Tadas Malinauskas², Gediminas Niaura¹, Martynas Skapas¹, Jan Devenson¹, Karolis Stašys¹ and Arūnas Krotkus¹

¹Center for Physical Sciences and Technology, Saulėtekio av. 3, Vilnius, Lithuania

²Institute of Photonics and Nanotechnology, Vilnius University, Sauletekio av. 3, Vilnius, Lithuania

Email: sandra.stanionyte@ftmc.lt.

Bulk bismuth is a semimetal, but when the thickness of Bi layer is decreased down to ~30 nm it becomes semiconductor. Recently, interest in such a layers increased because a few atomic layers of Bi can act as topological insulators [1] and can be used in many applications, such as sensors, contacts for Na-ion batteries, femtosecond optical switches, and etc.

In this work, thin bismuth layers (6–30 nm) were grown by molecular beam epitaxy (MBE) on Si (111) substrates. Bulk bismuth crystallizes in a rhombohedral structure, but depending on the technological growth conditions, thin layers grow in different orientations: homogeneous hexagonal symmetry (111)-oriented (β -Bi) and (110)-oriented (α -Bi) layers with different in plane orientation and β -Bi insets. In-plane and out-of-plane X-ray measurements have evidenced that α -Bi is compressively strained, while β -Bi layers are biaxially compressed in the layer plane and tensile in the growth direction. Their azimuthal orientations with the substrate were determined from XRD in-plane measurements (Fig. 1).

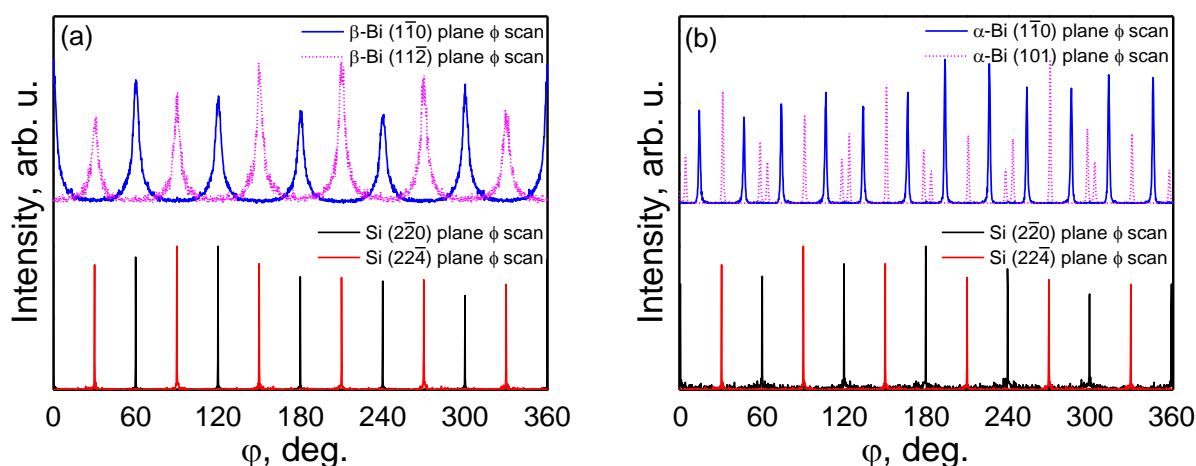


Fig. 1 In-plane relation between Si and Bi planes perpendicular to surface.

This research was funded by the European Social Fund under No. 09.3.3-LMT-K-712 “Development of Competences of Scientists, other Researchers and Students through Practical Research Activities” measure (Grant No. 09.3.3-LMT-K-712-23-0080).

REFERENCES

[1] Schindler, F.; Wang, Z.; Vergniory et al. *Nat. Phys.* **14** (2018) pp. 918–924.

Ultrafast long-distance electron-hole plasma expansion in GaAs mediated by stimulated emission of photons

T. Troha¹, F. Klimovič², T. Ostatnický², F. Kadlec¹, P. Kužel¹, and H. Němec¹

¹*Institute of Physics of ASCR, Na Slovance 2, 182 21 Prague 8, Czech Republic*

²*Faculty of Mathematics and Physics, Charles University, Ke Karlovu 6, 121 16 Prague 2, Czech Republic*

Email: troha@fzu.cz.

Transport of electrons and holes inside crystals is governed by the complex band structure. This puts some constraint on the maximum velocity of the charge transport, which is lower than $c/100$ even for (short-distance) ballistic transport in known materials. Here we report the ultrafast expansion of electron-hole plasma in GaAs by far exceeding this limit.

Using the technique of optical pump – THz probe spectroscopy we studied the expansion of electron-hole plasma (EHP) in direct band gap semiconductor GaAs on picosecond time scale. The THz spectroscopy is phase-sensitive and allows us to monitor the THz pulse arrival to the detector with a precision of a few femtoseconds. Firstly, an intense femtosecond optical pulse (800 nm) photoexcites the front surface of GaAs to create a dense EHP layer which acts as a metallic-mirror for THz radiation. The probing THz pulse impinges on EHP with variable delay from the opposite side of GaAs wafer and it is reflected from the inner EHP edge, thus serving as a time-of-flight probe of EHP expansion. From the time of arrival of THz pulse with respect to pump-probe delay we determined the expansion of the plasma layer. After the absorption of the pump pulse plasma starts to expand deeper into the material with velocity $c/10$ at 20 K and $c/30$ at 300 K which is significantly higher than permitted by the band structure. In addition, EHP expands over extremely large distances, 100 μm at 20 K and 50 μm at 300 K.

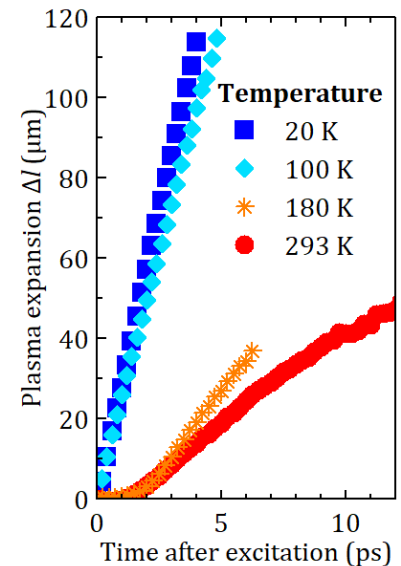


Fig. 1 Increase in plasma extent during its expansion at the excitation fluence 1.7×10^{16} photons/cm².

We explain the observed plasma dynamics by a coupling between the electron-hole system and the light field. Upon the absorption of the pump pulse the inversion of population rapidly develops slightly above the bandgap of the semiconductor leading to electron-hole recombination followed by the stimulated emission of radiation. The emitted photon bursts can then be reabsorbed only much deeper in the sample which is at the origin of the ultrafast plasma expansion. We believe that the observed process offers a potential for novel ultrafast optoelectronic elements.

REFERENCES

- [1] F. Kadlec, H. Němec, and P. Kužel; *Phys. Rev. B* **70**, 125205 (2004).
- [2] R. Ziebold, T. Witte, M. Hübner, and R. G. Ulbrich; *Phys. Rev. B* **61**, 16610 (2000).

POSTER SESSION

Bi-Quantum Dots Formation *in-situ* in MBE Reactor

Arnas Pukinskas¹, Nerijus Jurkūnas², Silvija Keraitytė¹, Algirdas Jasinskas^{1,3},
Andrea Zelioli¹, Bronislovas Čechavičius¹, Arnas Naujokaitis¹, Martynas Skapas¹,
Monika Jokubauskaitė¹, Evelina Dudutienė¹, and Renata Butkutė^{1,4}

¹ Centre for Physical Sciences and Technology, Saulėtekio av. 3, Vilnius, Lithuania

² Optonas Ltd., Savanorių av. 235, Vilnius, Lithuania

³ Light Conversion UAB, Keramiku st. 2B, Vilnius, Lithuania

⁴ Institute of Photonics and Nanotechnology, Vilnius University, Saulėtekio av. 3, Vilnius, Lithuania

Email: arnas.pukinskas@ftmc.lt

Several last decades scientists are focused into the miniaturization of the active area of devices by processing quantum structures, like quantum dots, quantum wells, quantum wires etc. Quantum effects applying various technological protocols – different designs of quantum well geometry, interruptions in processes for atom diffusion, *ex-situ* or *in-situ* annealing for smoothing of interfaces - allow to manipulate by characteristic parameters of devices. Moreover, scientists are exploring the modification of epitaxy methods for different formation of nanostructures that would lead to flexible properties of materials. The significant step into progress of A3-B5 family was the discovery of called bismides. Bismides are one of the most perspective compounds because of their unique properties – fast reduction of energy band gap replacing As by Bi atoms, and low energy band gap dependance on temperature [1]. Despite intensive bismide investigations their applications are hold-back by technological challenges. Both low epitaxy temperature and close to 1 arsenic and gallium ratio effect to poor crystalline quality and weak luminescent properties as well bismuth segregation to surface. Several thermal attempts to solve the problem of Bi agglomerations were tested. Our microscopical studies of post-annealing treatment demonstrated the formation of Bi nanoparticles emitting in the range of 1000 nm – 1300 nm [2]. In this work Bi quantum dots have been formed employing *in-situ* Bi segregation process in MBE reactor via annealing of GaAsBi quantum wells for a short time at 600-750°C temperatures under arsenic overpressure conditions (Fig. 1). HR-TEM and PL measurements were used to characterize the samples.

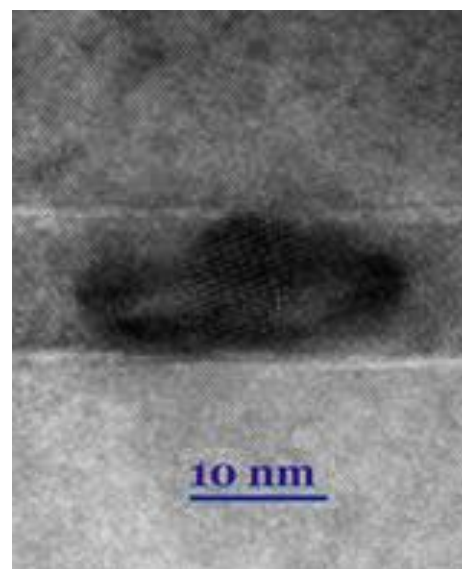


Fig. 1 HR-TEM cross-section image of Bi-QDs.

REFERENCES

- [1] S. Francoeur et al., *Appl. Phys. Lett.* 82, 3874 (2003).
- [2] R. Butkutė et al., *Nanoscale research letters* 12 (1), 436, 3 (2017).

Comparison of InAlGaN and AlGaN HEMT structures

J. Jorudas^{1,*}, A. Šimukovič¹, P. Prystawko², I. Kašalynas¹

¹Center for Physical Sciences and Technology (FTMC), Vilnius, Lithuania

²Institute of High Pressure Physics PAS, Warsaw, Poland

Email: justinas.jorudas@ftmc.lt

Gallium nitride (GaN) high electron mobility transistor (HEMT) structures possessing high density of two dimensional electron gas (2DEG) are investigated for the next generation of terahertz (THz) detectors, such as antenna coupled field effect transistor (TeraFET) detectors [1], bow-tie diodes [2], and plasmonic devices [3]. The heterostructures with sub-10 nm thick barrier, such as InAlGaN or ScAlN, would allow to maintain 2DEG parameters suitable for new applications in RF band and in the THz region [4], [5].

Here we investigate the three GaN-based HEMT structures grown by metalorganic vapour-phase epitaxy (MOCVD). One with the lattice matched thin InAlGaN barrier and the second one with buffer-free AlGaN/GaN design were developed and compared to a typical design AlGaN/GaN heterostructure. The heterostructures were simulated using Nextnano++ software and experimentally verified at 300 K and 77 K temperatures using Schottky contacts and Van der Pauw structures, the results of which are summarized in Table 1. Even with the lowest barrier thickness, the InAlGaN-based sample exhibited highest N_{2DEG} . Finally, the HEMTs ($L_G = 5 \mu\text{m}$, $L_{SD} = 14 \mu\text{m}$) and circular SBDs were fabricated. HEMTs demonstrated similar f_T values of about 1 GHz with extracted $f_T / f_{max} > 4$. Considering the dimensions of investigated transistors and their competitive performance in the S-band, the InAlGaN-based HEMT structures demonstrated great potential for new applications in high frequency electronic and plasmonic devices.

Table 1. Properties of 2DEG in studied HEMT structures at 300 K (at 77 K)

Sample	d_{2DEG} (nm)	U_{th} (V)	N_{2DEG} , ($\times 10^{13} \text{ cm}^{-2}$)	μ ($\text{cm}^2/\text{V s}$)
InAlGaN on Sapphire	10	-1.8	1.2 (1.2)	1660 (8830)
AlGaN “buffer-free” on SiC	19	-3.0	1.0 (1.0)	1590 (10140)
Typical AlGaN on SiC	19	-3.1	0.9 (0.8)	1900 (19690)

We acknowledge the support from the Research Council of Lithuania through the “T-HP” Project (No. 01.2.2-LMT-K-718-03-0096).

REFERENCES

- [1] M. Bauer *et al.*, *IEEE Trans. Terahertz Sci. Technol.*, **9**, 430–444 (2019)
- [2] J. Jorudas *et al.*, in *47th International Conference on Infrared, Millimeter, and Terahertz Waves*, 2022.
- [3] V. Janonis *et al.*, in *Terahertz Emitters, Receivers, and Applications XI*, 2020.
- [4] M. B. Tahhan *et al.*, “*IEEE Trans. Electron Devices*”, **69**, 962–967 (2022).
- [5] J. Jorudas *et al.*, *Materials (Basel)*, **15**, 1118 (2022).

Influence of the design of parabolic AlGaAs barriers on the optical properties of GaAsBi quantum wells

Monika Jokubauskaitė, Evelina Dudutienė, Andrea Zelioli, Arnas Pukinskas, Simona Pūkienė, Bronislovas Čechavičius and Renata Butkutė

Center for Physical Sciences and Technology, Saulėtekis ave. 3, Vilnius, Lithuania

Email: monika.jokubauskaite@ftmc.lt

It is known that only few percent of Bi incorporation in the lattice of GaAs to arsenic site significantly reduces the band gap of the semiconducting compound. It opens up possibilities to apply GaAsBi as an active media in fabrication of optoelectronic devices operating in IR spectrum range. Nevertheless, it is crucial to continue study of GaAsBi in order to explore the influence of design of active area to optical properties so that optimization of optoelectronic devices could be achieved. Recently our group [1] developed quantum structure design consisting of GaAsBi quantum wells with parabolically graded AlGaAs barriers (PGBs) and demonstrated that these structures exhibited by 50 times stronger photoluminescence at room temperature in comparison with rectangular quantum wells.

In this work the temperature- and excitation-dependent photoluminescence study of three different quantum structures of designs shown in Fig. 1 was performed. As it was expected higher PL intensity was observed for GaAsBi quantum structures containing multiple GaAsBi QWs. Excitation-dependent PL measurements showed that the radiative recombination in investigated GaAsBi quantum structures was of comparable rate with non-radiative recombination at room temperature. Almost two times stronger in magnitude localization effect was established for 2PQW and 3in1PQW structures assuming parabolic shape of barriers as an additional mechanism responsible for increased PL intensity at room temperature. Moreover, numerical calculation revealed that the design of AlGaAs PGB does not affect the energy of optical transitions between ground states of GaAsBi QW embedded in AlGaAs PGB.

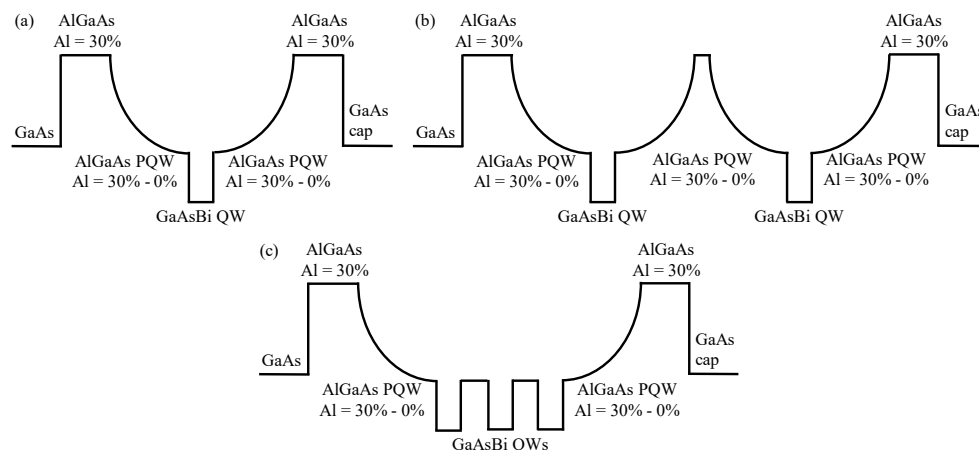


Fig. 1 Designs of the quantum structures: (a) 1PQW – GaAsBi SQW with AlGaAs PGBs, (b) 2PQW – GaAsBi MQW with AlGaAs PGBs and (c) 3in1PQW – three QWs embedded together in one pair of PGBs.

REFERENCES

[1] S. Pūkienė *et al.*, *Nanotechnology* **30** (2019).

Intentional modification of nanocrystalline graphene coatings by thermal annealing

Algimantas Lukša¹, Saulius Balakauskas¹, Virginijus Bukauskas¹, Viktorija Nargelienė¹, Marius Treideris¹, Martynas Talaikis², Arūnas Šetkus¹

¹Department of Physical Technologies, Center for Physical Sciences and Technology

²Department of Organic Chemistry, Center for Physical Sciences and Technology,
Saulėtekio ave. 3, LT-10257 Vilnius, Lithuania.

Email: algimantas.luksa@ftmc.lt.

Functional coatings with the properties sensitive to surrounding media physical and chemical influence are highly attractive for engineering of the key components in optoelectronics based detecting systems applied in diverse practical areas including medicine and life sciences [1]. Applications in chemical and biochemical sensing is typically dependent on possibilities to combine the detection methods with the controllable features of microfluidic systems as in [2]. According to our technological studies nanocrystalline graphene films are acceptable to produce a membrane with the properties comparable to that of the 2D materials and sensitive to media – membrane interaction.

The membranes can be formed on the surface of the optoelectronic elements at low temperatures and, therefore, can be used for modification of the surface in the photonic integrated circuits. Our present study improves the technology of these functional membranes.

The aim of this work is to investigate a thermal annealing effect for improvement of microcrystalline coatings. For this task several nanocrystalline graphene coatings with unique properties were grown by using Plasma-enhanced chemical vapor deposition. Coatings were deposited from methane precursor on dielectric substrates at different growing temperatures. The intensities of the Raman spectra in Fig. 1 revealed the relationship between the characteristics of the graphene membranes and the growth temperature. In addition, the membranes were modified by changing the distance between the substrate and the plasma source. The samples were annealed in vacuum at 450 °C. The Raman spectroscopy and AFM microscopy were used for experimental analysis of the coatings.

REFERENCES

- [1] Nelson, Gilbert L., et al. Enabling Microscale Processing: Combined Raman and Absorbance Spectroscopy for Microfluidic On-Line Monitoring. *Anal. Chem.* **93** (2021) pp. 1643-1651.
- [2] Alazzam, Anas, and Nahla Alamoodi. Microfluidic devices with patterned wettability using graphene oxide for continuous liquid–liquid two-phase separation. *ACS Appl. Nano Mater.* **3** (2020) pp. 3471-3477.

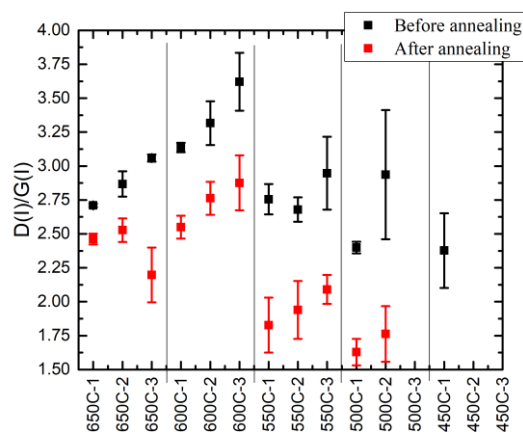


Fig. 1 Intensity ratio of D and G Raman modes for nanocrystalline graphene coatings before and after thermal annealing (Numbers 1; 2; 3 marks different distance from plasma source).

Transmission electron microscopy of Hybrid graphene-lanthanum perovskite structures

Martynas Skapas¹, Nerija Žurauskienė¹

¹ Center for physical science and technology, Saulėtekio av. 3, Vilnius, Lithuania.

Email: Martynas.skapas@ftmc.lt

The detection of magnetic fields with increased spatial resolution to micro-nanoscales is very important for magnetometry [1]. It is of great interest to have low-dimension sensors with increased sensitivity and extended capabilities. The discovery of magnetoresistive (MR) effects (AMR, TMR, GMR and CMR) in magnetic structures encouraged fundamental research leading to a number of laboratory-scale and commercially available devices [2]. Moreover, nowadays, the magnetosensorics becomes very important for wearable electronics and soft robotics. Each application has its specific requirements for sensitivity, temperature and magnetic field ranges of operation, accuracy, sensor's positioning, etc. Therefore, the choice of material with specific properties and design of sensing element becomes very important.

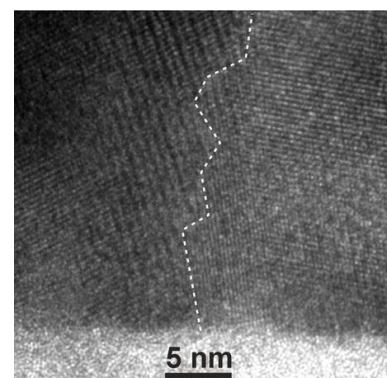


Fig. 1 High-resolution TEM images of an interface between intermixed layer (near the substrate) and two adjacent LSMO grains

High-resolution transmission electron microscopy (HRTEM) study of hybrid graphene-lanthanum perovskite structures is presented in this work. These graphene and lanthanum perovskite $\text{La}_{1-x}\text{Sr}_x(\text{Mn}_{1-y}\text{Co}_y)\text{O}_3$ (LSMCO) films were grown by using MW PECVD and pulsed-injection MOCVD and serves as a main active element of magnetoresistive sensor with tunable sensitivity. Such novel hybrid sensor would provide possibilities to decrease its dimensions for measuring magnetic fields in small volumes, especially for measurement of field direction in respect to reference plane, when in conventional methods three sensors are used.

High-resolution TEM image (Fig. 1) show smooth interface between LSMO and intermediate LSMO-SiO₂ layers, with a zigzag interface between LSMO grains and a wide boundary. In this case, crystallites grow on amorphous layer, thus initial crystallite is oriented randomly, and after their coalescence, smaller crystallites with a random orientation are formed.

These structural peculiarities, unresolvable by other techniques, affect magnetic properties, such as magnetoresistance anisotropy and sensor sensitivity, so in-depth structural analysis is crucial in sensor development and could be used for the development of magnetic field sensors with predetermined parameters for operation at low or high temperatures.

REFERENCES

- [1] Pisana et al. Nano Lett. 2010, 10, 341, DOI:10.1021/nl903690y
- [2] Zheng et al, IEEE Trans. Magn. 2019, 55, 0800130, DOI: 10.1109/TMAG.2019.2896036

Structural, optical, and mechanical properties of silicon nitride films deposited by inductively coupled plasma enhanced chemical vapor deposition

Ezgi Abacioğlu¹, José Luis Fernández Estévez¹ and Andreas Stöhr¹

¹Optoelectronics, University of Duisburg-Essen, Lotharstraße 55, 47057 Duisburg, Germany

Email: ezgi.abacioglu@uni-due.de

Silicon nitride (SiN_x) is a widely used dielectric material due to its superior optical properties and compatibility with processing techniques of semiconductor and microelectronics devices. Other than its potential applications, this material is regarded as a hard-mask material for patterning of such devices [1, 2] and as an alternative to traditional doped silica waveguide technology in indium phosphide-based photonic integrated circuits (InP PICs) [3]. In the context of the required SiN_x film thicknesses, which are generally greater than $1\text{ }\mu\text{m}$ for dry etching, the mechanical stress within these films can make processing steps such as photolithography extremely challenging along with affecting the integrity and performance of the PICs.

In this study, a low-temperature and low-pressure SiN_x film deposition on InP substrates is investigated using inductively coupled plasma enhanced chemical vapor deposition (ICPECVD) technology. Figure 1(a) shows the deposition rates of the SiN_x films deposited at different temperatures as a function of deposition time whereas Figure 1(b) demonstrates the dependency of the refractive index (n) on deposition temperature as a function of wavelength. We discuss herein the results of an extensive characterization of structural and mechanical properties of the ICPECVD- SiN_x films along with the results given in Figure 1.

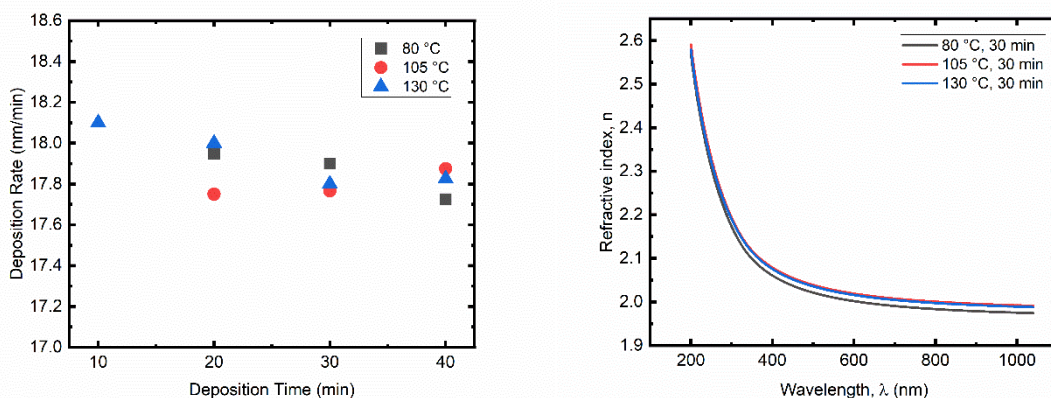


Fig. 1 Dependencies of deposition rate (a) and refractive index (b) of SiN_x films on deposition temperature.

REFERENCES

- [1] V. Jovanović *et al.*, "Sub-100 nm silicon-nitride hard-mask for high aspect-ratio silicon fins", *Proceedings of the International Convention MIPRO* (2007).
- [2] J. Haneveld *et al.*, "Nano-ridge fabrication by local oxidation of silicon edges with silicon nitride as a mask", *Journal of Micromechanics and Microengineering* (2016) 16 S24.
- [3] J. Klamkin *et al.*, "Indium Phosphide Photonic Integrated Circuits: Technology and Applications", *IEEE BiCMOS and Compound Semiconductor Integrated Circuits and Technology Symposium* (2018) pp. 8-13.

High-field electron transport measurements in (Be,Zn)MgO/ZnO heterostructures

Oleg Kiprijanovič¹, Linas Ardaravičius² and Emilis Šermukšnis²

¹Department of Functional Materials and Electronics, ²Department of Fundamental Research, Center for Physical Sciences and Technology, Saulėtekio av. 3, Vilnius LT-10257, Lithuania.
Email: linas.ardaravicius@ftmc.lt.

Zinc oxide (ZnO) is a wide-band gap semiconductor and has been used in a number of electronic, optoelectronic devices and sensors [1]. ZnMgO/ZnO heterostructures are promising when exploiting a high density two-dimensional electron gas (2DEG) channels (in excess of 10^{13} cm^{-2}) as a result of strong polarization fields [2].

The investigated ZnO-based heterostructures were grown by molecular beam epitaxy (MBE) at Virginia Commonwealth University (USA) [3,4]. The low-field electron mobility and electron density were estimated from Hall effect data or from measuring the sample resistance in TLM channel patterns. Studies of electron transport at high electric fields were performed with the use of nanosecond-pulsed technique to obtain current-voltage characteristics and estimate electron drift velocity [5].

In this work the measurements of the characteristics in ZnO 2DEG channels at ZnO/ZnMgO and BeZnMgO/ZnO heterointerfaces were made at room temperature with the pulses of 2-5 ns widths. The application of the pulses having few ns duration minimized Joule heating. The contact resistance was taken into account. The highest electric field strength of 360 kV/cm was attained in ZnO/ZnMgO heterostructures, while the highest drift velocity of $2.0 \times 10^7 \text{ cm/s}$ was achieved in BeZnMgO/ZnO heterostructures. The electron transport results at high electric fields (Fig. 1) are explained emphasizing the effect of non-equilibrium longitudinal optical phonons (hot-phonon effect).

REFERENCES

- [1] C. F. Klingshirn, A. Waag, A. Hoffmann, and J. Geurts, *Zinc Oxide: From Fundamental Properties Towards Novel Applications*, Berlin: Springer (2010); U. Ozgur, V. Avrutin, and H. Morkoc, in: *Molecular Beam Epitaxy*, Amsterdam: Elsevier (2018) pp. 343-375.
- [2] H. Tampo *et al.*, *Appl. Phys. Lett.* **93**, (2008) pp. 202104; R. Singh, Md. A. Khan, P. Sharma, M.T. Htay, A. Kranti, and S. Mukherjee; *J. Phys. D: Appl. Phys.* **51**, (2018) pp. 13LT02.
- [3] E. Šermukšnis, J. Liberis, A. Matulionis, V. Avrutin, M. Toporkov, U. Ozgur and H. Morkoc; *J. Appl. Phys.* **123**, (2018) pp. 175702.
- [4] K. Ding, V. Avrutin, N. Izyumskaya, U. Ozgur, and H. Morkoc; *J. Vac. Sci. Technol. A* **38**, (2020), pp. 023408.
- [5] L. Ardaravičius, O. Kiprijanovič, M. Ramonas, E. Šermukšnis, J. Liberis, A. Šimukovic, A. Matulionis, Md. B. Ullah, K. Ding, V. Avrutin, U. Ozgur, and H. Morkoc; *J. Appl. Phys.* **126**, (2019) pp. 185703.

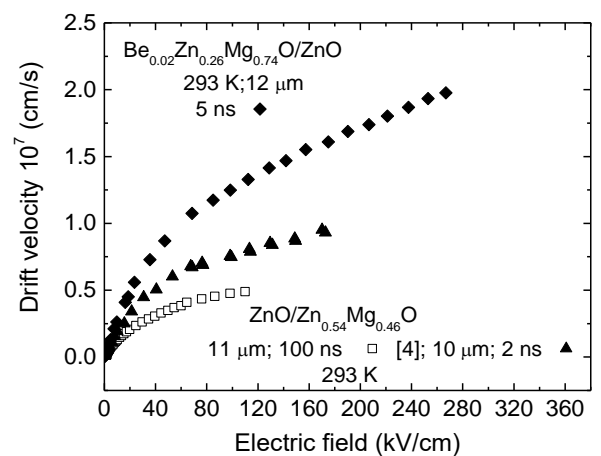


Fig.1. Experimentally obtained electron drift velocity versus the applied electric field in ZnO/ZnMgO (triangles, squares) and BeZnMgO/ZnO (diamonds) heterostructures at room temperature. Voltage pulse duration : 2 ns (triangles), 5 ns (diamonds), and 100 ns (squares [4]). Electron density: $7.7 \times 10^{12} \text{ cm}^{-2}$ (diamonds) and $6.1 \times 10^{12} \text{ cm}^{-2}$ (triangles, squares). Channel lengths are 10-12 μm .

Double Fano resonance in broken symmetry split-ring resonator array metasurface

Darius Urbonis¹, Paulius Ragulis¹, Gediminas Šlekas¹ and Žilvinas Kancleris¹

¹Department of Physical Technologies, Center for Physical Sciences and Technology, Saulėtekio av. 3, Vilnius, Lithuania.

Email: darius.urbonis@ftmc.lt

Fano resonance in metasurfaces is observed as a peak in transmission spectrum with asymmetric line shape. It arises due to constructive and destructive interference between discrete and continuum states. A common characteristic feature of such resonance is its high Q-factor which is important for many devices that exploit resonance [1].

In a microwave frequency range, we have found double Fano resonance in a split-ring resonator (SRR) array with broken symmetry (Fig. 1 a), which is achieved by displacing every second column of the SRRs from the symmetry position, decreasing the gap Δ . Even a small change of Δ , causes an appearance of the first resonance (f_1). As the gap decreases, the resonance amplitude grows, and the second resonance emerges (f_2). In Fig. 1 b calculated and experimentally measured transmittance spectra are shown for the SRR array fabricated on laminate FR-4 ($\Delta=1$ mm, dielectric thickness $d=1.5$ mm). The measured spectrum shows a good match with the simulation. It is also seen that amplitudes increase when the lossless material is applied. It seems that the nature of f_1 and f_2 is different. The first resonance appears due to the interaction of the lattice mode with the third plasmonic resonance [2], whereas the second resonance arises as a consequence of close proximity of the neighboring SRRs.

This work has received funding from the Research Council of Lithuania (LMTLT), project No S-SV-22-56.

REFERENCES

- [1] Khanikaev et al., Nanophotonics, vol. 2, no. 4, 2013, pp. 247-264.
- [2] D. Seliuta et al., Opt. Lett. 44, 759-762 (2019).

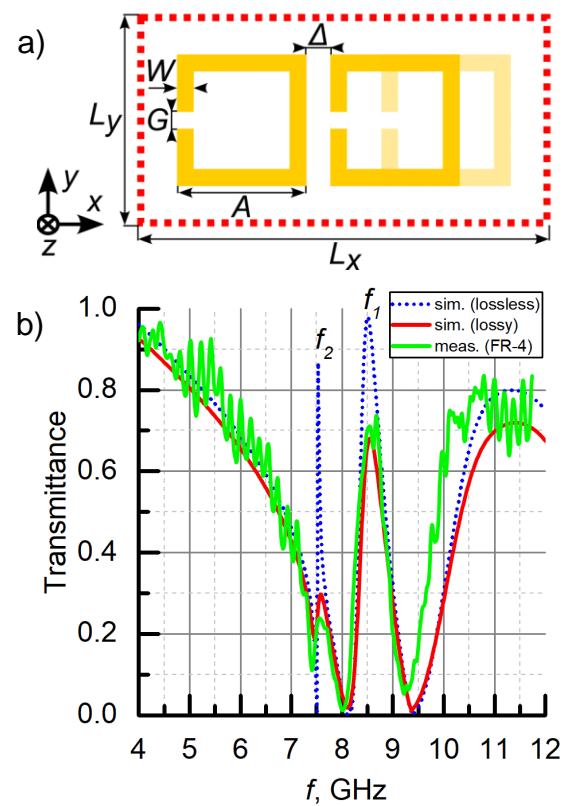


Fig. 1 a) metasurface unit cell, $L_x = 32$, $L_y = 16$, $A = 10$, $W = G = 1$, $d = 1.5$ (units in mm), b) transmittance spectrum with two Fano resonances (f_1 , f_2) excited by y-polarized electric field.

Compact rectennas for energy harvesting using SSAIL technique

Justina Žemgulytė¹, Paulius Ragulis¹, Gediminas Šlekas¹, Romualdas Trusovas², Karolis Ratautas², Rimantas Simniškis¹, Žilvinas Kancleris¹, Gediminas Račiukaitis²

¹ Department of Physical Technologies, Center for Physical Sciences and Technology, Lithuania

² Department of Laser Technologies, Center for Physical Sciences and Technology, Lithuania

Email: justina.zemgulyte@ftmc.lt

Energy harvesting is being heavily researched due to the possibility of replacing batteries in low-energy electronic devices and wireless sensor networks. The main requirements for such a system are that it has to be efficient and compact. The novel Selective Surface Activation Induced by Laser (SSAIL) technique allows to design more efficient and compact energy harvesting systems.

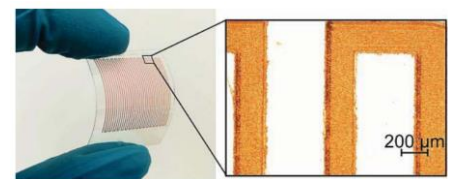


Fig. 1 Meander circuit on flexible PET using SSAIL [1]

The SSAIL technique has three main steps: surface sensitization by the laser; chemical treatment in an activator solution; and electroless plating. SSAIL enables one to be very flexible when choosing a substrate because metallization can be grown on rigid or flexible polymers (fig. 1) or glass. On top of that, using this technique, it is possible to integrate an antenna, matching impedance network, and rectifier on the same substrate plate. As a result, fewer connections and shorter traces increase the overall efficiency of the system.

We designed a Wi-Fi frequency energy harvester system which includes a slot antenna, a full-wave rectifier (fig. 2), and an impedance matching network. The system was manufactured on RO3210 dielectric material using the SSAIL method. System performance was measured and compared to an identical system manufactured on FR-4 dielectric material using traditional photolithography. Because of RO3210's higher dielectric constant, antenna size becomes significantly smaller.

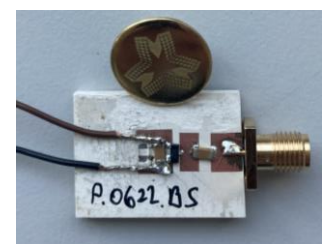


Fig. 2 Full wave rectifier without impedance matching circuit on RO3210 manufactured using SSAIL

REFERENCES

[1] Ratautas, K., Norkus, E., Jagminienė, A., Račiukaitis, G., & Stankevičienė, I. (2018). Laser Assisted Selective Metallization of Polymers; Laser Assisted Selective Metallization of Polymers. In 2018 13th International Congress Molded Interconnect Devices (MID).

This project has received funding from [European Social Fund] [European Regional Development Fund] (project No 01.2.2 LMT-K-718-03-0038) under a grant agreement with the Research Council of Lithuania (LMTLT)

Optically detected cyclotron resonance in CdTe-based quantum wells

Jerzy Łusakowski¹, Adam Siemaszko¹, Maciej Zaremba¹ and Tomasz Wojtowicz²

¹*Faculty of Physics, University of Warsaw, ul. L. Pasteura 5, 02-093 Warsaw, Poland*

²*Institute of Physics, Polish Academy of Sciences, al. Lotnikow 32/46, 02-668 Warsaw, Poland*

Email: jerzy.lusakowski@fuw.edu.pl

We present results of magnetospectroscopic studies on a single CdTe quantum well (QW) with Cd_{0.8}Mg_{0.2}Te barriers modulation-doped with Iodine donors. Experiments were carried out at temperature equal to 1.8 K as a function of magnetic field up to 10 T and included measurements of THz transmission, photoluminescence in the energy range of the fundamental band gap and optically detected cyclotron resonance (ODCR).

Transport measurements determined concentration of a two-dimensional electron gas (2DEG) in the CdTe QW to be $3.3 \times 10^{11} \text{ cm}^{-2}$ in the darkness $3.4 \times 10^{11} \text{ cm}^{-2}$ after over the barrier illumination. These values were used to establish the filling factors in the analysis of optical spectra.

THz transmission measurements allowed us to determine the effective mass of electrons which was to be $(0.1020 \pm 0.0006)m_e$, consistent with earlier studies on CdTe QWs. Magnetoluminescence spectra showed the Fermi-edge-singularity shape that is characteristic for QWs with such a high 2DEG concentration and allowed us to observe a band-to-band recombination between Landau levels in the conduction and valence bands. However, a complicated dependence of hole Landau levels on magnetic field did not allow us to estimate the value of the effective mass of holes which took part in the luminescence transitions. ODCR spectra showed that heating of 2DEG by absorption of a THz radiation leads to redistribution of electrons between all observable Landau levels, not just those adjacent to the Fermi energy.

In conclusion, we have shown on the example of CdTe/Cd_{0.8}Mg_{0.2}Te QW that the combination of magnetotransport with THz and VIS magnetospectroscopy allows for a thorough characterization of the structure of quantum levels in a two-dimensional system. The comprehensive procedure applied in our study show the way to plan and carry out experiments on less known semiconductor objects.

This research was partially supported by the Polish National Science Centre grant UMO-2019/33/B/ST7/02858.

Quantum well infrared photodetector operating at room temperature

Karolis Redeckas¹, Ignas Grigelionis¹, Vladislovas Čižas¹, Vytautas Jakštas²,
Renata Butkutė¹, Andrius Bičiūnas¹, Linas Minkevičius¹

1 Department of Optoelectronics, Center for Physical Sciences and Technology, Saulėtekio al. 3, Vilnius, Lithuania

2 Department of Physical Technologies, Center for Physical Sciences and Technology, Saulėtekio al. 3, Vilnius, Lithuania

Email: karolis.redeckas@ftmc.lt

In today's quickly technologically emerging world infrared frequency range sensing systems are becoming more and more involved in real applications like security, healthcare etc. [1]. However, since the first demonstration of quantum well infrared photodetector (QWIP) in early 90-ies, cryogenic cooling is still widely used to reduce the high detector's background noise. In the current study room temperature operating QWIPs were developed to respond to the high demand of infrared detectors for specific gas sensing [2].

In this work, the properties of GaAs/AlGaAs QWIP detectors designed and built using the FTMC facilities for 8-9 μm wavelength detection range are investigated. Characterization at room temperature as well as at the temperatures below 100 K was performed by measuring electrical properties and acquiring infrared photoresponse spectra in order to estimate signal to noise ratio and spectral responsivity.

Spectra were obtained using conventional infrared Fourier spectroscopy. The collimated radiation emanating from the spectrometer was focused onto a surface of the QWIP. It was placed in the cryostat and biased with the DC voltage. Photo response was measured by using the Lock-in technique, mechanically chopping output radiation at 211 Hz.

The obtained results give an opportunity for the development of room temperature QWIPs which in turn opens possibilities for compact and light-weight sensing systems to be developed and used in wide amount of practical applications.

REFERENCES

- [1] D. Tyagi, H. Wang, W. Huang et al., Recent advances in two-dimensional-material-based sensing technology toward health and environmental monitoring applications, *Nanoscale* 12, 3535-3559 (2020).
- [2] A. Agarwal et al., On-chip mid-infrared gas detection using chalcogenide glass waveguide, *Appl. Phys. Lett.* 108, 141106 (2016).

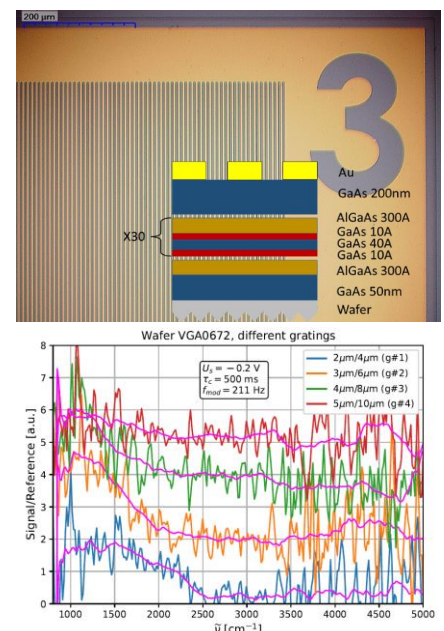


Fig. 1 The photo of the part of QWIP detector and its schematic cross section (upper). Spectra obtained at room temperature (lower)

Radiometric imaging and pulsed X-ray-based studies of light collection from scintillating crystals

Žygimantas Vosylius, Vincas Tamošiūnas, Maksim Jemeljanov,
and Gintautas Tamulaitis

*Institute of Photonics and Nanotechnology, Vilnius University,
Saulėtekio Ave. 3, LT 10257 Vilnius, Lithuania
E-mail: zygimantas.vosylius@ff.vu.lt*

Scintillator-based detectors are used in multiple advanced applications such as fast radiation detection systems used for high energy physics experiments or time-of-flight positron emission tomography (TOF-PET) in medical imaging. Light transfer efficiency (LTE) from the crystal bulk to the photodetector substantially affects as the coincidence time resolution (CTR) of the radiation detector [1].

In this contribution, we report on the photon transport investigation results obtained using two techniques. The pulsed X-ray system described in [2] was adapted to study the influence of excitation position within 40 mm × 3 mm × 3 mm Ce-doped gadolinium aluminum gallium garnet (GAGG:Ce) crystal on the signal generated in silicon photomultiplier (Onsemi MICROFC-SMA-60035-GEVB). The developed photon transport efficiency measurement technique serves as an alternative to the measurements using crystals of various lengths [1] and avoids the possible influence of crystal surface quality or wrapping variations.

The second technique was devoted to reveal more details about the light transport in the vicinity of the excitation point. We exploited UV excitation and radiometric imaging of the scaled scintillator model with the same wrapping. BC-408 organic scintillator slab of 100 mm × 25 mm × 30 mm in size was illuminated either by 365 nm or 395 nm light emitting diodes. The apparent radiance (Fig. 1) was evaluated by imaging performed by using a CCD camera. These imaging experiments revealed an efficient redistribution of the irradiance by the surface scattering of PTFE wrapping and the presence of significant specular reflection components despite the contact between the scintillator and PTFE.

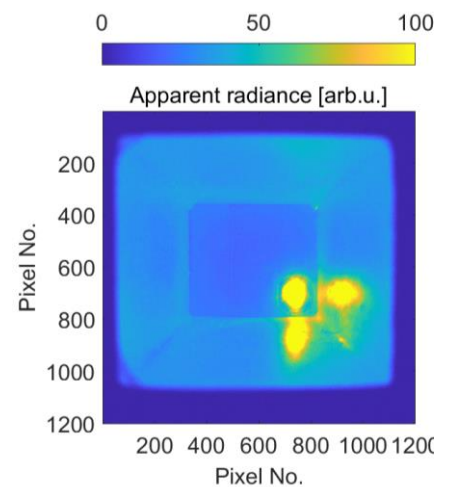


Fig. 1 False color image of interior surfaces of BC-408 scintillator slab under UV excitation. Yellow spots indicate the excitation area and specularly reflected images of it.

REFERENCES

- [1] S. Gundacker, A. Knapitsch, E. Auffray, P. Jarron, T. Meyer, P. Lecoq; *Nucl. Instrum. Methods. Phys. Res. A* **737** (2014) pp. 92-100.
- [2] K. Nomeika, Ž. Podlipskas, V. Tamošiūnas, J. Jurkevičius, M. N. Alsamsam, S. Nargelas, R. Aleksiejūnas, M. Korjik, G. Tamulaitis; *Nucl. Instrum. Methods. Phys. Res. A* **1029** (2022) 166408.

Study of thermo-refractive noise in solid-state dual frequency micro-lasers

Jose Javier Fernandez-Pacheco¹, Vincent Crozatier¹ and Loïc Morvan¹

¹Thales, Research & Technology, 1 Avenue Augustin Fresnel, 91120 Palaiseau, France
Email: jose-javier.fernandez-pacheco@thalesgroup.com.

Solid-state micro-lasers based on rare-earth ions doped active mediums are known to provide extremely low optical phase noise signals, down to 1 Hz linewidth. When using a dual-frequency cavity, they are then good candidates for the generation of ultra-low phase noise millimeter to THz beatnotes on high speed photomixers or photodiodes. However, this linewidth is far from the Schawlow-Townes limit (typ. 1 mHz): the temperature fluctuations of the medium, either induced by pump beam intensity noise, or due to intrinsic thermodynamic fluctuations, is the limiting factor. It induces intra-cavity index fluctuations through thermo-optic effect, and lead then to extra phase noise for the output signal. We plan to investigate this phenomena in a diode-pumped Er:Yb:glass laser, both theoretically and experimentally, and study the means to reduce this noise contribution.

For this purpose, we first implemented a specific temperature control of the active medium's temperature on a dedicated simplified laser setup, allowing several tens of degrees temperature variation. In parallel, we used a microlaser [1], shown on Figure 1, where the temperature of the whole cavity can also be changed. We also optimized a custom optical phase noise test bench. Due to the change of thermo-refractive coefficient over temperature of the active medium, and due to the spatial distribution of pump and laser beams, we expect to evidence phase noise changes. The preliminary results are shown in the next figure. Apart from a noise floor changes that may be related to measurement conditions, we were not able to see phase significant phase noise variations. Theoretical and experimental work will be pursued in order to explain the observed behavior.

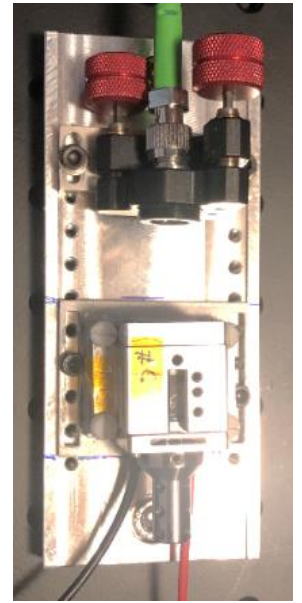
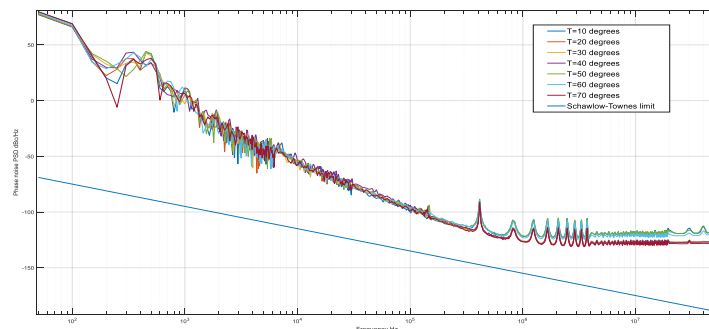


Figure 1. Dual Frequency Microlaser used



REFERENCES

[1] G. Pillet, L. Morvan, M. Brunel, F. Bretenaker, D. Dolfi, M. Vallet, J. Huignard and A. Le Floch (2008) Dual-Frequency Laser at 1.5 μm for Optical Distribution and Generation of High-Purity Microwave Signals. Journal of Lightwave Technology Vol 26.

Optimization of Coherent Thermal Emission from Circular Shape n-GaN Surface Relief Gratings

Vytautas Janonis¹, Pawel Prystawko², Evaldas Valasevičius¹, and Irmantas Kašalynas¹

¹*Center for Physical Sciences and Technology (FTMC), Vilnius, Lithuania.*

²*Institute of High Pressure Physics PAS (UNIPRESS), Warsaw, Poland.*

Email: vytautas.janonis@ftmc.lt

The periodic structures processed on the surface of various materials have been shown to possess extraordinary emission profiles facilitated by the evanescent surface wave excitation¹. Progress on the surface polaritons in metallic and in polar semiconductor structures accelerated development of coherent thermal emitters with exceptional temporal (narrow linewidth) and spatial (directive) coherence^{2,3}. The hybrid surface plasmon-phonon polaritons (SPPPhPs) were recently demonstrated in the linear surface relief gratings developed on high-crystal quality *n*-GaN semiconductor^{3,4}.

In this work we developed a circular shape design of the coherent thermal sources based on hybrid surface plasmon-phonon polaritons (SPPPhPs) excavated in the *n*-GaN surface relief gratings. In new design the propagation losses of SPPPhPs were optimized by considering the dispersion of polaritons^{3,4}. We found that the circular shape surface relief gratings (CSGs) with properly optimized values of the filling factor, *FF*, the groove height, *h*, and periodicity, *P*, show enhanced temporal and spatial coherence properties. For this reason, the emission performance of CSG with *h* = 1 μm and *P* = 17.5 μm was optimized at the target frequency of 570 cm⁻¹. With the change of *FF* from 50% to 25%, the improvement in the linewidth and the directivity of resonant emission peak was from 7 cm⁻¹ down to 1 cm⁻¹ and from 1.3 deg down to 0.24 deg, respectively.

Optimized parameter CSG samples of 5 mm in diameter were fabricated on the high-crystal quality *n*-doped GaN wafers. The emission characteristics of samples heated up to 500 C were measured by using a FTIR spectrometer without collimating optics exploring high beam coherence of the improved-design CSG. A good agreement between the theoretical and experimental spectra of all samples were found. While at normal direction (0 deg) the emission of linear- and circular-shape surface relief *n*-GaN gratings revealed very similar beam characteristics in experiment, only later design samples have demonstrated proper beaming at the design frequency with the highest angular directivity values found for a case of *FF*=25 % to be of about 0.2 deg and 2 deg in theory and experiment, respectively.

The work was supported by the Research Council of Lithuania through the “T-HP” project Grant No.01.2.2-LMTK-718-03-0096. The work at Warsaw was supported from the National Centre for Research and Development (Grant No.WPC/20/DefeGaN/2018).

REFERENCES

- [1] G. Lu et al, ACS Omega **5**, p. 10900 (2020), doi: 10.1021/acsomega.0c00600.
- [2] D. G. Baranov et al, Nat. Mater. **18**, p. 920 (2019), doi: 10.1038/s41563-019-0363-y.
- [3] V. Janonis et al. Appl. Phys. Lett **116**(11) (2020), doi: 10.1063/1.5143220.
- [4] V. Janonis et al, Opt. Express **29**, p. 13839 (2021), doi: 10.1364/OE.423397.

Application of terahertz time-domain spectroscopy in the study of air components and vapors of organic compounds

D.Sanda, I. Žičkienė, R. Adomavičius

*Center for Physical Sciences and Technology,
Savanorių Ave. 231, LT-02300 Vilnius, Lithuania.*

Email: dominykas.sanda@ff.stud.vu.lt

Both absorption and the refractive index of materials can be measured by terahertz time-domain spectroscopy (THz-TDS). In this work, THz-TDS is used to measure the refractive index of air components (carbon dioxide, oxygen, nitrogen) and study the absorption of chemical vapors. The values of the refractive index of gases have been of interest to scientists for a long period of years, and recently the field of communication and distance measurement has given a new impulse to the need for accurate values. At present, remarkable accuracy of measuring the refractive index of gases in the optical and acoustic ranges has been achieved. Meanwhile, in the terahertz range, accurate measurements of the refractive index of gases have not been performed [1]. Another part of our studies examines vapors of organic compounds that are of great importance in biology and industry. The work presents the results of studies of the following compounds: ammonia, isopropanol, propanol, ethyl acetate, acetone and ethanol.

The purpose of the refraction index research was to determine the factors the accuracy of THz TDS measurements depends on, as well as outline recommendations for improving the current measurement accuracy. It is established that the accuracy of the measurement of the time shift of the terahertz pulse, the mechanical stability of the measuring system and the control of the gas temperature are the most important factors that affect the accuracy of the determination of the refractive index. It was established that the accuracy of the measurements performed reached 2×10^{-5} , but it proved to be the case that after changing the design of the gas cell, it is possible to reach an accuracy of 1×10^{-6} .

A real-time spectroscopy technique was developed for vapor absorption measurement applications. The results obtained by this methodology can be represented in 3D space, the coordinates of which are time, frequency and vapor absorption. Such 3D measurement stores information about the vapor absorption spectrum and shows the variation of this spectrum with a temporal resolution of 100 ms. In our work, we demonstrate that real-time gas spectroscopy increases the probability of molecular recognition and allows the study of gas dynamic processes.

REFERENCES

[1] B. H. Sang and T.-I. Jeon; *Optics Express* **24** (2016) pp. 29040-29047.

Investigation of sensitivity limits of a near-field THz sensor based on a Si CMOS technology

Alexander V. Chernyadiev¹, Dmytro B. But¹, Cezary Kołaciński^{1,2}, Kęstutis Ikamas^{3,4},
and Alvydas Lisauskas^{1,3}

¹CENTERA Laboratories, Institute of High Pressure Physics PAS, Warsaw, Poland

²Łukasiewicz Research Network, Institute of Microelectronics and Photonics (Ł-IMI), Warsaw, Poland

³Institute of Applied Electrodynamics and Telecommunications, Vilnius University, Lithuania

⁴General Jonas Žemaitis Military Academy of Lithuania, Vilnius, Lithuania

Email: acherniadev@unipress.waw.pl

Resonator-based sensors became a promising concept for label-free detection of biological substances with high values of sensitivity and low detection limit. Ideally, the sensitivity down to a single molecule is required which was already achieved with an optical microresonator-based sensor [1]. At terahertz (THz) frequencies a big step towards such sensitivity was made this year [2], when the authors managed to couple free-space THz radiation to a single subwavelength split-ring resonator and estimate the number of electrons from the two dimensional electron gas coupled to the single metallic planar resonator. Systems of coupled resonators may propel the sensitivity values even further due to their asymmetrical resonance profile and steep resonance slope [3]. Recent works of P.H. Bolivar group in the THz frequency range have proved the applicability of frequency selective surfaces for biosensing applications [4]. Here we propose our own solution of a future near-field THz sensor based on vertically coupled planar resonators (Fig.1). Such detectors can be fabricated using the commercial Si CMOS platform with a prospect of enabling to detect low sample volumes.

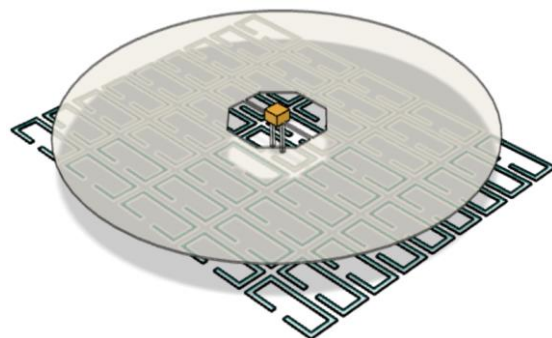


Fig. 1 Schematic illustration of the near-field THz sensor based on vertically coupled resonators: a slot-dipole antenna and a surface of split-ring resonators. The yellow cube in the figure represents the dielectric material loading the antenna and causing detuning of the coupled system.

REFERENCES

- [1] A. M. Armani, R. P. Kulkarni, S. E. Fraser, R. C. Flagan, and K. J. Vahala; *Label-free, single-molecule detection with optical microcavities*, Science 317 (2007) pp.783-787.
- [2] S. Rajabali, S. Markmann, E. Jöchl, M. Beck, C. A. Lehner, W. Wegscheider, J. Faist, and G. Scalari; *An ultrastrongly coupled single terahertz meta-atom*, Nature Communications, vol. **13**, 2528 (2022).
- [3] Y.-F. Xiao, V. Gaddam, and L. Yang; *Coupled optical microcavities: an enhanced refractometric sensing configuration*, Optics Express, vol. **16**, no. 17 (2008) pp. 12538-12543.
- [4] C. Weisenstein, D. Schaar, A. K. Wigger, H. Schäfer- Eberwein, A. K. Bosserhoff, and P. H. Bolívar; *Ultra-sensitive thz biosensor for pcr-free cdna detection based on frequency selective surfaces*, Biomed. Opt. Express, vol. **11**, no. 1 (2020) pp. 448–460.

Development of an integrated Schottky based heterodyne THz receiver at 300 GHz using power combining approach

H. Gohil^{1,2}, H. Wang¹, C. Renaud² and P. Huggard¹

¹ RAL Space, Science and Technologies Facilities Council, UKRI, UK.

² Department of Electronic and Electrical Engineering, UCL, UK.

Email: himanshu.gohil@stfc.ac.uk

The aim of this research is to develop a heterodyne THz receiver using a sub-harmonic Schottky mixer pumped by a photonic local oscillator for detection above 300 GHz.

The photonic local oscillator (LO) pumping the mixer will be based on Uni-travelling carrier (UTC) photodiodes (>75 GHz). The photodiode output will then be doubled using a frequency multiplier to generate the LO signal for the sub-harmonic mixer. To produce a suitable amount of LO power while overcoming the frequency multiplier losses, power combining will be implemented to the UTC photodiodes outputs. The mixer for down-conversion will use the Schottky barrier diode, which offers excellent sensitivity for THz detection at room temperature with wide Intermediate Frequency (IF) Bandwidth.

The components of the receiver viz. power combined UTC photodiodes, frequency multiplier, Schottky mixer, bias unit, etc. will be incorporated into a single device block using hybrid integration. Such integration would improve the overall performance of the receiver through optimization of interconnection, amplification, etc. and miniaturize the device, making it suitable for several applications.

The project objectives are to study the receiver performance characteristics improvement due to the photonic local oscillator approach in contrast to the conventional electronic sources, and the benefits of integration in the receiver device.

ACKNOWLEDGEMENT

The TERAOPTICS project has received funding from the European Union's Horizon 2020 research and innovation programme under the Marie Skłodowska-Curie grant agreement No. 956857.

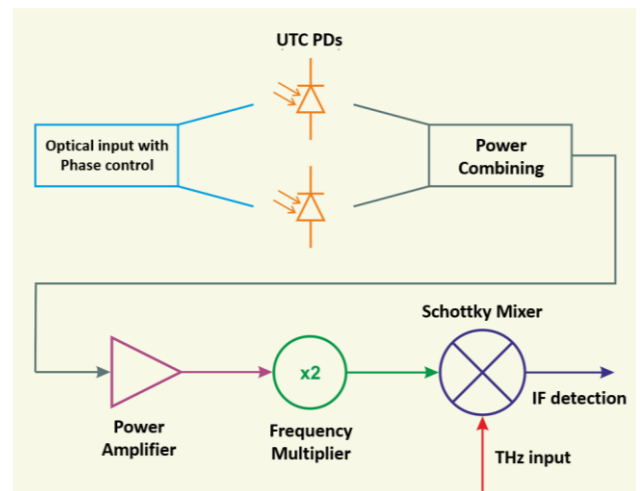


Fig. 1 Schematic of the Integrated heterodyne THz receiver (>300 GHz)

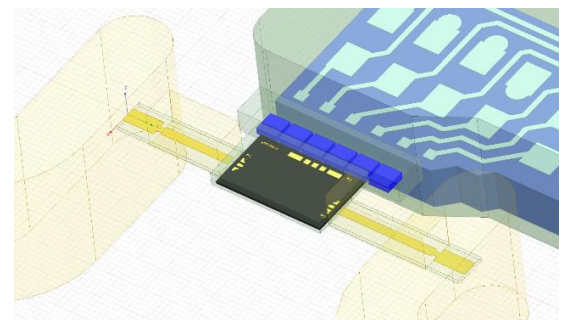


Fig. 2 WR10 Waveguide to micro-strip transition for MMIC Power Amplifier in the receiver block.

270-320 GHz Low Barrier Schottky Diode Mixer

Javier Martinez¹, Diego Moro¹ and Oleg Cojocari¹

¹ACST GmbH, Josef-Bautz Strasse 15, 63457 Hanau, Germany.

Email: javier.martinez-gil@acst.de

We report the fabrication of a sub-harmonic Mixer at 270-320 GHz, featuring discrete anti-parallel low barrier Schottky diode. The mixer presents a typical Noise Figure of 16 dB in the middle of the band and lower than 18dB all over the band. The reduction in local oscillator (LO) input power requirements is as low as 170 μ W for optimal operation conditions. The mixer noise performance remains low when additional LO input power of 500 μ W is applied. Both the mixer and the diodes have been fully designed and fabricated at ACST GmbH.

The state of the art of SHM at 300GHz presents LO powers between 1-4mW [1,2] thus, we present a SHM which only requires 170 μ W of LO power, keeping its main features using 10 times less power. This reduction of LO power requirements in the receiver has a direct impact in the total DC power consumption of the LO source. This also opens the possibility to offer simpler and more compact receivers in the THz range.

The designed and fabricated 270-320 GHz SHM requires LO power levels comparable to SIS and HEB technologies [3], but it can operate at room temperatures and performs noise levels acceptable for a wide range of applications.

The double side band (DSB) Noise Figure of the tested receiver is illustrated in Fig. 1. It has been obtained using the Y-factor measurements [4]. The receiver DSB NF includes a WR-3.4 horn antenna, the low barrier mixer and a ~ 2 dB NF LNA in the 2-18 GHz bandwidth. The Y-factor was measured using a power sensor head in the 5 MHz to 50 GHz. The NF of this receiver remains constant and flat in all the band, being the typical 16 dB with a minimum of 15dB and maximum of 18 dB.

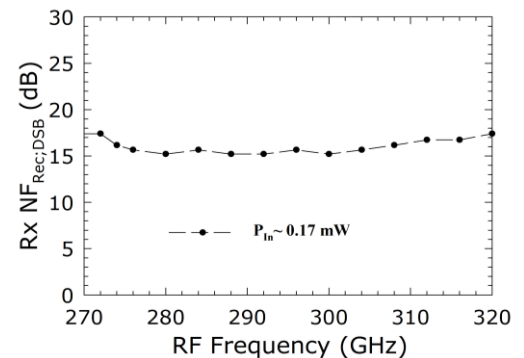


Fig. 1 DSB Noise Figure of the receiver with a constant LO input power of 0.17 mW.

REFERENCES

- [1] Bertrand Thomas, "Low-Noise Fixed-Tuned 300–360-GHz Sub-Harmonic Mixer Using Planar Schottky Diodes", IEEE Microwave and Wireless Components Letters, Dec. 2005.
- [2] Cheng Guo, "A 290–310 GHz Single Sideband Mixer With Integrated Waveguide Filters", IEEE Transactions on Terahertz Science and Technology, Jul. 2018.
- [3] Shoichi Shiba, "Temperature Dependence of HEB Mixer Performance", 19th International Symposium on Space Terahertz Technology, April 2008.
- [4] Shunyou Qin, "Uncertain analysis of antenna noise temperature measurement using Y-factor method", 11th International Symposium on Antennas, Propagation and EM Theory, Oct. 2016.

3D printed THz MIMO diffractive structures

Mateusz Kaluza¹, Pawel Komorowski², Patrycja Czerwińska¹, Mateusz Surma¹,
Przemysław Zagrajek² and Agnieszka Siemion¹

¹*Faculty of Physics, Warsaw University of Technology, 00-662 Warsaw, Poland*

²*Institute of Optoelectronics, Military University of Technology, 00-908 Warsaw, Poland*

Email: Mateusz.kaluza.dokt@pw.edu.pl

The development of telecommunication systems requires fast, wireless signal transmission. One of the possible solutions is a multiple-input multiple-output (MIMO) system for the terahertz (THz) radiation range, which significantly increases the optical channel data transfer ratio. The MIMO system can be realized using two different types of diffractive optical elements (DOEs): multiple-input single-output (MISO) used for coupling (multiplexing) of the THz radiation into a single, free space optical channel and single-input multiple-output (SIMO) for demultiplexing of THz radiation to spatially separated detectors.

SIMO and MISO structures were designed using the iterative ping-pong algorithm [1], known from computer-generated holography. SIMO hologram in the form of the grey-scale bitmap is presented in Fig. 1a. Simulation results indicate its correct numerical performance (Fig. 1c).

During the design of 3D models, a novel method was applied that allows more accurate simulation results for THz DOEs. The aim is to create mesh based on the shape of particular pixels and extrude it into particular levels. The method is described in our previous work [2].

Fused deposition modeling (FDM) technology was used in the manufacturing process of structures with respect to simulation sampling. Our research and material measurements show that in the THz radiation range, some polymer materials like Cyclic Olefin Copolymer (COC) or Styrene Butadiene Copolymer (SBC) have desired optical properties and can be used in the manufacturing of phase structures [3]. The fabricated MISO structure is shown in Fig. 1b.

The obtained experimental results are in accordance with simulation results. MISO structure combines and focuses incoming radiation on the optical axis. SIMO structure splits radiation asymmetrically to the optical axis, which can be applied in time-division multiplexing.

The research was funded by the National Science Centre, Poland under the OPUS-18 programme (2019/35/B/ST7/03909).

REFERENCES

- [1] R.G. Dorsch, A.W. Lohmann, and S. Sinzinger; *Appl. Opt.*, 33(5) (1994) pp. 869.
- [2] M.S. Surma, M. Kaluza, A. Siemion, et al.; *Photonics Letters of Poland*, 13(4) (2021) pp. 88-90.
- [3] A. Siemion; *Sensors*, 21(1) (2020) pp. 100.

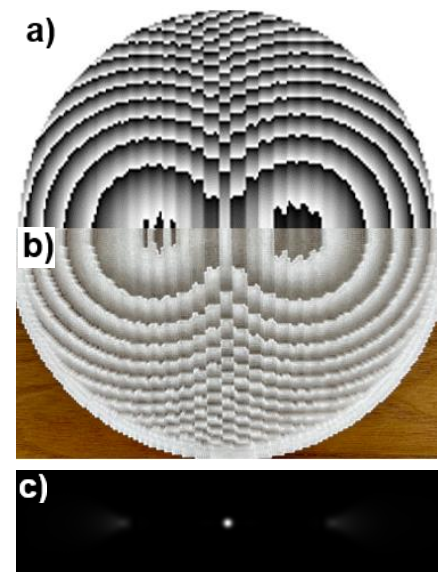


Fig. 1 MISO structure, **a)** phase distribution generated with iterative algorithm, **b)** lens fabricated with FDM 3D printing technique from SBC material, **c)** numerical simulation results – intensity distribution 100 mm after DOE.

THz achromatic lens from 3D printing materials

Mateusz Surma¹, Mateusz Kałuża¹, Paweł Komorowski², Wiktoria Sajda¹,
and Agnieszka Siemion¹

¹*Faculty of Physics, Warsaw University of Technology, Koszykowa 75, 00-662 Warsaw, Poland*

²*Institute of Optoelectronics, Warsaw Military University of Technology, gen. S. Kaliskiego 2, 00-908 Warsaw, Poland*

Email: mateusz.surma.dokt@pw.edu.pl

Further developments in THz optical components may require achieving wide-band (achromatic) operation. The rudimentary method used in the optical spectral range is the design of an achromatic doublet. This requires two materials with the right set of optical properties. 3D printing, another quickly growing industry, may provide certain solutions for the production of achromatic optical elements. This work investigates the properties of commercially available 3D-printable materials for the design of achromatic doublets in the THz range.

Optical properties, that is absorption and refractive indices of the materials, have been tested with THz-TDS [1]. Based on the obtained results and available sources Abbe diagrams [2] have been generated (example shown in Fig. 1). The resulting material information allowed to identify possible material combinations and design of test achromatic doublet.

After the material selection and design process, an achromatic doublet has been 3D modeled and printed with material extrusion method [3]. Obtained lenses have been measured in an experimental setup with a reference refractive lens for comparison. The dependence of the focal spot position on the frequency has been gathered for both lenses in the sub-THz spectral range.

Research funded by the National Center for Research and Development under the LIDER program (LIDER /11/0036 / L-9/17 / NCBR / 2018).

REFERENCES

- [1] J. Neu and C. A. Schmuttenmaer, *Journal of Applied Physics* **124** (2018), no. 23, pp. 231101.
- [2] M. Schaub, and A. Symmons; "Abbe Diagram" in *Field Guide to Molded Optics*, 1st ed., Bellingham, Washington USA: SPIE PRESS, 2016, pp. 9.
- [3] N. Shahrubudin, T. C. Lee, and R. Ramlan, *Procedia Manufacturing* **35** (2019), pp. 1286–1296.

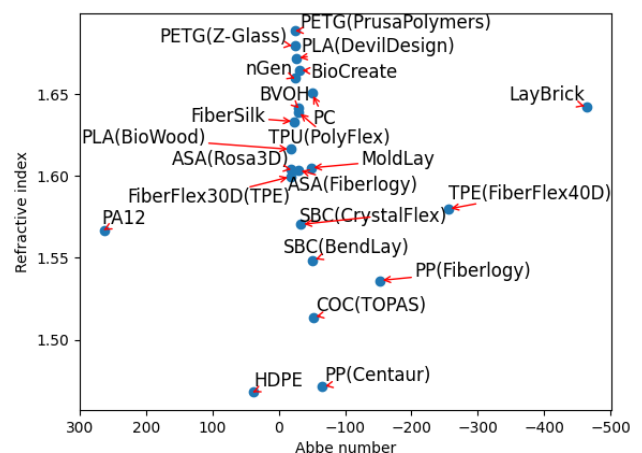


Fig. 1 Abbe diagram for the measured materials. Calculations are based on the frequencies of 100 GHz, 300 GHz, and 600 GHz

Cost-effective high pass filter for dielectric rod waveguides

Ashish Kumar, Daniel Gallego, Mushin Ali,

Daniel Headland, and Guillermo Carpentro

Optoelectronics and Laser Technology Group (GOTL),

University Carlos III de Madrid, 28911 Madrid, Spain.

Email: akumar@ing.uc3m.es.

All-silicon dielectric rod waveguides (DRW) show promise for integrated systems in the mm-wave and terahertz regions [1]. In this frequency band, applications such as communications, sensing, spectroscopy, and imaging are being accelerated by passive devices such as integrated multiplexers to divide the broad spectral bandwidth into manageable allocations [2]. It is desirable to enhance the isolation between adjacent channels in order to improve signal integrity. Thus, there is a need for compatible cost-effective filters.

We present a contactless technique to realize high-pass filters in mm-waves which does not require modification to the DRW itself. We place an electrically conductive metal post on either side of DRW, as shown in fig 1(a). This encloses the DRW within a short section of parallel-plate waveguide, raising the cutoff of the tangentially-polarized mode. The curvature of the cylindrical metal posts provides progressive matching for the passband.

The experimental results given in Fig 1(b), show that the isolation is 10 dB over the range of 55-87 GHz. The fluctuation in the measured result is due to the presence of higher-order modes in the hollow metallic waveguide feed, which is operated above its single-mode range due to limited available equipment. The fact that two plots track closely above 87 GHz indicates high efficiency.

We have demonstrated a contactless technique for filtering lower frequencies in mm-wave DRWs using two inexpensive metal posts. The fact that it is contactless offers the potential for reconfigurability, to realize bespoke filters as-needed. Furthermore, DRWs are viable in the terahertz range [1,2], and so the overall structure can be rescaled for higher frequencies. This concept therefore holds the potential to enhance signal integrity in terahertz-range applications.

The authors wish to acknowledge support from: TERAOPTICS project (Grant No: 956857), TERAWAY project (Grant No: 871668), and TERAmesure Grant No: 862788 funded from the European Union's research.

REFERENCES

- [1] Rivera-Lavado, Alejandro, Sascha Preu, Luis Enrique García-Muñoz, Andrey Generalov, Javier Montero-de-Paz, Gottfried Döhler, Dmitri Lioubtchenko et al.. " *IEEE Transactions on Antennas and Propagation* **63.3** (2015): 882-890.
- [2] Headland, Daniel, Withawat Withayachumnankul, Masayuki Fujita, and Tadao Nagatsuma. " *Optica* **8.5** (2021): 621-629.

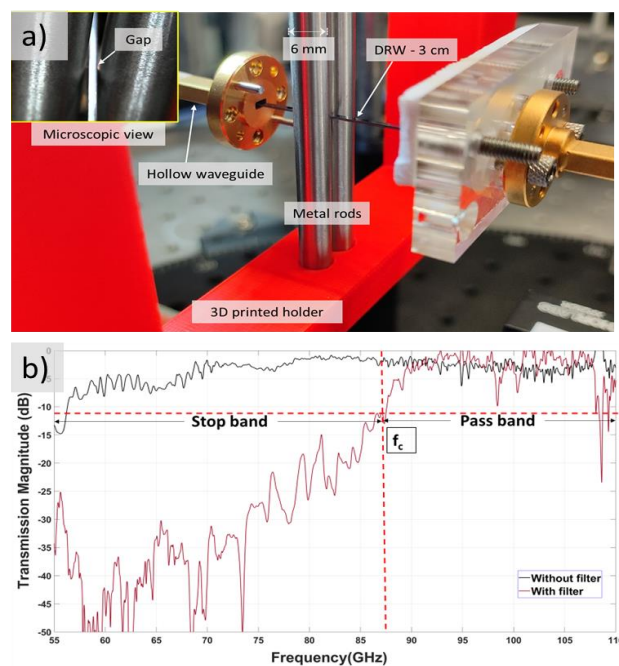


Fig. 1 a) Photo of experiment experimental setup, and b) measured results

Low Loss Topological Silicon Valley Photonic Crystal waveguides in Terahertz regime

Abdu Subahan Mohammed¹, Edouard Lebouvier²; Gaëtan Lévêque¹, Alberto Amo³, Yan Pennec¹, Pascal Szriftgiser³, Guillaume Ducournau¹, Marc Faucher¹

¹IEMN, University of Lille, 59650 Villeneuve d'Ascq, France.

²V-MICRO SAS, Avenue Poincaré, 59650 Villeneuve d'Ascq, France.

³PhLAM, University of Lille, 59000 Lille, France.

Email: abdu-subahan.mohammed@iemn.fr

Terahertz (THz) technology is becoming attractive for the future technology due to its unbeatable range of applications in sensing, safety imaging and data communications. The majority of the current THz systems has not much enjoyed the silicon based chip scale integrated technology but rely on voluminous and bulky systems. Currently silicon photonic integrated circuits are very crucial for wide range of applications. Conventional THz photonic circuits used are suffering from back scatterings, sensitivity defects and structural perturbations, which will be more prominent upon the further miniaturization of devices. Hence, the recent progress in Valley Photonic Crystal (VPCs), which is known for its topological protection, holds much promise for high-performance photonic circuits densely integrating various optical components.

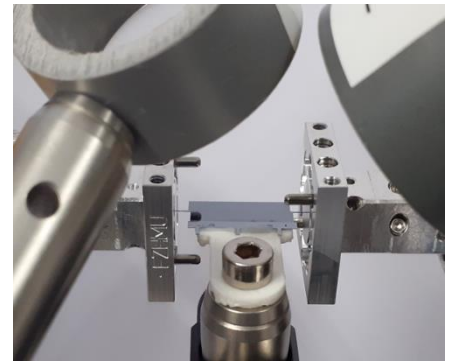


Fig. 1 Experimental setup during VNA measurement

Extremely low loss and low dispersion topological THz VPC waveguides using high resistivity ($>10 \text{ k}\Omega \text{ cm}$) silicon (of relative permittivity 11.7) have already been designed and demonstrated in the 300 Gigahertz (GHz) frequency region and its high performance in data communication applications [1],[2]. In this work, building on the topological phase of light, we design, fabricate and experimentally demonstrate a low-loss and low-cost, silicon based VPC waveguide for the 570-630 GHz frequency region. Specifically, we measure the transmission and group delay for the straight waveguide fabricated with length 9.2 mm with well known graphene-like lattice containing equilateral triangle holes. These results prove that topological valley kink states are promising for THz communication applications enabling high speed 6G data transfer systems.

REFERENCES

- [1] Yang, Y., Yamagami, Y., Yu, X. *et al.* Terahertz topological photonics for on-chip communication. *Nat. Photonics* **14**, 446–451 (2020). <https://doi.org/10.1038/s41566-020-0618-9>.
- [2] J. Webber et al., "Terahertz Band Communications With Topological Valley Photonic Crystal Waveguide," in *Journal of Lightwave Technology*, vol. 39, no. 24, pp. 7609-7620, 15 Dec.15, 2021, doi: 10.1109/JLT.2021.3107682.

Cascaded wideband RoF links with LWA for enabling mobile 5G base stations

Yilmaz Ucar¹, Thomas Haddad², Peng Lu², Sumer Makhlouf^{1,2}, Andreas Stöhr^{1,2}

¹Microwave Photonics GmbH, Essener Str. 5, 46047 Oberhausen, Germany

²ZHO/ Optoelektronik, Universität Duisburg-Essen, Lotharstr. 55, 47057 Duisburg, Germany

Email: yilmaz.ucar@microwave-photonics.com

Vast increase in number of mobile devices which involves inevitable internet applications emerged the need of wider bandwidth with enhanced coverage. Especially, higher data rates are demanded for train journeys since passengers desire to access internet including high quality streaming services.

Often, railway communications suffers from connection interruptions due to hard handover process between base transceiver stations (BTS) or simply because of poor coverage. In order to overcome these issues, we propose mounting the BTS on the train and providing backhaul connectivity using a cascaded RoF and Leaky-Wave Antenna (LWA) system (Figure 1). In this approach, the RF signals are modulated onto optical signals using an Electro-absorption Modulated Laser (EML) and then the modulated RF signals are transmitted over optical fiber (RoF) which are deployed along the railway track. Subsequently, RF signals are recovered using a photodiode (PD) and radiated to the train via a low-cost LWA. For V-band operation, fabricated LWA yield a steering angle of 40° in the H-plane [1]. The concept of a planar LWA monolithically integrated with a PD is illustrated in Figure 2. Optical switches are utilized to enable the necessary node which requires tracking of the train. As already demonstrated, LWAs are also capable of tracking objects in a joint communication-sensing (JCS) approach [2]. For 3D localization, two linearly polarized LWAs for azimuth and elevation are used [2].

In conclusion, a joint communication-localization system consisting of subsequent RoF sections with LWA is proposed to enable 5G access to trains.

REFERENCES

- [1] M. Steeg, N. Yonemoto, J. Tebart, and A. Stöhr; *Electronics* **6** (2017) pp. 107.
- [2] M. Steeg, J. Tebart, K. Neophytou, M. A. Antoniadis, S. Iezekiel and A. Stöhr; *2019 International Topical Meeting on Microwave Photonics (MWP)* (2019) pp. 1-4.
- [3] Peng Lu, et al.; *IEEE Transactions on Terahertz Science and Technology* **11.2** (2020): pp. 218-230.

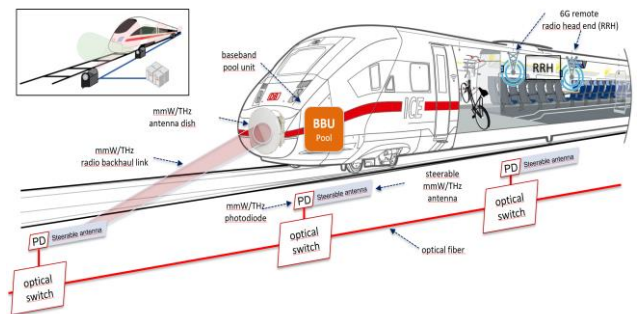


Figure 1: Proposed Xhaul system for mobile base located on a high-speed-train.

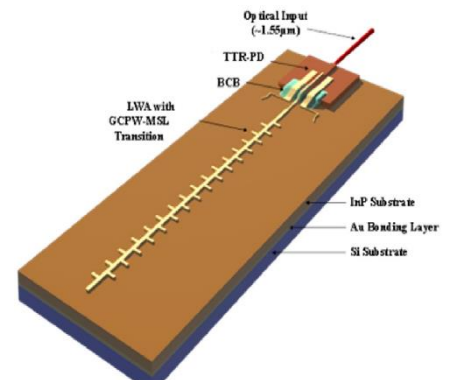


Figure 2: Concept of monolithic integration [3]

Exploiting 3D metal printing for additive manufacturing of waveguide and antenna structures for THz-applications

Jonas Tebart¹, Michael Staiger¹, Tim Brüning¹, Marcel Grzeslo¹, Andreas Stöhr¹ and Andreas K. Klein¹

¹Department of Optoelectronics, University of Duisburg-Essen, Lotharstr. 55, 47057 Duisburg, Germany

Email: jonas.tebart@uni-due.de

Due to the continuously improving technology in the field of additive manufacturing, nowadays, it is possible to fabricate metal structures for millimeter wave and THz applications by means of 3D printing [1]. In addition to the production of simple structures such as waveguide sections, complex and integrated features can also be processed through the use of 3D printing technology. The work presented here includes designing, optimizing, and fabricating of several WR3 components, all intended for an application in the context of interconnecting waveguide-bound to wireless transmission. In terms of waveguides components, this comprises the fabrication of short waveguide sections (Fig. 1(a)) to determine the inherent losses of the feeding structures (Fig. 1(b)) as well as the design and production of T-junctions (Fig. 1(c) and (d)) to allow for splitting of the EM-wave to feed more than just a single antenna. On the antenna side itself, the focus here is on the utilization of 3D-printed helical antennas that allow a circularly polarized wave to be radiated into free space. Thereby, the directivity of the antenna is increased via a cone (Fig.1(e)). Furthermore, the excitation of higher order modes is possible by enlarging the antenna's geometry and offers the capability of orbital angular momentum multiplexing [2].

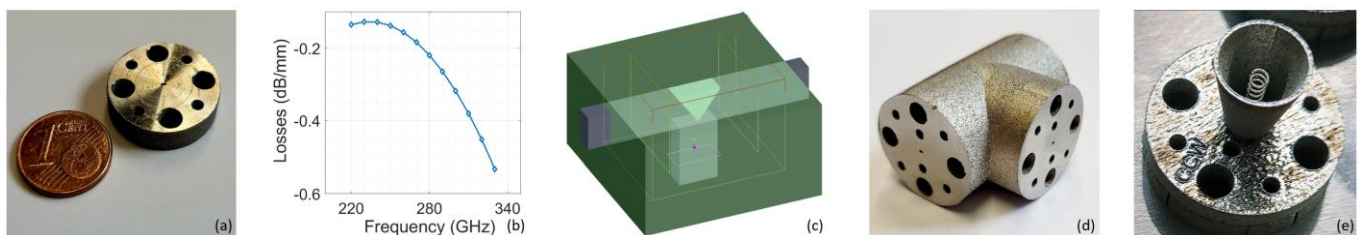


Fig. 1 A WR3 waveguide section of 6 mm length is shown in (a) while the corresponding measured losses in dB/cm are depicted in (b). The Lumerical model of the WR3 T-junction is illustrated in (c) together with the 3D-printed module in (d). Additionally, a fabricated version of the helical antenna with an integrated cone is seen in (e).

The components are optimized for applications in the WR3 range (220 GHz-330 GHz) using finite difference time domain simulations (Lumerical). For manufacturing, a Trumpf TruPrint 1000 laser metal fusion system with a laser spot size of 30 μm and stainless steel powder (316L) are used. First characterizations of the printed structures are carried out, showing a loss of less than 0.15 dB/cm within the frequency range of 220-255 GHz.

REFERENCES

- [1] B. Zhang, W. Chen, Y. Wu, K. Ding, R. Li, "Review of 3D Printed Millimeter-Wave and Terahertz Passive Devices", *International Journal of Antennas and Propagation*, vol. 2017, Article ID 1297931, 10 pages, 2017.
- [2] D. Weiguo, Y. Zhu, Y. Yang, Z. Kaiwei, "A Miniaturized Dual-Orbital-Angular-Momentum (OAM)-Mode Helix Antenna". *IEEE Access*, 6, 57056-57060.

Metamaterial based Antenna integrated UTC-PD array for THz communications in 270-330 GHz band

Fasil Bashir Wani¹, Cyril Renaud¹, and Chin-Pang Liu¹

¹Ultrafast Photonics Group, Electronic and Electrical Engineering Department
Roberts Building, WC1E 7JE, University College London, London, UK
Email: fasil.wani.21@ucl.ac.uk

The data traffic is expected to rise from 47 Exabytes/month in 2020 to 4700 Exabytes/month in 2030[1], most of which will be wireless. There will be a huge demand for lightning fast data transfer which in turn requires more bandwidth. Given that the current technology is incompatible, we need to look for alternative solutions. Terahertz based technologies, which work in frequency range of 0.1 to 10 THz, offer some unprecedented advantages in terms of higher bandwidth, faster speed, compact devices, and a potential to be integrated with the current telecom technology, making them one of the most desired solutions. THz communications make use of the uni-travelling-carrier photodiode (UTC-PD) photomixers in the transmitter side, which have demonstrated superior performance over other technologies.

Although a significant amount of work has been done in this domain in the last two decades, some difficulties still persist. Using Optical Delay Lines for beam steering poses challenges in device alignment. Adding a Si lens increases the device size and limits the number of elements in an array and thus hinders the monolithic integration for smaller form factor and ease of fabrication. As the impedance of UTC-PD is frequency dependent, it is hard to match the component impedances over a large frequency range and this mismatch causes inefficient energy coupling and power transfers. Substrate absorption and mutual coupling causes on-chip interferences and cross talk in arrays.

Metamaterials exhibit extraordinary properties that are not available in nature and have the potential to overcome the aforementioned limitations. We are focusing on creating a Metamaterial based antenna array driven by the InGaAs-based UTC-PD, as a transmitter (and possibly a receiver). This will make use of metamaterial for antennas and power combining, a phase gradient metasurface for beam steering, and a meta-lens for beam focusing. Given their sub-wavelength unit cell sizes and being linear, the devices shall be compact and offer potential for monolithic integration.

REFERENCES

- [1] International Telecommunications Union "IMT traffic estimates for the years 2020 to 2030" (07/2015).
- [2] Chong Han, Yongzhi Wu, Zhi Chen, and Xudong Wang "Terahertz Communications (TeraCom): Challenges and Impact on 6G Wireless Systems".

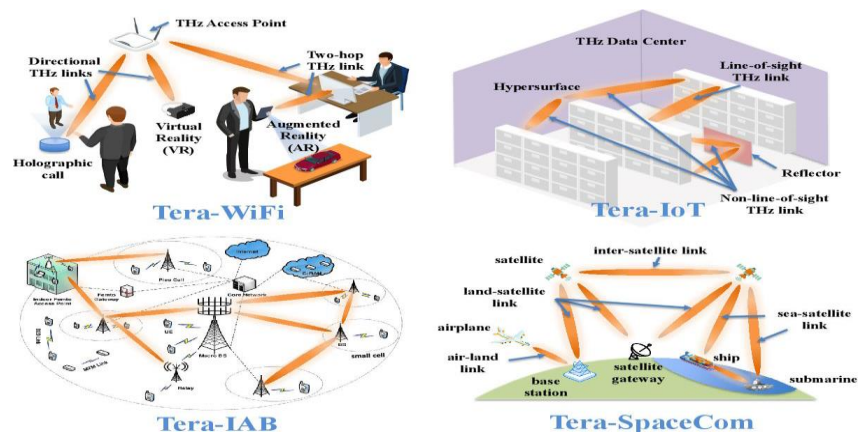


Figure 1: Applications of THz communication system [2]

Triple cation perovskite/silicon tandem solar cell

Ašmontas S., Gradauskas J., Grigučevičienė A., Leinartas K., Lučun A., Mujahid M.,
Petrauskas K., Selskis A., Sužiedėlis A., Šilėnas A., and Širmulis E.

Center for Physical Sciences and Technology, Saulėtekio Avenue 3, 10257 Vilnius, Lithuania
office@ftmc.lt

Owing to its excellent power conversion efficiency (PCE) and extremely cheap material prices, perovskite solar cells based on organometal halide light absorbers have been highlighted as a plausible photovoltaic technology. Nowadays, almost 90% of solar cells (SC) manufactured in the market are comprised of silicon [1]. Perovskite and silicon SC successfully linked together to form tandem solar devices have the significance of surpassing cutting-edge silicon SC. In the two-terminal (2T) arrangement, both SC are monolithically incorporated, and the wide-bandgap cell is placed precisely on the narrow-bandgap cell. [2]. The two cells are mechanically connected in the four-terminal (4T) arrangement, with the wide-bandgap cell stacked on top of the narrow-bandgap cell [3].

We explored the photovoltaic characteristics of a triple cation perovskite/silicon tandem SC with four terminals $\text{Cs}_{0.06}(\text{MA}_{0.17}\text{FA}_{0.83})_{0.94}\text{Pb}(\text{I}_{0.83}\text{Br}_{0.17})_3$ layer-based perovskite cell integrated on an industrial n-type monocrystalline bifacial PERT silicon SC. According to the SEM image of the triple cation perovskite film formed on the mesoporous titanium dioxide layer, there are various grain sizes, some of which are larger than 1000 nm. The perovskite layer's measured transmittance spectrum reveals an excellent absorber of visible light and semitransparent in the infrared range. In the 800–1100 nm wavelength region, the transmittance is considerably larger than 80%.

Open circuit voltage, short-current density, fill factor (FF), and PCE of the top perovskite solar cell are 1.11V, 23.6mA, 74 %, and 19.4 %, respectively. As far as the bottom cell is concerned, it shows 0.64V Open circuit voltage, 15.8mA short-current density, 71%FF, and 7.2% PCE. Thus, the 4T perovskite/silicon tandem solar cell's overall PCE of 26.6 % is substantially greater than the efficiency of each subcell.

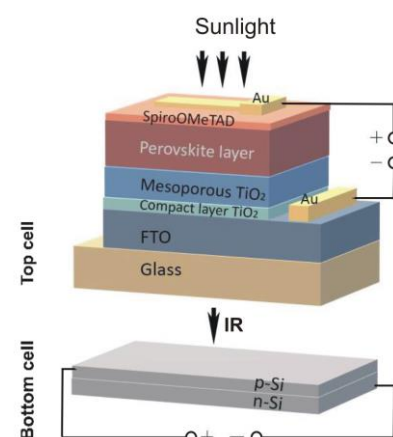


Fig. 1. Architecture of the triple cation perovskite/silicon tandem solar cell composed of perovskite top cell and bottom silicon cell

REFERENCES

1. Yu C, Xu S, Yao J, and Han S; *Crystals* **8** (2018) pp. 430–41.
2. Albrecht S, Saliba M, Baena J P C, Lang F, Kegelmann L, Mews M, Steier L, Abate A, Rappich J, Korte L, Schlattmann R, Nazeeruddin M K, Hagfeldt A, Grätzel M, and Rech B; *Energy Environ. Sci.* **9** (2015) pp. 81–88.
3. Polman A, Knight M, Garnett E C, Ehrler B, and Sinke W C; *Science*. **352** (2016) pp.4424-1-442-10.

Strong inverse piezoelectric response in graphene - dielectric structures induced by nanosecond electric pulse

Linās Ardaravičius, Oleg Kiprijanovič

Center for Physical Sciences and Technology, Vilnius, Saulėtekio al. 3, LT-10257, Lithuania

oleg.kiprijanovic@ftmc.lt

The application of the unique graphene properties in electronics is still at an early stage. More accessible for investigation are phenomena known from semiconductor electronics. These include the acoustic-electronic interaction [1].

Monolayer graphene grown by chemical vapor deposition was transferred on 50 nm thick HfO_2 , and bilayer one was transferred by dry method on 50 nm thick SiO_2 , which were preliminarily deposited by plasma atomic layer deposition on p+Si substrate.

Fabricated 100 μm wide structures with a channel length of $L = 10\text{--}12\ \mu\text{m}$ were used to investigate the current carrying characteristics of graphene transistor channels up to high electric fields. A probe station was used to connect the samples into the circuit capable of transmitting ns duration pulses. Pulsed I - V characteristics of the samples were measured, and electron drift velocity was estimated. A wave packet superimposed with the transmitted pulse was observed. The basic oscillations of wave packets have frequencies of 8.5 and 10.1 GHz. Signal analysis showed that the presence of some other modes distorted the wave packet shapes. These frequencies allowed us to conclude that there is an inverse piezoelectric response of the dielectrics to the fast voltage growth with frequencies close to their surface acoustic waves (SAW). When applied electric field strength approaches 100 kV/cm, the inverse piezoresponse amplitudes become about 20% of the pulse amplitude.

Analysis of the spectra lines showed the modes having frequencies as the bisected SAW ones. Moreover, this bisected line is split, and its splitting is more pronounced for HfO_2 and less for SiO_2 (see Fig.1). The authors note a strong bond between C atoms in graphene and O ones in dielectrics, which can lead to the appearance of forced or parametric oscillations of graphene at bisected frequency [2]. The splitting indicates that the two identical submeshes of graphene interact as coupled oscillatory circuits, and the coupling is stronger for the monolayer on HfO_2 .

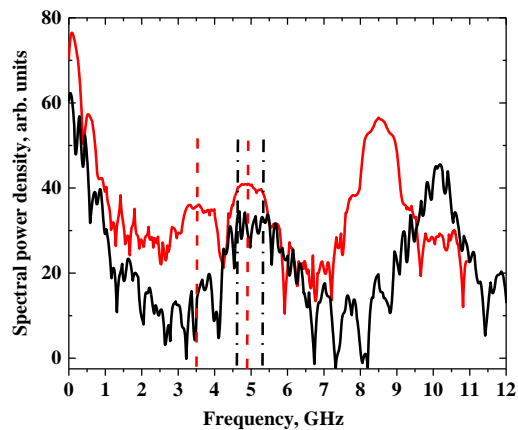


Fig. 1 Spectra of the piezoresponse. Dashed lines denote the splitting of bisected oscillations. Red indicates HfO_2 and black indicates SiO_2 dielectric.

REFERENCES

- [1] V. Miseikis, J. E. Cunningham, K. Saeed, R. O'Rourke, A. G. Davies, *Appl. Phys. Lett.* **100** (2012) p. 133105.
- [2] J. Awrejcewicz, G. Kudra, O. Mazur, *Nonlinear Dyn.* **105** (2021) pp. 2173–2193.

Low and high photon energy induced photoresponse in single junction solar cells

Jonas Gradauskas^{1,2}, Steponas Ašmontas¹, Ihor Zharchenko¹, Oleksandr Masalskyi^{1,2}, Algirdas Sužiedelis¹, Aldis Šilenas¹, Aurimas Cerškus^{1,2}, Aleksej Rodin¹ and Petrulėnas Augustinas¹

¹Lab. of Electronic Processes, Center for Physical Sciences and Technology, Saulėtekio av. 3, LT-10257 Vilnius, Lithuania

²Dept. of Physics, Vilnius Gediminas Technical University, Saulėtekio av. 11, LT-10223 Vilnius, Lithuania

Email: ihor.zharchenko@ftmc.lt

The practically achieved record level of 26.1% efficiency is still far below the theoretical 32% Shockley-Queisser limit of a silicon cell. The theory implies that photons with energy lower than a semiconductor band gap (E_g) are not absorbed at all, while the residual energy of the high energy photons is accounted only via the process of lattice heating after the hot carrier thermalization.

In this communication we demonstrate that 33.6% of the incident AM 1.5 G solar radiation high energy photons ($h\nu > E_g$) and 19.3% of the low energy ones have a potential to heat the free carriers in silicon. In the case of GaAs, the values are 21.7% and 33.0% respectively [1].

The present work gives experimental evidence that low and high energy photons participate in the formation of hot carrier photovoltage (HCPV). Fig. 1 shows that HCPV demonstrates polarity opposite to the generation induced PV, and this way has a harmful influence on the effective operation of solar cell.

When Si and GaAs p-n junctions were illuminated by 1.06 μm , 1.34 μm and 2 μm -long laser light pulses, the photoresponse composed of opposite polarity components was observed under certain experimental conditions. Analysis of the components' properties with regard to their polarity, response speed, dependence on bias voltage and spectral excitation gives proof that before cooling down the hot carriers give rise to the HCPV.

To conclude, conditions minimizing the HCPV will support rise of the efficiency of a single-junction solar cell. If the S-Q theory were revised by taking into account the direct negative impact of the hot carriers, the theoretical limit will come down closer to the practically achieved solar cell efficiency.

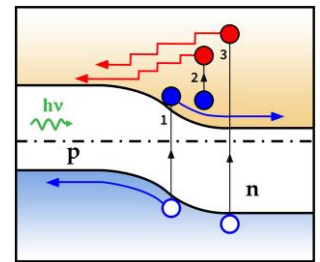


Fig. 1 Schematic formation of generation-induced photovoltage (blue arrows) and hot carrier photovoltage (red arrows) across a p-n

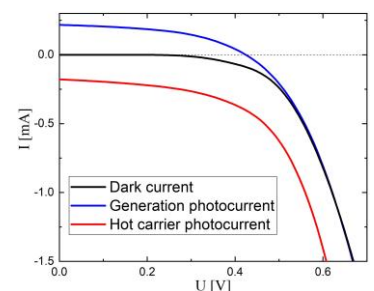


Fig. 2 I-V characteristic of Si solar cell exposed to 1.34 μm laser light ($h\nu = 0.93 \text{ eV} < E_g$): black – in dark, blue – generation, red – hot carrier photocurrent.

REFERENCES

[1] O. Masalskyi and J. Gradauskas; *Ukr. J. Phys. Opt.* 23 (2022) pp. 117–125.

Collagen orientation index determination in wide-field SHG microscopic images of lung tissue

Yaraslau Padrez¹, Lena Golubewa^{1,2}, Renata Karpicz¹ and Danielis Rutkauskas¹

¹Center for Physical Sciences and Technology, Vilnius, Lithuania

²Department of Physics and Mathematics, University of Eastern Finland, Institute of Photonics, Joensuu, Finland

Email: yaraslau.padrez@ftmc.lt

Second Harmonic Generation (SHG) microscopy is a second-order non-linear optical method for tissue analysis. It provides high-contrast, label-free, non-destructive imaging of biological samples with a sub-micron resolution, through visualizing non-centrosymmetric molecules in the tissue [1]. Collagen satisfies this condition and thus can be successfully visualized via SHG without any specific labelling. The collagen fiber network transformations lead to fibrosis and indicate development of many diseases including pulmonary arterial hypertension (PAH). The collagen orientation index (OI) shows the anisotropy of the collagen fiber network and may be used as a specific marker of disease progression [2].

In the present study we analyzed collagen structure modification during PAH progression from 0 to 8 weeks in rats. We performed wide-field SHG microscopic image analysis using Fast Fourier Transform (FFT) processing for determining OI using the formula (1):

$$OI = \left[1 - \left(\frac{\text{short axis}}{\text{long axis}} \right) \right], \quad (1)$$

where short and long axes are extracted from FFT images using Wolfram Mathematica (Wolfram Research, Champaign, Illinois). It was demonstrated that OI changes during PAH progression with significant increase on the second week of the disease (Fig. 1). The lung tissue of healthy rats has lower OI than that during PAH progression, meaning that it is associated with ordering of collagen fibers. Significant increase of OI by the second week indicates fiber elongation and their protrusion in the lung tissue. Subsequently OI decreases, because collagen fibers reorganize and form more isotropic collagen network.

Thus, FFT and statistics analysis of the SHG images [3] is a useful tool for revealing changes of collagen morphology and their interpretation in terms of different stages of PAH progression.

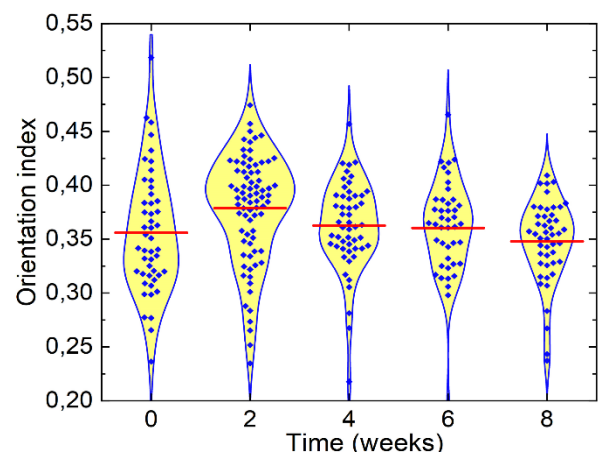


Fig. 1 OI values, calculated using SHG images of control samples (0 weeks) and samples at different stages of PAH progression. Violin plot is used to visualize the distribution of calculated OIs.

REFERENCES

- [1] P. J. Campagnola and L. M. Loew, *Nat Biotechnol* **11** (2003) pp. 1356-1360.
- [2] S. Wu, H. Li, H. Yang, et. al., *JBO* **4** (2011) p. 040502
- [3] Y. Padrez, L. Golubewa, T. Kulahava, et al., *Sci Rep* **1** (2022)

Investigation of surface modification of polycarbonate by picosecond Nd:YVO₄ laser pulses for selective chemical copper deposition

Šarūnas Mickus, Vytautas Vosylius, Evaldas Kvietkauskas, Viktorija Vrubliauskaitė, Karolis Ratautas

3D Technologies and Robotics Laboratory, Department of Laser Technologies, Center for Physical Sciences and Technology, Savanorių ave. 231, Vilnius LT-02300, Lithuania.

Email: sarunas.mickus@ftmc.lt

Our daily lives are packed with number of integrated, functional, and miniaturized devices. The amount of these devices is still increasing therefore high demand for fast and cheap manufacturing methods arise. One of the newer method for molded interconnect devices (MID) [1] production is Selective Surface Activation Induced by Laser (SSAIL) [2, 3]. Technology copes with complex 3D surfaces and allows varied materials metallization by electroless metal plating. However, several challenges related to selection of optimal surface modification parameters for different surfaces and copper adhesion strength are yet to overcome.

The work is focused on SSAIL process application on engineering polycarbonate (PC) polymer as well as its impact on its surface properties. The main goal was to find out laser beam angle of incidence impact for this technology. Various surface roughness properties including root mean square height (S_q) and core void volume (V_{vc}) parameters were thoroughly researched. All the measured parameters exhibited no correlation with different laser modification angles. The successful selective metallization window for all the tested AOI appeared on the sample areas with irradiation dose values between 40 and 190 J/cm².

The SSAIL method is successfully applicable on PC surface. Already mentioned window, where good copper deposition quality can be expected for specified laser modification angles shows enormous potential for SSAIL technology on complex 3D structures but requires further investigation.

REFERENCES

- [1] A. Islam, H. N. Hansen, and N. Giannakas, *CIRP Ann.*, vol. 64, no. 1, pp. 539–544, 2015.
- [2] K. Ratautas, V. Vosylius, A. Jagminienė, I. Stankevičienė, E. Norkus, and G. Račiukaitis, *Polymers (Basel)*, vol. 12, no. 10, pp. 1–16, 2020.
- [3] K. Ratautas, A. Jagminienė, I. Stankevičienė, E. Norkus, and G. Račiukaitis, *Procedia CIRP*, vol. 74, pp. 367–370, 2018.

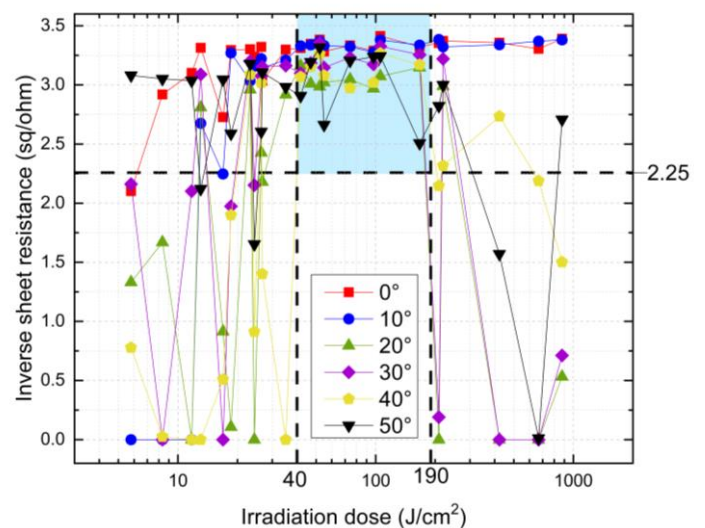


Fig. 1 Dependence of the inverse sheet resistance on the laser irradiation dose for various laser beam angles of incidence.

In vivo imaging of human retina with Fourier-Domain Full-Field Optical Coherence Tomography and a Multimode Fiber for Coherence Noise Reduction

K. Adomavičius¹, D. Borycki², P. Wegrzyn², I. Žičkienė¹, M. Wojtkowski²,
E. Aukorius^{1,2}

¹Department of Semiconductors, ¹Center for Physical Sciences and Technology, Vilnius, Lithuania

²Institute of Physical Chemistry, Polish Academy of Sciences, Warsaw, Poland

karolis.adomavicius@ftmc.lt

Optical coherence tomography (OCT) is an interferometric imaging method widely used for 3D retinal imaging that can image deep in tissue. Full-field OCT (FF-OCT) has significantly improved imaging speed by using an ultrafast CMOS camera and a swept laser source. However, crosstalk – a coherent noise – appearing from use of a spatially coherent laser (and widefield detection) has been limiting the technique's performance, preventing from seeing choroid and other deeper retinal layers. It is important to image choroid in human eye as it is a crucial determinant in the pathogenesis of many ocular diseases, since its principle role is to supply oxygen to the outer retina [1]. A light source with reduced spatial coherence can be used to remove crosstalk, as was shown previously by the help of an ultrafast deformable membrane. Here we show that using a multimode fiber with carefully chosen parameters, the entire thickness of the retina and choroid can be acquired in one volume *in vivo* with suppressed crosstalk and high contrast [2], as shown in Fig. 1. Specifically, the laser was coupled into 300 meters-long multimode fiber with 50 μm core, where it broke down into hundreds of modes that reduced the spatial coherence, and created a homogenous light distribution at the distal end of the fiber and illumination on the retina. This implementation can speed up the clinical adaptation of FF-OCT technology.

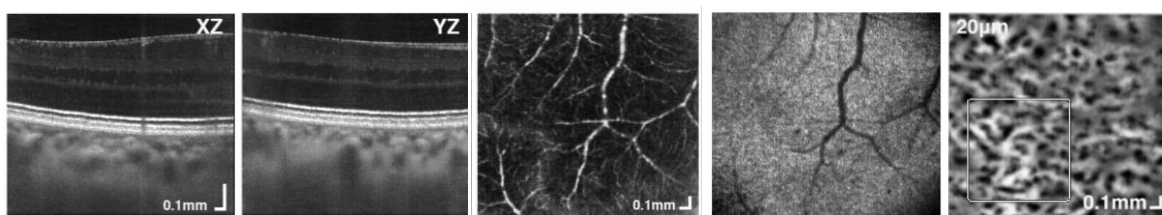


Fig. 1 FF-OCT images of a retina acquired in less than 0,1s. Axial views (1, 2) and *en face* views (3,4) of the retina and choroid (5), which were derived from the acquired retinal data, shows high resolution and high contrast.

REFERENCES

- [1] H. Lavers and H. Zambarakji, "Enhanced depth imaging-OCT of the choroid: a review of the current literature," *Graefes Archive for Clinical and Experimental Ophthalmology*, vol. 252, no. 12, pp. 1871-1883, 2014.
- [2] E. Aukorius *et al.*, "Multimode fiber as a tool to reduce cross talk in Fourier-domain full-field optical coherence tomography," *Opt. Lett.*, vol. 47, no. 4, pp. 838-841, 2022/02/15 2022, doi: 10.1364/OL.449498.

Characterization of Metal-Organic Frameworks Using THz Techniques

Faustino Wahaia^{1,*}, Irmantas Kašalynas², Gintaras Valušis², Mindaugas Karaliunas²,
Andžej Urbanovič², Birger Seifert¹

¹*Institute of Physics - Millennium Institute for Research in Optics, Chile*

²*FTMC - Terahertz Photonics Laboratory, Optoelectronics Department, Center for Physical Sciences and Technology, Vilnius, Lithuania*

Email: fwahaia@fis.puc.cl

Through the present work we intend to demonstrate the potential of THz spectroscopy to provide insights into the dynamics of the photoconductivity of metal-organic frameworks (MOFs) with a resolution of sub-picoseconds and, the precise determination of the lifetime of their carriers. In addition, we will go toward the determination of the photoconductivity dependent upon its frequency.

In addition, we will go through the detection of the basic phenomenon of molecular rotors in MOFs structure and comb the reticular dynamics that accompanies it including the characterization of the vibrational dynamics of MOFs to understand the complex physical mechanisms that control their core functions and related structure.

We expect that this work will underline a knowledge of vital importance in the development of the next generation of cutting-edge functional materials.

Special session

3 MIN AWARD PRESENTERS SESSION



Young researcher award

- Science Award by Teltonika IoT: Master student **Lukas Naimovičius (Vilnius University)**
- Technology Award by Light Conversion: Bachelor student **Silvija Keraitytė (Vilnius University and FTMC)**
- Innovation Award by Science and Technology Park of Institute of Physics: PhD student **Rusnė Ivaškevičiūtė-Povilauskienė (FTMC)**
- Presentation Award by Inospectra: shared by Bachelor student **Monika Jokubauskaitė (Vilnius University and FTMC)** and **Dr. Martynas Skapas (FTMC)**

Author index

A	Abacıoğlu Ezgi	S1-P6	79
	Adomavičius Karolis	S5-I3	32
		S4-P6	104
	Adomavičius Ramūnas	S3-P1	88
	Ayyagari Surya Revanth	S6-O5	48
	Alekseev Kirill	S2-O2	20
		S5-O5	37
	Alexeeva Natalia	S5-O5	37
		S9-O1	67
	Ali Muhsin	S6-O9	52
		S3-P7	94
	Alkauskas Audrius	S5-O4	36
	Amo Alberto	S3-P8	95
	Andresen E.	S6-O7	50
	Apostolakis A.	S2-O2	20
	Ardavičius Linas	S1-P7	80
		S4-P2	100
	Astachov Vladimir	S8-O3	64
	Ašmontas Steponas	S4-P1	99
		S4-P3	101
	Auksorius Egidijus	S5-I3	32
		S4-P6	104
B	Balagula Roman M.	S5-O3	35
		S6-O3	46
	Balakauskas Saulius	S8-O3	64
		S1-P4	77
	Balanov A. G.	S2-O2	20
	Balevičius Saulius	S5-O2	34
	Bandyopadhyay Artrio	S6-O7	50
	Baranowski M.	S2-I3	18
	Baronas Paulius	S8-O2	63
	Bässler Heinz	S5-I2	31
	Baudelle K.	S6-O7	50
	Belio-Apaolaza Inigo	S6-O6	49
	Bičiūnas Andrius	S2-P4	84
	Bigot Laurent	S6-O7	50
	Bleizgys Vytautas	S5-O2	34
	Boeck Jo	S-I2	14
	Borycki Dawid	S5-I3	32
		S4-P6	104
	Bouet M.	S6-O7	50
	Bouwman G.	S6-O7	50

	Breuer S.	S2-O1	19
	Brüning Tim	S3-P10	97
	Bukauskas Virginijus	S8-O3	64
		S9-O2	68
		S1-P4	77
	But Dmytro B.	S5-O1	33
		S5-O6	38
		S6-O4	47
		S6-O10	53
		S3-P2	89
	Butkutė Renata	S6-O1	44
		S9-O2	68
		S9-O3	69
		S9-O4	70
		S1-P1	74
		S1-P3	76
		S2-P4	84
C	Carpintero Guillermo	S6-O9	52
		S6-O11	54
		S3-P7	94
	Castaneda M.	S8-I1	60
	Cesiul Albert	S6-O10	53
	Chang J.	S8-I1	60
	Chatinovska Barbara	S8-O1	62
	Chen Yang-Zhen	S2-I2	17
	Chernyadiev Alexander	S6-O4	47
		S3-P2	89
	Chiu Yi-Jen	S2-I2	17
	Cywinski Grzegorz	S5-O3	35
		S5-O6	38
	Cywiński Grzegorz	S5-O1	33
	Cohen S.	S8-I1	60
	Cojocari Oleg	S6-O6	49
		S3-P4	91
	Crozatier Vincent	S2-P6	86
	Czerwińska Patrycja	S3-P5	92
	Čechavičius Bronislavas	S9-O2	68
		S9-O3	69
		S1-P1	74
		S1-P3	76
	Čerškus Aurimas	S4-P3	101
	Čižas Vladislovas	S5-O5	37
		S6-O1	44
		S2-P4	84

D	Deumer M.	S2-O1	19
	Devenson Jan	S9-O5	71
	Dyksik M.	S2-I3	18
	Dilys Justas	S5-O2	34
	Doherty Marcus W.	S5-O4	36
	Dorenbos S.	S8-I1	60
	Dub Maksym	S5-O1	33
		S5-O3	35
		S5-O6	38
	Ducournau Guillaume	S6-O7	50
		S3-P8	95
	Dudutienė Evelina	S9-O2	68
		S9-O3	69
		S1-P1	74
		S1-P3	76
	Dumbrė Dominykas	S9-O4	70
	Dzisevič Jaroslav	S8-O3	64
E	Elshaari A.	S8-I1	60
F	Fang Yi-Xin	S2-I2	17
	Faucher Marc	S3-P8	95
	Fedorov Georgy	S4-I1	25
	Fernández-Estévez José Luis	S1-P6	79
		S6-O9	52
	Fernandez-Pacheco Jose Javier	S2-P6	86
	Filipiak M.	S5-O6	38
	Fognini A.	S8-I1	60
G	Gaillot Davy P.	S6-O7	50
	Gallego Daniel	S3-P7	94
	Garcia-Meca Carlos	S6-O2	45
	Getautis Vytautas	S1-I2	12
	Gyger S.	S8-I1	60
	Globisch B.	S2-O1	19
	Gohil H.	S3-P3	90
	Golubewa Lena	S4-P4	102
	Gourgues R.	S8-I1	60
	Gradauskas Jonas	S4-P1	99
		S4-P3	101
	Graham Chris	S6-O6	49
	Gramlich M.	S2-I3	18
	Grigelionis Ignas	S6-O1	44
		S2-P4	84
	Grigucevičienė Asta	S4-P1	99
	Grzeslo Marcel	S3-P10	97
	Guerrero Luis	S6-O11	54

	Gulbinas Vidmantas	S7-I1	56
	Guzman Robinson	S6-O11	54
H	Haddad Thomas	S3-P9	96
	Headland Daniel	S3-P7	94
	Hyart Timo	S5-O5	37
	Hsiao Chung-Wei	S2-I2	17
	Hübers Heinz-Wilhelm	S6-I1	40
	Huggard P.	S3-P3	90
I	Ikamas Kęstutis	S6-O1	44
		S6-O4	47
		S6-O10	53
		S9-O1	67
		S3-P2	89
	Ikari Tomofumi	S2-I1	16
	Indrišiūnas Simonas	S6-O5	48
	Ivaškevičiūtė-Povilauskienė Rusnė	S9-O1	67
		3 min award	106
	Ivonyak Yu.	S5-O6	38
	Iwamatsu Shuya	S6-O9	52
J	Jakštas Vytautas	S6-O1	44
		S9-O4	70
		S2-P4	84
	Janonis Vytautas	S2-P7	87
	Jasinskas Algirdas	S9-O3	69
		S1-P1	74
	Jelezko Fedor	S4-I2	26
	Jemeljanov Maksim	S2-P5	85
	Jokubauskaitė Monika	S9-O2	68
		S9-O3	69
		S1-P1	74
		S1-P3	76
		3 min award	106
	Jorudas Justinas	S5-O1	33
		S5-O3	35
		S1-P2	75
	Jovaišaitė Justina	S8-O2	63
	Jukubauskis Domas	S6-O1	44
		S9-O1	67
	Jurkūnas Nerijus	S1-P1	74
	Juršėnas Saulius	S8-O2	63
	Juzeliūnas Gediminas	S4-I3	27
K	Kadashchuk Andrey	S5-I2	31

Kadlec F.	S9-O6	72
Kałuża Mateusz	S3-P5	92
	S3-P6	93
Kancleris Žilvinas	S2-P1	81
	S2-P2	82
Karaliūnas Mindaugas	S9-O4	70
	S4-P7	105
Karpicz Renata	S4-P4	102
Kašalynas Irmantas	S5-O1	33
	S5-O3	35
	S6-O3	46
	S6-O5	48
	S1-P2	75
	S2-P7	87
	S4-P7	105
Kazlauskas Karolis	S8-O1	62
Keraitytė Silvija	S9-O2	68
	S1-P1	74
	3 min award	106
Keršulis Skirmantas	S5-O2	34
Kiprijanovič Oleg	S1-P7	80
	S4-P2	100
Kirshner Sven	S8-O2	63
Kizevičius Paulius	S9-O1	67
Klein Andreas K.	S7-O1	58
	S3-P10	97
Klimovič F.	S9-O6	72
Knap Wojciech	S3-I2	23
	S5-O1	33
	S5-O6	38
	S6-O4	47
Köhler Anna	S5-I2	31
Köhler Klaus	S5-O5	37
Kohlhaas R. B.	S2-O1	19
Kołacinski Cezary	S6-O4	47
	S3-P2	89
Komorowski Paweł	S3-P5	92
	S3-P6	93
Korotyeyev V.V.	S5-O6	38
Kreiza Gediminas	S8-O2	63
Krotkus Arūnas	S9-O5	71
Kumar Ashish	S3-P7	94
Kumar Krishna	S6-O2	45
Kusmartsev F. V.	S2-O2	20
Kužel P.	S9-O6	72

	Kvietkauskas Evaldas	S4-P5	103
L	Lampe C.	S2-I3	18
	Lauck S.	S2-O1	19
	Lebouvier Edouard	S3-P8	95
	Leinartas Konstantinas	S4-P1	99
	Leo Karl	S1-I1-P	11
	Lettner T.	S8-I1	60
	Lévêque Gaëtan	S3-P8	95
	Lyaschuk Yu. M.	S5-O6	38
	Liebermeister L.	S2-O1	19
	Lisauskas Alvydas	S6-O4	47
		S6-O10	53
		S9-O1	67
		S3-P2	89
	Liu Chin-Pang	S3-P11	98
	Lizewski Kamil	S5-I3	32
	Lo Robert	S-I1	14
	Lu Peng	S3-P9	96
	Lučun A.	S4-P1	99
	Lukša Algimantas	S1-P4	77
	Łusakowski Jerzy	S2-P3	83
M	Maciaszek Marek	S5-O4	36
	Makhlouf Sumer	S6-O9	52
		S3-P9	96
	Malinauskas Tadas	S9-O5	71
	Martinez Javier	S3-P4	91
	Masalskyi Oleksandr	S4-P3	101
	Matulaitienė Ieva	S8-O3	64
	Maude D. K.	S2-I3	18
	Mickus Šarūnas	S4-P5	103
	Minkevičius Linas	S6-O1	44
		S9-O1	67
		S2-P4	84
	Mironas Audružis	S8-O3	64
	Mittleman Daniel	S6-I3	42
	Mohammed Abdu Subahan	S3-P8	95
	Morkūnaitė Ieva	S6-O4	47
	Moro Diego	S3-P4	91
	Moro-Melgar Diego	S6-O6	49
	Morvan Loïc	S2-P6	86
	Mujahid M.	S4-P1	99
N	Nacius Ernestas	S9-O1	67
	Nagatsuma Tadao	S6-I4	43

	Naimovičius Lukas	S8-O1	62
		3 min award	106
	Name Rih-You	S2-I2	17
	Nargelas Saulius	S8-O4	65
	Nargelienė Viktorija	S1-P4	77
	Naujokaitis Arnas	S1-P1	74
	Němec H.	S9-O6	72
	Nguyen Chris Phong Van	S2-O1	19
	Niaura Gediminas	S8-O3	64
		S9-O5	71
O	Orbe Luis	S6-O11	54
	Orentas Edvinas	S8-O1	62
	Orlov Sergey	S9-O1	67
	Ostatnický T.	S9-O6	72
	Otani Chiko	S2-I1	16
	Otsuji Taiichi	S3-I1	22
P	Padrez Yaraslau	S4-P4	102
	Pashnev Daniil	S5-O3	35
	Pennec Yan	S3-P8	95
	Petrauskas K.	S4-P1	99
	Petrauskas Rimvydas	S5-I1	30
	Petrulėnas Augustinas	S4-P3	101
	Plaušinitienė Valentina	S5-O2	34
	Plochocka P.	S2-I3	18
	Prystawko P.	S6-O3	46
		S1-P2	75
		S2-P7	87
	Pūkienė Simona	S1-P3	76
	Pukinskas Arnas	S1-P1	74
		S1-P3	76
R	Račiukaitis Gediminas	S6-O5	48
		S2-P2	82
	Radiunas Edvinas	S8-O1	62
	Ragulis Paulius	S2-P1	81
		S2-P2	82
	Raišys Steponas	S8-O2	63
	Ratautas Karolis	S2-P2	82
		S4-P5	103
	Razinkovas Lukas	S5-O4	36
	Redeckas Karolis	S2-P4	84
	Reinhard Friedemann	S5-O4	36
	Renaud Cyril C.	S6-O6	49
		S3-P3	90

		S3-P11	98
	Rodin Aleksej	S4-P3	101
	Roskos Hartmut G.	S6-I2	41
	Rumyantsev Sergey L.	S5-O1	33
		S5-O6	38
	Rutkauskas Danielis	S4-P4	102
S	Sai Pavlo	S5-O1	33
		S5-O3	35
		S5-O6	38
	Sajda Wiktoria	S3-P6	93
	Sakowicz Maciej	S5-O3	35
		S5-O6	38
	Sanda D.	S3-P1	88
	Sasaki Yoshiaki	S2-I1	16
	Sawadogo Bewindin A.	S6-O7	50
	Saxena Rishabh	S5-I2	31
	Schell M.	S2-O1	19
	Seddon James	S6-O6	49
	Seifert Birger	S4-P7	105
	Seliuta Dalius	S5-O5	37
	Selskis A.	S4-P1	99
	Serevičius Tomas	S7-I2	57
	Siemaszko Adam	S2-P3	83
	Siemion Agnieszka	S3-P5	92
		S3-P6	93
	Simniškis Rimantas	S2-P2	82
	Skapas Martynas	S9-O3	69
		S9-O5	71
		S1-P1	74
		S1-P5	78
		3 min award	106
	Słowikowski M.	S5-O6	38
	Spanidou Kalliopi	S6-O11	54
	Spigulis Janis	S8-I2	61
	Staffas T.	S8-I1	60
	Staiger Michael	S3-P10	97
	Stanionytė Sandra	S9-O2	68
		S9-O3	69
		S9-O5	71
	Stankevych Andrei	S5-I2	31
	Stankevič Voitech	S5-O2	34
	Stašys Karolis	S9-O5	71
	Steinhauer S.	S8-I1	60
	Stelmaszczyk K.	S5-O6	38
	Stöhr Andreas	S6-O9	52

		S1-P6	79
		S3-P9	96
		S3-P10	97
	Subačius Liudvikas	S5-O3	35
		S5-O5	37
		S6-O3	46
	Surma Mateusz	S3-P5	92
		S3-P6	93
	Surrente Alessandro	S2-I3	18
	Sutton J.	S8-I1	60
	Sužiedelis Algirdas	S4-P1	99
		S4-P3	101
	Szriftgiser Pascal	S6-O7	50
		S3-P8	95
	Šermukšnis Emilis	S1-P7	80
	Šetkus Arūnas	S8-O3	64
		S1-P4	77
	Šilėnas Aldis	S4-P1	99
		S4-P3	101
	Šimukovič A.	S1-P2	75
	Širmulis E.	S4-P1	99
	Šlekas Gediminas	S2-P1	81
		S2-P2	82
T	Talaikis Martynas	S1-P4	77
	Talochka Y.	S8-O4	65
	Tamošiūnaitė Milda	S6-O8	51
	Tamošiūnas Vincas	S6-O8	51
		S2-P5	85
	Tamulaitis Gintautas	S8-O4	65
		S2-P5	85
	Tebart Jonas	S3-P10	97
	Tomczewski Slawomir	S5-I3	32
	Treideris Marius	S6-O1	44
		S8-O3	64
		S1-P4	77
	Troha T.	S9-O6	72
	Trusovas Romualdas	S2-P2	82
U	Ucar Yilmaz	S3-P9	96
	Urban A. S.	S2-I3	18
	Urbanovič Andžej	S6-O1	44
		S4-P7	105
	Urbonis Darius	S2-P1	81
V	Vaitkevičius A.	S8-O4	65

	Valasevičius Evaldas	S2-P7	87
	Valušis Gintaras	S5-O5	37
		S6-O8	51
		S9-O1	67
		S9-O4	70
		S4-P7	105
	Vertelis Vilius	S5-O2	34
	Vidal Borja	S6-O2	45
	Viliūnas Mindaugas	S5-O2	34
	Vosylius Vytautas	S4-P5	103
	Vosylius Žygimantas	S2-P5	85
	Vrubliauskaitė Viktorija	S4-P5	103
W	Wagner Matthias	S8-O2	63
	Wahaia Faustino	S4-P7	105
	Wang H.	S3-P3	90
	Wang S.	S2-I3	18
	Wani Fasil Bashir	S3-P11	98
	Wegrzyn Piotr	S5-I3	32
		S4-P6	104
	Winnerl Stephan	S4-I4	28
	Wojtkowski Maciej	S5-I3	32
		S4-P6	104
	Wojtowicz Tomasz	S2-P3	83
Z	Zadeh I.	S8-I1	60
	Zagrajek Przemysław	S3-P5	92
	Zaknounge M.	S6-O7	50
	Zaremba Maciej	S2-P3	83
	Zdaniauskis Ernestas	S-I3	14
	Zegaoui M.	S6-O7	50
	Zelioli Andrea	S9-O2	68
		S1-P1	74
		S1-P3	76
	Zharchenko Ihor	S4-P3	101
	Žičkienė Ieva	S5-I3	32
		S3-P1	88
		S4-P6	104
	Zwiller Val	S8-I1	60
	Žemgulytė Justina	S2-P2	82
	Žurauskienė Nerija	S5-O2	34
		S1-P5	78

